

Ph.D. Dissertation



**International Doctoral School in Information
and Communication Technology**

DISI - University of Trento

**WILDLIFE ROAD CROSSING: INNOVATIVE
SOLUTION FOR PREVENTING VEHICLE COLLISION
BASED ON PERVASIVE WSN MONITORING SYSTEM**

Fabrizio Robol

Tutor:

Andrea Massa, Full Professor
University of Trento

Advisor:

Paolo Rocca, Associate Professor
University of Trento

Co-Advisor:

Federico Viani, Assistant Professor
University of Trento

April 2015

To my parents and my family, for their continuous and kind participation during this travel.

A special thanks to all friends and colleagues of the ELEDIA Research Center and an additional thanks to Ing. S. DeVigili and Ing. G. Benedetti of the 'Servizio Gestione Strade', of the Autonomous Province of Trento (PAT), Italy, for the support during pilot site definition and system deployment.

Abstract

The study, design and development of a monitoring system for wildlife road crossing problem is addressed in this thesis. Collisions between fauna and vehicles is a relevant issue in several mountain and rural regions and a valuable low-cost solution has not yet been identified. In particular, the proposed system is composed by a network of sensors installed along road margins, in order to detect wildlife events, (e.g., approaching, leaving or crossing the road), thus to promptly warn the incoming drivers. The sensor nodes communicate wirelessly among the network thus collecting the sensed information in a control unit for data storage, processing and statistics. The detection process is performed by the wireless nodes, which are equipped with low-cost Doppler radars for real-time identification of wildlife movements. In detail, different technologies valuable for solving the problem and related off-the-shelf solutions have been investigated and properly tested in order to validate their actual performance considering the specific problem scenario. A final classification based on specific parameters has allowed identifying the Doppler radar system as the better low-cost technology for contributing to the problem objective. The performance of the proposed system has also been investigated in a real scenario, which has been identified to be the actual pilot site for the monitoring system. This confirms the system capability of movements detection in the road proximity, thus defining a security area along it, where all occurring events may be identified.

Keywords

Wireless Sensor Network, Smart Environment, Road Safety, Sensors and Actuators, Distributed Monitoring

Published Conference Papers

- [C1] G. Oliveri, F. Robol, M. Carlin, and A. Massa, "Synthesis of large sparse linear arrays by bayesian compressive sensing," *5th European Conference on Antennas and Propagation (EuCAP 2011)*, Rome, Italy, pp. 2203-2206, April 11-15, 2011.
- [C2] G. Oliveri, P. Rocca, F. Viani, F. Robol, and A. Massa, "Latest advances and innovative solutions in antenna array synthesis for microwave wireless power transmission," *IEEE MTT-S International Microwave Workshop Series on "Innovative Wireless Power Transmission: Technologies, Systems, and Applications" (IMWS-IWPT 2012)*, Kyoto, Japan, pp. 71-73, May 10-11, 2012.
- [C3] G. Franceschetti, P. Rocca, F. Robol, and A. Massa, "Innovative rectenna design for space solar power systems," *IEEE MTT-S International Microwave Workshop Series on "Innovative Wireless Power Transmission: Technologies, Systems, and Applications" (IMWS-IWPT 2012)*, Kyoto, Japan, pp. 151-153, May 10-11, 2012.
- [C4] G. Franceschetti, P. Rocca, F. Robol, and A. Massa, "Design and optimization of efficient rectenna systems for space solar power applications," *International Conference on Electromagnetics and Advanced Applications (ICEAA 2012)*, Cape Town, South Africa, September 2-7, 2012 (Invited paper; Session title: "Wireless power transmission" - G. Franceschetti and N. Shinohara).
- [C5] F. Viani, F. Robol, M. Salucci, E. Giarola, S. De Vigili, M. Rocca, F. Boldrini, G. Benedetti, and A. Massa, "WSN-based early alert system for preventing wildlife-vehicle collisions in Alps regions - From the laboratory test to the real-world implementation," *7th European Conference on Antennas and Propagation (EuCAP 2013)*, Gothenburg, Sweden, pp. 1857-1860, April 8-12, 2012.
- [C6] G. Menduni, F. Viani, F. Robol, E. Giarola, A. Polo, G. Oliveri, P. Rocca, and A. Massa, "A WSN-based architecture for the E-Museum - The experience at "Sala dei 500" in Palazzo Vecchio (Florence),"

Proc. 2013 IEEE AP-S International Symposium, Lake Buena Vista, Florida, USA, pp. 1114-1115, July 7-12, 2013.

- [C7] F. Viani, F. Robol, A. Polo, E. Giarola, and A. Massa, "Localization strategies in WSNs as applied to landslide monitoring," *2013 American Geophysical Union Fall Meeting*, San Francisco, USA, p. A5, December 9-13, 2013 (Invited paper; Session title: "New technologies in landslide monitoring and risk management" - A. Pasuto and L. Schenato).
- [C8] F. Viani, F. Robol, E. Giarola, G. Benedetti, S. Devigili, and A. Massa, "Advances in wildlife road-crossing early-alert system: new architecture and experimental validation," *8th European Conference on Antennas and Propagation (EUCAP 2014)*, The Hague, The Netherlands, pp. 3457-3461, April 6-11, 2014.
- [C9] A. Polo, F. Robol, C. Nardin, S. Marchesi, A. Zorer, L. Zappini, F. Viani, and A. Massa, "Decision support system for fleet management based on TETRA terminals geolocation," *8th European Conference on Antennas and Propagation (EUCAP 2014)*, The Hague, The Netherlands, pp. 1195-1198, April 6-11, 2014.
- [C10] F. Viani, A. Polo, F. Robol, G. Oliveri, P. Rocca, and A. Massa, "Crowd detection and occupancy estimation through indirect environmental measurements," *8th European Conference on Antennas and Propagation (EUCAP 2014)*, The Hague, The Netherlands, pp. 2127-2130, April 6-11, 2014.
- [C11] F. Viani, A. Polo, E. Giarola, F. Robol, P. Rocca, P. Garofalo, S. De Vigili, G. Benedetti, L. Zappini, A. Zorer, S. Marchesi, and A. Massa, "Semantic wireless localization for innovative indoor/outdoor services," *Proc. 2014 IEEE AP-S International Symposium and USNC-URSI Radio Science Meeting*, Memphis, Tennessee, USA, pp. 402-403, July 6-12, 2014.
- [C12] F. Viani, E. Giarola, F. Robol, G. Oliveri, and A. Massa, "Distributed monitoring for energy consumption optimization in smart buildings," *Proc. 2014 IEEE Antenna Conference on Antenna Measurements and Applications (IEEE CAMA 2014)*, Antibes Juan-les-Pins, France, pp. 1-3, November 16-19, 2014.
- [C13] F. Viani, E. Giarola, F. Robol, A. Polo, A. Lazzareschi, T. Moriyama, and A. Massa, "Passive wireless localization strategies for security in large indoor areas," *Proc. 2014 IEEE Antenna Conference on Antenna Measurements and Applications (IEEE CAMA 2014)*, Antibes Juan-les-Pins, France, pp. 1-3, November 16-19, 2014.

-
- [C14] F. Viani, F. Robol, E. Giarola, A. Polo, A. Toscano, and A. Massa, "Wireless monitoring of heterogeneous parameters in complex museum scenario," *Proc. 2014 IEEE Antenna Conference on Antenna Measurements and Applications (IEEE CAMA 2014)*, Antibes Juanles-Pins, France, pp. 1-3, November 16-19, 2014.
- [C15] F. Viani, F. Robol, E. Giarola, P. Rocca, G. Oliveri, and A. Massa, "Passive imaging strategies for real-time tracking of non-cooperative targets in security applications," *9th European Conference on Antennas and Propagation (EUCAP 2015)*, Lisbon, Portugal, April 12-17, 2015 (Invited paper; Session title: "Wave-based sensing and imaging for security applications" - J. Martinez and C. Rappaport).
- [C16] F. Robol, F. Viani, A. Polo, E. Giarola, P. Garofalo, C. Zambiasi, and A. Massa, "Opportunistic crowd sensing in WiFi-enabled indoor areas," *Proc. 2015 IEEE AP-S International Symposium and USNC-URSI Radio Science Meeting*, Vancouver, BC, Canada, July 19-25, 2015 (Submitted).
- [C17] F. Viani, M. Salucci, F. Robol, E. Giarola, and A. Massa, "WSNs as enabling tool for next generation smart systems," *Atti XIX Riunione Nazionale di Elettromagnetismo (XIX RiNEm)*, Roma, pp. 393-396, 10-14 Settembre 2012.
- [C18] E. Giarola, S. Marchesi, A. Polo, F. Robol, F. Viani, L. Zappini, A. Zorer, and A. Massa, "Innovative wireless solutions for smart cities," *Atti XX Riunione Nazionale di Elettromagnetismo (XX RiNEm)*, Padova, pp. 385-388, 15-18 Settembre 2014.

Published Journals Papers

- [R1] F. Viani, M. Salucci, F. Robol, G. Oliveri, and A. Massa, "Design of a UHF RFID/GPS fractal antenna for logistics management," *Journal of Electromagnetic Waves and Applications*, vol. 26, pp. 480-492, 2012.
- [R2] F. Viani, M. Salucci, F. Robol, and A. Massa, "Multiband fractal ZigBee/WLAN antenna for ubiquitous wireless environments," *Journal of Electromagnetic Waves and Applications*, vol. 26, no. 11-12, pp. 1554-1562, 2012.
- [R3] F. Viani, L. Poli, G. Oliveri, F. Robol, and A. Massa, "Sparse scatterers imaging through approximated multi-task compressive sensing strategies," *Microwave and Optical Technology Letters*, vol. 55, no. 7, pp. 1553-1557, July 2013.
- [R4] F. Viani, F. Robol, A. Polo, P. Rocca, G. Oliveri, and A. Massa, "Wireless architectures for heterogeneous sensing in smart home applications - Concepts and real implementations," *Proceedings of the IEEE - Special Issue on 'The Smart Home,' Invited Paper*, vol. 101, no. 11, pp. 2381-2396, November 2013.
- [R5] G. Oliveri, L. Lizzi, F. Robol, and A. Massa, "Polarization-agile ADS-interleaved planar arrays," *Progress in Electromagnetic Research*, vol. 142, pp. 771-798, 2013.
- [R6] G. Oliveri, E. Bekele, F. Robol, and A. Massa, "Sparsening conformal arrays through a versatile BCS-based method," *IEEE Transactions on Antennas and Propagation - Special Issue on "Innovative Phased Array Antennas based on Non-regular Lattices and Overlapped Sub-arrays"*, vol. 62, no. 4 (Part 1), pp. 1681-1689, April 2014.
- [R7] B. Majone, F. Viani, E. Filippi, A. Bellin, A. Massa, G. Toller, F. Robol, and M. Salucci, "Wireless sensor network deployment for monitoring soil moisture dynamics at the field scale," *Procedia Environmental Sciences*, vol. 19, pp. 426-235, 2013.

- [R8] T. Moriyama, F. Viani, M. Salucci, F. Robol, and E. Giarola, "Planar multiband antenna for 3G/4G advanced wireless services," *IEICE Electronics Express*, vol. 11, no. 17, pp. 1-10, 10 September 2014.

Contents

1	Introduction	1
2	Wildlife Road Crossing Problem and Solutions	5
2.1	Roadside characteristics which may attract wildlife	6
2.1.1	Wildlife Road Crossing Problem in the Province of Trento	6
2.2	State of the Art Solutions	10
3	Proposed Solution, Prototype and Validation	13
3.1	Proposed Solution: System Architecture	14
3.2	Technology Scouting	18
3.2.1	Radar Technology	18
3.2.2	Ultrasound Technology	19
3.2.3	Infrared Technology	19
3.2.4	Thermal Technology	20
3.3	Off-The-Shelf Sensor Selection	21
3.4	Sensor Preliminary Setup and Testing	23
3.4.1	Radar Sensor RSM-1650	23
3.4.2	Ultrasound Sensor SRF485WPR	31
3.4.3	Infrared Sensor PIR-SMD	38
3.4.4	Thermal Sensor TPA81	45
3.5	WSN Node Architecture	51
3.5.1	WSN Node 3Mate Architecture	51
3.5.2	Power Consumption and Management of the Integrated Solution	53
3.5.3	Hardware Interface of the Integrated Sensor Node	59
3.6	Wireless Network Architecture	66
3.6.1	Linear Network Architecture	66
3.6.2	Ring Network Architecture	66
3.6.3	Star Network Architecture	67
3.6.4	Mesh Network Architecture	68
3.6.5	Application Scenarios and Network Topology	68
3.7	Testing of the WSN Monitoring System in controlled Test-site . .	73
3.7.1	Test in Deer Fence	74

4	Engineering and Pilot Site Extension	79
4.1	Doppler Radar	80
4.2	WSN Sensor Node Engineering	85
4.2.1	WSN Node Platforms	89
4.2.2	Prototype Layout Optimization	94
4.2.3	Radar Sensor Support	98
4.2.4	Optimal Case Definition	100
4.2.5	Integration Testing	101
4.2.6	Controller Firmware	103
4.2.7	Event Detection Methodologies	107
4.3	Experimental Validation	110
4.4	Pilot Site Identification and Sensor Node Installation	114
4.4.1	Experimental Testing	119
5	Conclusions	129
5.1	Conclusion and Future Development	130
A	Complete Circuital Scheme of the WSN Node-Sensors Interfacing Board	143

List of Tables

2.1	Fauna species on the provincial territory: species, number and expected trend.	7
2.2	Fauna collisions in the last decades.	8
3.1	Radar technology: available off-the-shelf products.	21
3.2	Ultrasound technology: available off-the-shelf products.	21
3.3	Infrared technology: available off-the-shelf products.	21
3.4	Thermal technology: available off-the-shelf products.	22
3.5	Power budget: main components of the integrated sensor node and related current consumption using 12Volt battery.	54
3.6	Power budget: main components of the integrated sensor node and related power consumption using 12Volt battery.	55
3.7	Power budget: main components of the integrated sensor node and related current consumption using 6Volt battery.	55
3.8	Power budget: main components of the integrated sensor node and related power consumption using 6Volt battery.	56
3.9	Electrical and communication characteristics of sensors and WSN node.	60
3.10	Specific input and output connections of the analog switch for sensors management.	64
3.11	Sensors evaluation on the basis of four main parameters given by the experimental tests outcome and specific technology features.	77

LIST OF TABLES

List of Figures

2.1	Risk map of the roads in the Province of Trento.	8
2.2	Reflective device used on road delimiters.	9
2.3	Example of active wildlife monitoring system [5]: (a) device, (b) animal wearing the device.	12
2.4	Typical road infrastructures: (a) fence applied to road overpass, (b) wildlife eco-pass over road, (c) wildlife underpass near flood, (d) wildlife underpass in rural area.	12
3.1	Wildlife road crossing monitoring system: risk definition scheme.	14
3.2	WSN system architecture: sensor and actuator devices for the detection of wildlife movement along road stretches and prompt alert.	15
3.3	Radar sensor RSM-1650: dimensions and connection pins.	24
3.4	High pass filter: cut frequency 154Hz.	25
3.5	Low pass filter: cut frequency 3.39KHz.	25
3.6	Double semi-wave rectifier.	26
3.7	Schmidt trigger with hysteresis and tunable threshold.	26
3.8	Radar sensor interface board: processing of output signal.	27
3.9	Radar sensor testing setup.	28
3.10	Radar sensor testing setup: (a) active LED for movement detection, (b) LED off for no movement detection.	28
3.11	Radar sensor testing: target with constant speed 1Km/h.	29
3.12	Radar sensor testing: target with speed in the range 3.5-5Km/h.	29
3.13	Radar sensor testing - target moves away from the sensor plane with constant speed: (a) experimental scenario, (b) radar output signal.	30
3.14	Radar sensor testing - target moves towards the sensor plane with constant speed: (a) experimental scenario, (b) radar output signal.	30
3.15	Radar sensor testing - target is still in front of the radar sensor: (a) experimental scenario, (b) radar output signal.	31
3.16	Ultrasound sensor testing setup: (a) sensor view, (b) sensor connection scheme.	32
3.17	RS-485 protocol: transmission example.	32

LIST OF FIGURES

3.18	Ultrasound sensor testing setup: USB-RS485 converter and SRF485WPR sensor.	33
3.19	Ultrasound sensor testing setup: reception data on Matlab workspace.	34
3.20	Ultrasound sensor testing: log file with the measured data.	35
3.21	Ultrasound sensor validation setup.	35
3.22	Ultrasound sensor testing setup.	36
3.23	Ultrasound sensor testing: (a) target approaching the sensor, (b) target in steady position in front of the sensor.	37
3.24	Ultrasound sensor testing setup.	37
3.25	Infrared sensor: (a) front view, (b) bottom view.	39
3.26	Infrared sensor testing setup.	40
3.27	Infrared sensor testing: (a) target approaching the sensor, (b) sensor output signal acquired with oscilloscope.	41
3.28	Infrared sensor testing: sensor output signal acquired with oscilloscope while target leaves the sensor plane.	42
3.29	Infrared sensor testing: (a) sensor output signal acquired with oscilloscope while target approaches the sensor plane starting from 7.0m, (b) sensor output signal acquired with oscilloscope while target leaves the sensor plane from 4.5m.	42
3.30	Infrared sensor testing: (a) target moving tangentially in front of the sensor, (b) sensor output signal acquired with oscilloscope while the target moves tangentially at 3.5m.	43
3.31	Infrared sensor testing: sensor output signal acquired with oscilloscope while the target moves tangentially at 7.0m.	44
3.32	Infrared sensor testing: (a) target standing in front of the sensor, (b) sensor output signal acquired with oscilloscope while the target stands in front of the sensor at 2m distance.	44
3.33	Thermal sensor TPA81: (a) connection pins, (b) sensor dimension.	46
3.34	Thermal sensor TPA81 connected to the I2C-USB converter.	46
3.35	Thermal sensor TPA81: (a) data acquisition example in Matlab workspace, (b) real-time color map generated on data acquisition.	47
3.36	Thermal sensor TPA81 testing setup.	48
3.37	Thermal sensor TPA81: color map representative of a target placed on the left side of the sensor field-of-view.	49
3.38	Thermal sensor TPA81: color map representative of a target moving at 2m distance from the sensor plane.	49
3.39	WSN node 3Mate: (a) front side, (b) back side.	51
3.40	WSN node 3Mate: (a) programmer board, (b) 3Mate device with programmer board.	52
3.41	WSN node 3Mate: connection strips.	52
3.42	WSN node 3Mate: integration scheme.	53

3.43	Voltage regulators circuitual scheme: (a) step-down regulator 6.0V-3.3V, (b) step-down regulator 6.0V-5.0V, (c) step-up regulator 6.0V-12.0V.	61
3.44	Radar sensor conditioning stages and connection to WSN node controller: circuitual scheme.	62
3.45	Ultrasound sensor connection to WSN node controller: circuitual scheme.	63
3.46	Infrared sensor connection to WSN node controller: circuitual scheme.	63
3.47	Analog switch connection to WSN node controller and sensors: circuitual scheme.	64
3.48	Integrated sensor node prototype: (a) circuitual board, (b) integrated device.	65
3.49	Linear network architecture scheme.	66
3.50	Ring network architecture scheme.	67
3.51	Star network architecture scheme.	67
3.52	Mesh network architecture scheme.	68
3.53	WSN node radio transceiver coverage: scheme and diameter of the covered area.	69
3.54	Controlled environment of reduced dimensions.	70
3.55	Controlled environment of medium/large dimensions.	70
3.56	Experimental test site: network topology sketch.	72
3.57	WSN monitoring system testing: (a) approaching event, (b) graphical interface showing the event detection.	73
3.58	WSN monitoring system testing: (a) lateral movement, (b) graphical interface showing the event detection.	74
3.59	WSN monitoring system testing: sensor node position inside the deer fence.	74
3.60	WSN monitoring system testing: (a) lateral approaching movement, (b) leaving movement, (c) graphical interface showing the approaching event detection, (d) graphical interface showing the leaving event detection.	75
3.61	WSN monitoring system testing: (a) deers movement, (b) graphical interface showing the event detection.	76
4.1	Doppler effect scheme.	81
4.2	Doppler radar scheme.	82
4.3	WSN sensor node field-of-view: (a) single radar module, (b) double radar module.	85
4.4	Block diagram of the conditioning stage in case of double radar module.	86
4.5	Radar signal output of the first amplifier stage: (a) leaving movement, (b) approaching movement.	87

LIST OF FIGURES

4.6	Radar signal output of the complete conditioning stage: (a) leaving movement, (b) approaching movement.	88
4.7	WSN node platforms: 3Mate device.	90
4.8	WSN node platforms: TinyNode device.	90
4.9	WSN node platforms: Flyport device.	91
4.10	WSN node platforms: Arduino and XBee devices.	92
4.11	WSN node platforms testing: experimental test scenario map and altitude measurements.	92
4.12	WSN node platforms testing: experimental setup and nodes position.	93
4.13	WSN sensor node prototype optimization: circuital scheme.	97
4.14	WSN sensor node prototype optimization: board layout.	98
4.15	WSN sensor node prototype optimization: radar sensor axial joint.	99
4.16	WSN sensor node prototype optimization: radar sensors and supports.	99
4.17	Optimal case definition: (a) front view and dimensions, (b) back view and fixing holes.	101
4.18	Optimal case definition: (a) sliding profile for board insertion, (b) insertion guide and lock.	102
4.19	Controller firmware flux diagram.	105
4.20	Controller firmware flux diagram: battery voltage check and adaptive sensor node activity regulation.	106
4.21	Movement event: radar signal output of the hardware pre-processing methodology.	108
4.22	Experimental testing: (a) sensor node installation support, (b) sensor node installation height.	110
4.23	Experimental testing sensor node installation distance.	111
4.24	Experimental testing: data log file.	112
4.25	Experimental testing: lateral movement in sensor nodes field-of-view.	113
4.26	Pilot site: (a) map location, (b) node installation sketch.	114
4.27	Wildlife road crossing monitoring system: risk definition scheme.	115
4.28	Sensor nodes under construction.	115
4.29	Sensor nodes installation on the pilot site.	116
4.30	Pilot site: (a) variable message panel and position of some sensor nodes signed by red marker, (b) variable message panel and position of gateway node signed by yellow marker, (c) gateway node installation, (d) gateway node Yagi antenna and verification system.	118
4.31	Pilot site experimental testing: (a) approaching, leaving and lateral movements, (b) road crossing movements.	119
4.32	Experimental testing: (a) processed radar signal during approaching event, (b) processed radar signal during leaving event.	120

4.33	Pilot site experimental movement tests: <i>(a)</i> - <i>(b)</i> orthogonal to node #5 and processed radar signal, <i>(c)</i> - <i>(d)</i> orthogonal to node #6 and processed radar signal, <i>(e)</i> - <i>(f)</i> lateral to node #5 and processed radar signal, <i>(g)</i> - <i>(h)</i> lateral to node #6 and processed radar signal.	121
4.34	Pilot site experimental movement tests: <i>(a)</i> - <i>(b)</i> lateral to node #6 and processed radar signal, <i>(c)</i> - <i>(d)</i> lateral to nodes #5 and #6 and processed radar signal, <i>(e)</i> - <i>(f)</i> lateral approach to nodes #6 and #5 and processed radar signal.	122
4.35	Pilot site experimental tests: <i>(a)</i> target moving out of the security area, <i>(b)</i> processed radar signal when target moving out of the security area, <i>(c)</i> target moving inside the security area, <i>(d)</i> processed radar signal when target moving inside the security area.	123
4.36	Pilot site experimental tests: <i>(a)</i> - <i>(b)</i> road crossing near nodes #5 and #1 and processed radar signal, <i>(c)</i> - <i>(d)</i> road crossing near nodes #6 and #2 and processed radar signal, <i>(e)</i> - <i>(f)</i> road crossing near nodes #5 and #2 and processed radar signal, <i>(g)</i> - <i>(h)</i> road crossing near nodes #6 and #3 and processed radar signal. . . .	124
4.37	Pilot site experimental tests: <i>(a)</i> - <i>(b)</i> road crossing near nodes #7 and #2 and processed radar signal, <i>(c)</i> - <i>(d)</i> road crossing near nodes #5 and #3 and processed radar signal, <i>(e)</i> - <i>(f)</i> road crossing near nodes #7 and #1 and processed radar signal.	125
4.38	Pilot site: battery recharge.	126
4.39	Pilot site: <i>(a)</i> - <i>(b)</i> - <i>(c)</i> roe-deer road crossing event, successive time instants, <i>(d)</i> processed radar signal acquired for the roe-deer road crossing event.	127
5.1	Actuator node of the monitoring system: <i>(a)</i> developed prototype, <i>(b)</i> proposed final solution.	131
A.1	Circuitual scheme of the WSN node-sensors interfacing board. . . .	143

LIST OF FIGURES

Chapter 1

Introduction

Wildlife monitoring has attracted more and more attention during the last decades. In this framework, the problem of wildlife road-crossing is here considered. In the last years, most of the mountain roads in Alps regions have been affected by an increasing number of wildlife-vehicle collisions mainly due to the high flow of tourism and the climatic changes that force animals to move at different altitudes. The negative effects of roads on wildlife are well documented and the animal mortality because of vehicle collisions is constantly increasing [1]. The problem of crossing-event also constitutes a major public safety concern for transportations especially in mountain regions. Many solutions have been introduced in road facilities to minimize the wildlife-vehicle collisions, mainly based on fencing and crossing structures that prevent ungulates to access the road. Unfortunately, the costs of road upgrades limit a wide diffusion of preventive structures. Therefore, finding reliable and cost-effective methods for collision prevention represents a challenging objective for many wildlife management agencies. State-of-the-art studies are devoted to monitor wildlife activities for tracking and behavior analysis [2, 3] with integrated often wearable sensors. The most diffused technological solutions are based on global positioning systems (GPSs), radio-frequency identification (RFIDs), and video cameras. Unfortunately, these active (i.e. with wearable devices) systems cannot be exploited for road crossing-event detection of non-controlled species. Other studies are focused on the understanding of animal behavior, their physiology, socialization, and diffusion [4, 5]. To this end, researchers have proposed many autonomous monitoring systems mainly based on wireless sensor network (WSN) infrastructures [6, 7]. Thanks to their scalability and pervasiveness, WSN-based systems have been widely adopted for the monitoring of heterogeneous real-world data and events, such as the soil characteristics in precision agriculture [8], the electromagnetic pollution in urban areas [9, 10], the artworks preservation in museums [11], up to the localization and tracking of transceiver-free targets [12, 13, 14, 15, 16, 17, 21]. The compact size, the robustness and the long lifetime of WSNs have been exploited in those solutions where animals are equipped with battery powered sensors (e.g. collars)

able to collect heterogeneous spatio-temporal data related to movements and positions. However, this system architecture composed by wearable devices is valuable only when a known and finite set of animals is monitored. A different approach is needed for the passive monitoring of transceiver-free (i.e. not equipped with active devices) animals.

This work deals with a prevention system for wildlife-vehicle collisions based on a sensor/actuator network able to detect the presence of animals in the proximity of the road and to immediately alert the drivers. More specifically, a wireless sensor network (WSN) infrastructure is exploited as a powerful platform for processing data collected from the environment and for the event signaling [18]. The nodes of the WSN consist of low-cost and compact devices, installed on the road sides, with sensing and processing capabilities. Each node is wirelessly connected to the others to perform distributed and cooperative sensing tasks. The nodes are equipped with specific sensors able to effectively detect the presence and the movements of animals (e.g., ungulates) approaching the road proximity. Additional parameters may be evaluated, like the direction and the velocity of wildlife movement, in order to enable a reliable and real-time false alarm detection [19, 20, 22, 23, 24]. Each sensing device allows identifying a finite-size warning area along the road path, which corresponds to the sensors field-of-view. The real-time event detection is shared among the WSN nodes thus to promptly monitor not only the area surrounding the WSN node, which firstly detects the events, but also the area monitored by the other sensing devices in the proximity. This information, then, may trigger the actuation policies to alert drivers of the risky condition. In fact, once the sensed information is interpreted as a crossing-event, the actuators of the WSN platform could be activated to warn the alarm for driver security (e.g., a light signal system installed on the roadside). The collected information is also transmitted to a remote control unit for successive data analysis and statistics. The proposed early-alert system has been experimentally validated through a real small-scale deployment in Alps region. Preliminary results have assessed the potentialities of the approach in dealing with ungulates road crossing detection and signaling.

Therefore, the conducted technology transfer activity has been aimed at designing and developing a system able to monitor and alert drivers of the presence of wildlife animals approaching the monitored road in order to prevent wildlife-vehicle collision. Actually there is no an effective solution to the presented problem, which in turns produces huge costs for Public Administration. As an example, in the Province of Trento, there are about 600 wildlife to vehicle collisions per year and till the year 2014, drivers refund for the accident was about up to the 70% of the experienced damages. Nowadays, the restriction policies have implied to neglect this reimbursement formula and hence solutions like the one proposed may be valuable approaches to the problem.

Thesis outline

The thesis is organized as follows. Firstly, the wildlife road crossing problem is discussed, by analyzing the actual solutions to the problem used nowadays in Chapter 2. Then, the approach to the problem is presented in Chapter 3, by describing the proposed solution to prevent wildlife-vehicle collision. In this context, the technological solutions identified to be integrated in the sensing device are described, analyzing the features for each adopted technology. An experimental validation campaign emphasizes advantages and disadvantages of each technology and in particular of the specific off-the-shelf devices, which has been chosen for the integration with the sensing WSN device. On the basis of the outcomes obtained during the experimental validation, the final technological choice is defined in Chapter 4 together with the engineering process on the basis of the prototypal platform, which is conducted in order to improve the performance, while reducing dimensions and energy consumption. Then the actual installation on the experimental test-site is presented and final conclusions are drawn in Chapter 5.

Chapter 2

Wildlife Road Crossing Problem and Solutions

In this chapter, the problem concerning wildlife road crossing is presented. State-of-the-art studies are mainly devoted to monitor wildlife activities for tracking and behavior analysis [2, 3] by exploiting integrated sensors most of which are wearable ones. Many actual solutions have also been introduced in road facilities in order to minimize wildlife-vehicle collisions, mainly based on fencing and crossing structures, which should prevent ungulates to access the road. The huge number of incidents registered nowadays lead to infer the reduced effectiveness of the experimented solutions, thus motivating the definition of a more efficient system to address the problem.

2.1 Roadside characteristics which may attract wildlife

Wildlife-collision areas exhibit some common feature, which appeal wildlife thus increasing the risk of collision with in transit vehicles. Some of these characteristics are listed below and their knowledge may be exploited in order to clearly identify more risky road areas and to increase driver awareness about the problem:

- Areas of good forage: on the basis of the particular periodicity, animals moves from more remote areas down into the valley looking for food, given that at higher altitudes the food resources may be depleted or nature is still frozen, if we consider autumn and winter seasons.
- Proximity to water sources: wildlife is attracted to fresh water sources, often placed in creeks parallel or intersecting roads.
- Wide open and/or isolated, clear stretches of road: wildlife-vehicle collisions occur most of the times during clear nights, on dry roads conditions and on straight stretches of road or quite isolated areas. In fact, animals are attracted by these conditions, since there are few vehicles and human activity is quite reduced. At the same time, the same conditions give more confidence to drivers on behalf of higher visibility and a false sense of increased security.

In addition to these features, it is possible to identify other characteristics in common to many collisions registered in last years. In particular, dawn and sunset are peak activity times for wildlife collisions and most of incidents happen between 7:00pm and midnight. This is due to the fact that animals exploit first and last glimmers of light, respectively, for looking forward for food and forage, given also the reduced traffic activity along roads during these hours.

Therefore these simple rules may be of public domain in order to increase citizen awareness to the problem and to improve their forecast and reaction ability, establishing a virtuous behavior.

2.1.1 Wildlife Road Crossing Problem in the Province of Trento

The provincial territory is mainly characterized by Alps regions over an area of about 620668 hectares, the 70% of which present an altitude higher than 1000m to the sea level. The actual surface covered by forests is around 345000 hectares, namely the 56% of the entire provincial territory. Grazing land represents about the 17% and the remaining is mainly divided among agricultural activities and urban areas. Over this area a great variety of flora and fauna is present, ranging

CHAPTER 2. WILDLIFE ROAD CROSSING PROBLEM AND SOLUTIONS

from mediterranean species to mountain and sub-alpine woods. Concerning fauna, instead, Table 2.1 reports the main species present on the territory, their actual number and the expected trend (data given by the 'Servizio Gestione Strade' of the Province of Trento).

<i>Species</i>	<i>Individual Number</i>	<i>Trend</i>
Roe Deer	26016	increasing
Deer	9123	increasing
Chamois	24520	stable
Wild Boar	150	/
Steinbock	400	stable
Mouflon	860	decreasing
Hare	5000-6000	decreasing
Marmot	10000-12000	stable
Bear	23-25	increasing

Table 2.1: Fauna species on the provincial territory: species, number and expected trend.

The roads in the Trentino Region are classified as state and provincial roads, for a total length of about 2375Km, divided in 1511Km of provincial roads and 864Km of state roads. In particular, the mountain roads covers around 2140Km, while the remaining 235Km are represented by valley roads.

In addition, the Province of Trento is in charge of monitoring roads status and guarantee security also considering the incidents prevention due to the local fauna. To this end, risk maps have been generated on the basis of the registered incidents along the roads of the province, as shown in Fig. 2.1. In particular, the risk level is classified in four main categories, namely low-, moderate-, risk, high- risk conditions to which a color is assigned for the map generation.

In Trentino, the data related to incidents due to fauna are stored on a database since the year 1993 in fulfillment of a specific legislation, which implies the collision communication to the authority. Table 2.2 reports the data related to fauna incidents of the last decades.

2.1. ROADSIDE CHARACTERISTICS WHICH MAY ATTRACT WILDLIFE

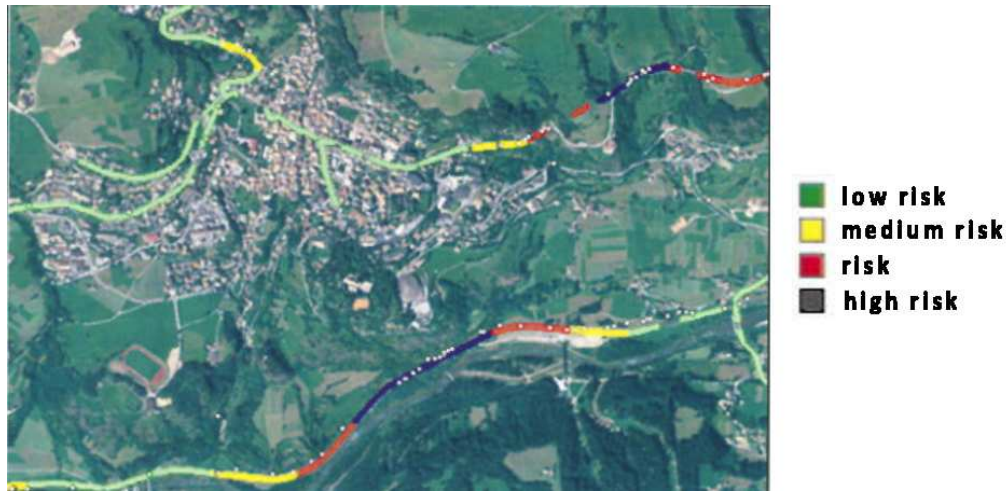


Figure 2.1: Risk map of the roads in the Province of Trento.

<i>Year</i>	<i>Roe Deer</i>	<i>Deer</i>	<i>Chamois</i>	<i>Wild Boar</i>	<i>Mouflon</i>	<i>Total</i>
1993	193	30				223
1994	182	25				207
1995	207	23				230
1996	255	38		2		295
1997	210	44				254
1998	217	41				258
1999	291	38				329
2000	345	52	1	1		399
2001	281	43		2		326
2002	320	65	2	6		393
2003	340	82	1		2	425
2004	317	84		2		403
2005	266	78	2	3		349
2006	405	97	2	1		505
2007	389	125	1	2		517
2008	495	110	2	9		616

Table 2.2: Fauna collisions in the last decades.

It is worth noting that the data shown in Table 2.2 are related to reported collisions. In addition to these values the number of non-declared incidents may be considered.

Nevertheless, by looking at the total incidents reported, deer and roe deer are the two species more involved in the collisions. In particular, the collisions

CHAPTER 2. WILDLIFE ROAD CROSSING PROBLEM AND SOLUTIONS

peaks are registered during autumn and spring seasons in relation to the higher mobility of the fauna during such periods of the year.

In addition, also birds and small size species are victims of vehicle collisions, but given their reduced size, the gathering data process is quite difficult and thus such incidents may escape from the survey.

Among the intervention conducted by the Province of Trento in order to limit the fauna collisions, barriers, fences and reflective devices have been actuated. In particular, regarding the reflective devices (Fig. 2.2), the Province of Trento started with their installation in the 1998 along 160 stretched of roads for about 101Km, as an experimental test. Such devices should reflect the vehicles lights towards the external section of the road, such that an approaching animal should be scared by the reflected light stopping and leaving the scene. Nevertheless, a study conducted in order to evaluate the effectiveness of the implemented solution states that no actual benefit is given by the presence of the reflective devices, given that the actual number of collisions do not decrease since their presence on the road margins. Therefore this may suggest that fauna incidents are mainly related to seasonal conditions and thus the effectiveness of such devices has already to be evaluated.



Figure 2.2: Reflective device used on road delimiters.

Additional interventions regard the installation of illuminated road signs, placed along high-risk roads and equipped with traffic sensors, thus activating the signal when vehicles transit over the road.

2.2 State of the Art Solutions

Several technological solutions have been investigated to monitor, analyse and preventing animal behaviour. In particular, we can distinguish between two main classes of solutions, namely monitoring systems, addressed to improve knowledge about wildlife habits [25, 26, 27, 28], and structural systems, used to allow wildlife crossing roads in safety condition.

Let us consider the former case. Several monitoring systems have been developed in the last years [29], based on some main technologies like identification and localization technologies, such as radio-frequency identification (RFID) [30], global positioning system (GPS) [5] (Fig. 2.3) and video cameras [2, 31]. One main drawback of such systems is represented by the need of specific setup in order to allow the monitoring process. In particular, animals should be equipped with specific devices able to interact with the monitoring system. It may appear clear that such condition may not always be applied to some animals typology, like ungulates and wildlife in general, considering the huge number of animals in each single herd. In addition, the specific case of video cameras based systems imply the need of clear vision in the monitored area, therefore fog and bad weather conditions may limit their applicability.

Regarding monitoring systems for wildlife, a brief review of the various available solutions at the state-of-the-art is presented hereafter. In the last decades several improvements have been obtained for wildlife monitoring [32, 33, 34, 35, 36, 5]. The use of collars to be worn by animals is widely spread and for instance [37] propose an animal tracking system, which exploits Arduino platforms equipped with several sensors. The location and sensor information are spread over the network by using GSM and radio frequency technologies thus allowing monitoring animals in their habitat. Also [5] proposed a monitoring system based on WSNs and off-the-shelf devices for gathering wildlife information, which may be of large interest for scientists like disease control and sustainable ecological development. Particular attention may also be given to the radio frequency used for communication and in this view [38] presents a communication study defining the more useful radio frequency considering the testing scenario used by authors. In addition, the need of insight into animal habitat, for monitoring animal state and behaviour, is very important mainly for biologists, but considering that many species are widespread over large areas the direct monitoring may be quite difficult [4]. [39] proposes a monitoring system based on light-weight collars able to communicate among them collecting useful information and trying overcoming the problem related to the actual network nodes position, which, due to continuous and random animals movements, do not allow exploiting fixed network infrastructures.

As already described, a possible solution for wildlife monitoring is based on the use of video camera. In particular [2] designs an integrated video system for deer monitoring. Additional sensors are also used like GPS technology and the

system objective is mainly focused on the understanding and analysis of animals behaviour.

Another important issue regards the detection algorithms implemented generally on board of WSN devices, as described in [40, 41], where the sensor nodes are considered not only as sensing devices but also including processing capabilities useful for detection making.

[42, 43, 44, 45, 46, 47, 48, 49, 50], instead, are mainly focused on designing energy-efficient routing protocols, given the limited resources of the system devices batteries, which may not easily accessed for long periods of time. Similar, [51] proposes a novel dissemination protocol, called Seal-2-Seal, for data gathering through sparse nodes, which are intermittently connected to the network, allowing the deployment of larger number of sensor nodes rather than done before.

An approach to wildlife crossings is presented in [52], where the problem of elephants rail track crossing is addressed. In particular, the use of sensing and infrasonic actuator nodes should deter animals by crossing the rail track.

Let us now focus on the road infrastructures for preventing wildlife-vehicle collisions. Common solutions are represented by fencing and crossing structures used to limit wildlife access to roads. The combined use of such structures leads directing animals towards under- or over- passes, which allow the safe coexistence of wildlife, vehicles and roads. The main problem with this kind of solutions is represented by the huge costs required for their realization, which brings Public Administrations to apply such technology only for specific cases or whenever nature may give aid to the actual creation (i.e., particular geological shape). Fig. 2.4 shows some examples of the mentioned road infrastructures widely used in order to limit wildlife crossing roads.

Alternative to fencing and crossing structures is represented by reflective devices mounted on road delimiters specifically designed to re-direct car lights towards external road areas, thus alerting animals and diverting them to approach that zone. These devices are widely used nowadays, given the quite reduced cost, the low maintenance level and the easy of installation.

In addition, road stretches equipped with these devices are in general combined with the installation of specific road signs, raffigurating an ungulate, which may be printed or composed by led-lights, thus allowing the actual sign in presence of moving vehicles. Nevertheless, the static and repeated presence of such road-signs lead drivers to decrease their attention level along the affected roads, because of the habit-phenomenon.

2.2. STATE OF THE ART SOLUTIONS

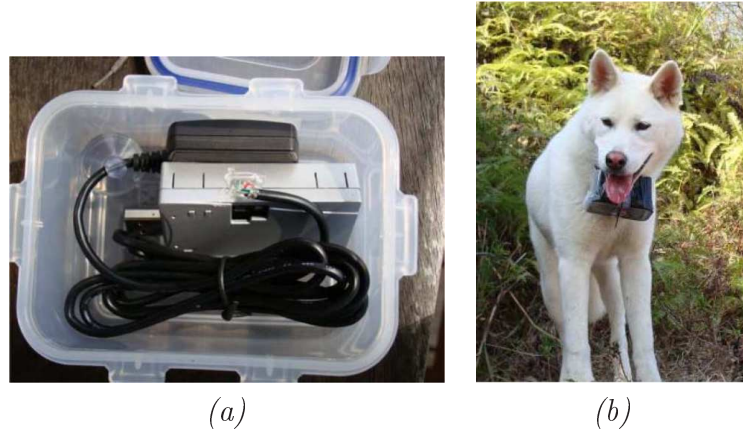


Figure 2.3: Example of active wildlife monitoring system [5]: (a) device, (b) animal wearing the device.

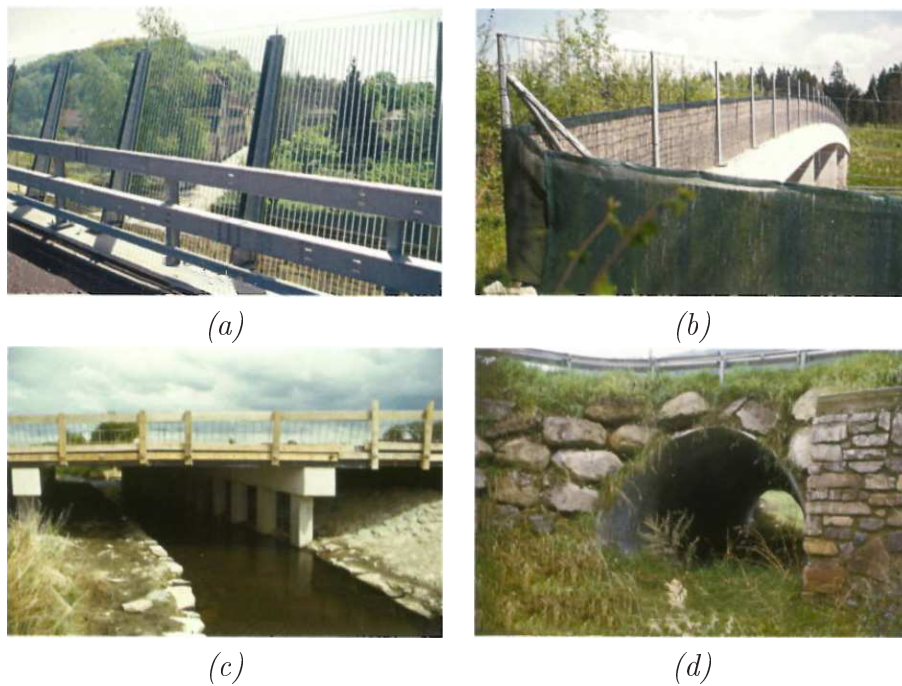


Figure 2.4: Typical road infrastructures: (a) fence applied to road overpass, (b) wildlife eco-pass over road, (c) wildlife underpass near flood, (d) wildlife underpass in rural area.

Chapter 3

Proposed Solution, Prototype and Validation

This chapter is devoted to the description of the proposed solution to the wildlife road crossing problem. In particular, the system architecture is presented together with the technology scouting process carried out in order to define which technologies should be used for the system integration. In addition, validation test are reported, thus evaluating the system working in real scenarios.

3.1 Proposed Solution: System Architecture

Starting from the considerations explained in the previous chapter, the proposed solution to the wildlife-road crossing problem is based on the use of low-cost and compact devices, to be installed on the road sides, with specific sensing capabilities, thus to allow monitoring the road proximity for detecting presence and movement of animals approaching, staying or leaving the road.

In particular, the system main objective regards the capability to alert drivers only when the actual risk is present, thus avoiding the habit effect in looking at static road signs, improving the risk awareness and inspiring virtuous behaviour. All these key aspects should contribute in reducing the actual number of incidents due to wildlife road crossing. Therefore the meaning of actual risk may be defined. To this end, Fig. 3.1 shows a graphical scheme of the system working. The yellow dots represent the sensing devices installed at the road edge and the so-called detection area is defined in relation to the sensors field-of-view integrated on such devices. More specifically, three main areas should be identified, distinguished on the basis of the risk level for drivers given the presence/movement of a wildlife in one of those areas. The danger is therefore classified on the basis of the target position and trajectory, thus diversified warnings may be generated.

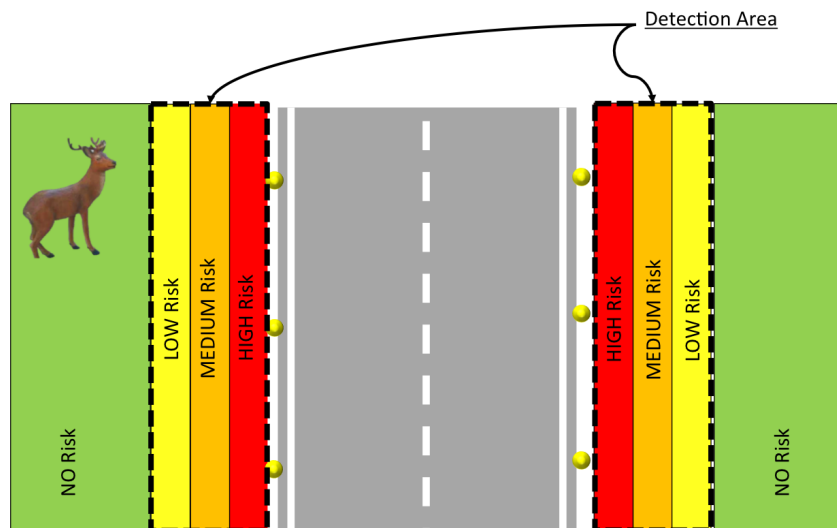


Figure 3.1: Wildlife road crossing monitoring system: risk definition scheme.

In detail, a wireless sensor network (WSN) infrastructure is exploited, taking

advantage of the several features this technology carries [53, 54, 55, 56, 57, 58]. Each single WSN node is capable to communicate with the other devices in the network, thus allowing distributed, pervasive and cooperative sensing and actuating tasks. Several studies have been conducted in order to properly manage the network possibilities, considering also the reduced computational capabilities of the network nodes microcontrollers[59, 60, 61, 62, 63]. These devices are equipped with specific sensors useful for effectively detecting presence and movements of animals in the road proximity. Thus the real-time sensing feature allows the network sharing the information and triggering the actuation devices if needed, on the base of the movement typology, which has been sensed. In fact, once the sensed information is processed and interpreted as crossing-event, the actuators of the WSN platform activate the warning alarm for in transit drivers. In addition, the collected information is also transmitted to a remote control unit for successive data analysis and statistics.

Therefore, it should appear clear that no habit-effect should be generated by such a system, given that actuators and road signs alarm drivers only in the actual case of risky conditions, namely wildlife approaching the road or staying in the road stretch proximity.

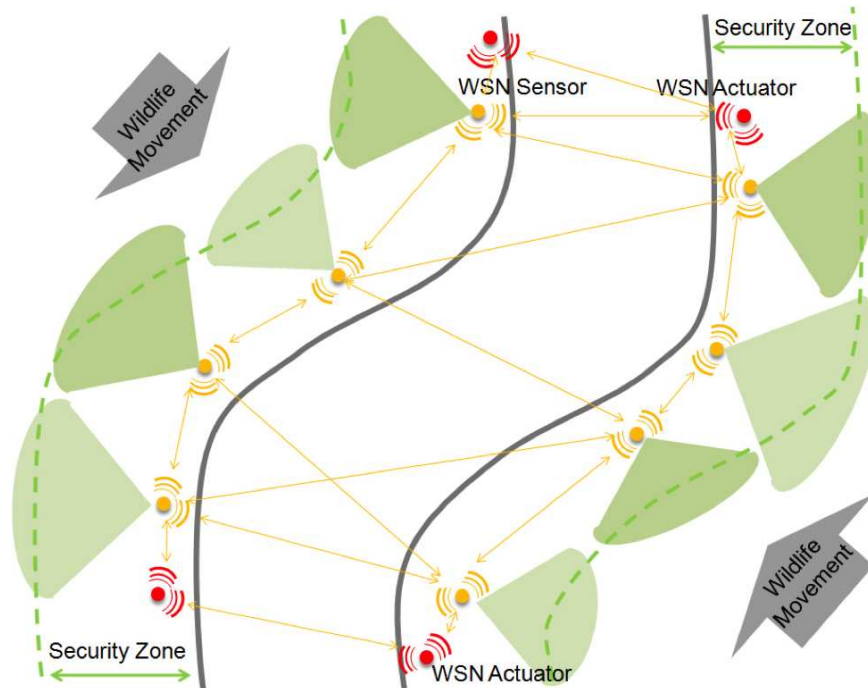


Figure 3.2: WSN system architecture: sensor and actuator devices for the detection of wildlife movement along road stretches and prompt alert.

3.1. PROPOSED SOLUTION: SYSTEM ARCHITECTURE

Fig. 3.2 shows a simple sketch raffigurating an example of the WSN system architecture, composed mainly by two node typologies, namely:

- Sensor node, in charge of sensing the nearby environment by using the specific sensors with which it is equipped and performing first step data processing;
- Actuator node, in charge of activating actuation device for warning drivers of the risky condition sensed by the sensor nodes.

Besides this first node classification, two additional node typologies may be considered, namely:

- Anchor node, devoted to wireless network management via multihop architecture for coverage extension along road sides;
- Gateway node, dedicated to data collection and forwarding to the control unit.

With reference to Fig. 3.2, let us consider to compose the WSN of N nodes installed in known positions in the road proximity, such as (x_n, y_n) , $n = 1, \dots, N$. Together with a precise analysis of sensor field-of-view, sensor nodes position (x_n, y_n) should be strategically defined to enable good detection of moving targets, while being as less invasive as possible with respect to the real installation scenario. As Fig. 3.2 clearly shows, the sensor nodes define the so-called security zone, whose size is determined by the sensors coverage capability installed on each single device. The security zone, therefore, defines the area in the road proximity within which the presence and possible movement of animals is detected, giving raise to the complete monitoring and actuating process (i.e., sensing, processing, actuation).

The WSN network typology may be customized in relation to the particular scenario in which the system may be installed, thus exploiting the actual node position in the real scenario to extend network capabilities. In general, the WSN nodes may be interconnected via multihop wireless links, thus increasing the network coverage and its robustness.

In addition, each single device, being a sensor-, an actuator- or an anchor-node, has to be properly designed in order to minimize the overall dimensions, thus simplifying installation and camouflage processes, the energy consumption, thus limiting the maintenance intervention and extending at the same time the device lifetime. Therefore, each node is equipped with solar panels for energy management and lifetime optimization, together with an efficient control firmware, which allows limiting power losses due e.g. to non synchronized wireless transmissions.

The data collected by the gateway node are sent to the control unit for on-line storage and processing. In particular, the system generates different data categories:

- Diagnostic data: the data sent periodically by each sensor node, such as battery and solar panel voltages, internal temperature and humidity, wireless link quality. These information allows monitoring the status of the system and detecting potential malfunctioning to promptly intervene with proper maintenance process.
- Detection event: when sensors detect animals presence or movements in the security zone, the respective sensor node immediately sends the event data to the gateway node with the time, position and direction information of the event. The gateway node forwards the event to the control unit, in charge of processing the information and evaluating the optimal feedback according to the adopted strategy.
- Signalling event: in case a real event has been detected and the related data have been processed by the control unit, a signalling message is sent to the actuator nodes closest to the area in which the event has been detected in order to activate the signalling devices installed on the road sides.

3.2 Technology Scouting

First step in the design process of the proposed monitoring system regards the definition of the specific technologies to be integrated in the sensor node devices, thus enabling the sensing capability of the system.

In particular, in order to design low-cost devices, as defined in the proposed solution scheme in the previous section, it is necessary to identify off-the-shelf solutions, which may be adopted to achieve the system objective. Therefore, the main technologies identified as valuable ones are presented, together with advantages and disadvantages proper of the considered technology or deduced if applied to the proposed system.

3.2.1 Radar Technology

The radar technology (RAdar Detection And Ranging) is widely known and used nowadays as one of the major systems for target localization applied to several applications. This system is based on the electromagnetic propagation of radio waves. In particular, the transmitting antenna sends a radio or microwave pulse, a small portion of which, once it impinges on the target, is reflected towards the receiving antenna, usually co-positioned with the transmitting one.

A radar sensor allows determining several parameters useful for the object detection, either moving either static. Some of these parameters are: distance, altitude, direction and speed of the movement.

Nevertheless, not all the radar sensors are able to supply such parameters. In particular, some sensors are only able to detect movements and accelerations along orthogonal directions to the sensor plane or with non-null angle between the movement direction and the tangential direction to the sensor plane. Therefore, by using such sensors, it is not possible to detect the presence of static targets or movements perfectly directed along the tangential direction to the sensor plane.

Some advantages of the radar technology if applied to the sensor device are:

- the use of radio waves, which allows locating targets even at large distances, given the reduced attenuation phenomena through the propagation media or for atmospheric agents;
- large field of view;
- availability of low-cost solutions.

One major disadvantage of this technology regards the sensors based on continuous wave with no frequency modulation, since these devices do not allow evaluating the target distance and therefore neither the presence of static objects in the sensor field of view.

3.2.2 Ultrasound Technology

The ultrasound sensors are based on a functional principle similar to the one used by radar technology. In fact, the reflected section of the transmitted wave is gathered by the sensors and properly processed in order to determine target characteristics. These sensors generate sound waves at high frequency and computing the time between transmission and the reception of the echo the distance of the target in the sensor field of view can be computed. This technology is widely used in medical and industrial fields, for instance in sonogram or in non-invasive control systems.

Among the advantages of such technology let us consider the following ones, useful for the investigated problem:

- it allows computing the distance of the target, without any specific wave modulation as instead in the radar technology case;
- enables the detection of still targets;
- availability of low-cost solutions.

Major disadvantages of such technology are the reduced field of view and the physical characteristics that the target should have in order to be properly detected by the sensor. In particular, material density and composition affect the reading capability of the ultrasound sensor, by varying the portion of reflected wave towards the sensor itself, thus in turn leading to more ambiguous readings.

3.2.3 Infrared Technology

Infrared sensors are particular devices able to measure the radiation emitted in the infrared spectrum by any target in the field of view of the sensor. This technology is largely used for the detection of humans and targets able to radiate in the infrared spectrum. The detection is based on the variation of infrared radiation registered in the field of view of the sensor, thus even a target with temperature equal to the environmental one and moving in front of the sensor can be detected since it generates a field change, which is detected by the infrared sensor.

Advantages of such technology are:

- passive detection of targets, which implies reduced energy consumption;
- medium size field of view, with in general wide aperture angle;
- availability of low-cost solutions.

The main disadvantage regards the huge attenuation this technology suffers due to atmospheric agents, which perturbates the scenario thus decreasing the detection capability of the sensor.

3.2.4 Thermal Technology

Thermal sensors measure the temperature of anything in the sensor field of view, being an actual target or the surrounding environment. In particular, this technology exploits thermal emission of any object and specifically considering medium infrared radiation (i.e., thermal infrared).

This technology, similarly to the infrared technology, allows the passive detection of targets, also considering low-cost solutions available off-the-shelf. Nevertheless, this technology is strongly affected by atmospheric agents and the off-the-shelf solutions show in general a reduced size field of view. Improved performance may be obtained with specific thermal sensors, whose cost increases prominently.

3.3 Off-The-Shelf Sensor Selection

In the following, the available off-the-shelf sensors per each of the presented technologies are reported, with some specification, which allow determining the possibility of integrating such devices in the sensor node for the development of the monitoring system. Additional information may be retrieved in the sensor datasheets.

It is worth noting that the robustness parameter is defined on the basis of the actual physical robustness of the considered sensor, together with additional features it may present (e.g., waterproof). Therefore three main values are given, namely low, medium and high robustness.

Model	Cost	Power Consumption	Field-of-View	Robustness	Output Signal	Dimensions [mm]
RSM-1650	\$19.65	5V, 30-40mA	15-20m, 80°/32° (H/V)	medium	analog	25x25x12.7
RSM-1700	\$19.65	5v, 30-40mA	15-20m, 70°/70° (H/V)	medium	analog	25x25x12.7
R-GAGE QT50R	\$530.00	12-30V, 100mA	12m, 15°/15° (H/V)	high	digital	74.1x46.1x66

Table 3.1: Radar technology: available off-the-shelf products.

Model	Cost	Power Consumption	Field-of-View	Robustness	Output Signal	Dimensions [mm]
UB6000-30GM-E2-V15	\$175.00	20-20V, 200mA	6m, 20°	medium	digital PNP	73x73x112
MIC+600/D/TC	\$445.00	9-30V, 80mA	6m, 10°	high	digital PNP	65x65x105
SRF485WPR	\$30.63	8-14V, 10mA	0.6-5m, 30°	high	RS-485 protocol	40.5x40.5x20
SRF10	\$31.80	5V, 15mA	0.06-6m, 72°	medium	I2C protocol	32x15x10
SRF02	\$10.60	5V, 4mA	0.16-6m, 55°	medium	I2C and serial protocols	24x20x15
SRF01	\$21.20	3.3-12V, 25mA	0-6m	medium	serial protocol	25x25x20

Table 3.2: Ultrasound technology: available off-the-shelf products.

Model	Cost	Power Consumption	Field-of-View	Robustness	Output Signal	Dimensions [mm]
IRA-E700ST0	\$3.30	2-15V, -	12m, 45°	medium	analog	9.1x9.1x4.7
LHI 878	\$3.60	2-15V, -	- , 95°	medium	analog	9.1x9.1x4.2
EW-AMN34111	\$38.52	3-6V, 170-300uA	10m, 110°	medium	digital	17.4x17.4x18.5
GP2Y0A02YK0F	\$29.50	4.5-5.5V, 33mA	0.2-1.5m, -	high	analog	18.9x13.5x44.5
GP2Y0A710K0F	\$23.40	4.5-5.5V, 30mA	1-5.5m, -	high	analog	58x17.6x22.5
GP2Y3A003K0F	\$61.93	4.5-5.5V, 30mA	0.4-3m, -	high	analog	68x20x18
PIR SMD 3-5V/80UA	\$27.06	3-5V, 40uA	12m, 120°	medium	analog and digital	25x25x20
PIR SMD 3-12V/2MA	\$17.07	3-12V, 2mA	12m, 120°	medium	analog and digital	25x25x20

Table 3.3: Infrared technology: available off-the-shelf products.

3.3. OFF-THE-SHELF SENSOR SELECTION

Model	Cost	Power Consumption	Field-of-View	Robustness	Output Signal	Dimensions [mm]
TPA81	\$59.19	5V, 5mA	4-100°C, 8 pixels 5°x6°	medium	I2C protocol	31x18x10
ZTP-135S	\$16.29	5V, 3.9mA	-20-100°C, -	low	analog	5.4x5.4x5
D203S	\$0.98	3-15V, -	-30-70°C, 130°	low	analog	10x10x5
TMP006	\$7.18	2.2-5.5V, 240uA	-40-125°C, 60°	low	digital	1.6x1.6x2

Table 3.4: Thermal technology: available off-the-shelf products.

On the basis of the available off-the-shelf solutions and considering the known specifications for each of the devices, the sensor selection can be performed and the outcome is reported in the following section considering each technology separately.

3.4 Sensor Preliminary Setup and Testing

3.4.1 Radar Sensor RSM-1650

3.4.1.1 Setup

Multipurpose radar sensor, especially suitable for movement detection applications in compact and low power systems. This sensor is composed by separated transmitting and receiving antennas for better sensitivity.

Technical parameters:

- reduced cost: \$19.65
- voltage source: 4.75-5.25V
- current drain: 30-40mA
- field-of-view: 15-20m
- aperture angle (H/V): 80°/32°
- signal frequency band: 6-600Hz
- operating frequency: 24.0-24.5GHz
- signal type: continuous wave without frequency modulation
- emitted power: 16dBm
- operating temperature: [-20,60]°C
- output signal: frequency modulated signal, modulation based on the object speed and amplitude proportional to dimensions and distance of the target to the sensor
- dimensions (LxWxH): 25x25x12.7mm

In order to perform a preliminary experimental validation of the radar sensor RSM-1650, a dedicated interface board has been developed, thus allowing the measure of controlled desired movements.

The radar sensor RSM-1650 is equipped with three connection pins, devoted to 1) power supply, 2) analog output, 3) ground connection respectively (Fig. 3.3).

3.4. SENSOR PRELIMINARY SETUP AND TESTING

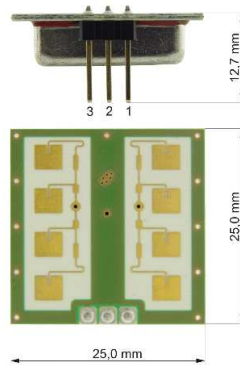


Figure 3.3: Radar sensor RSM-1650: dimensions and connection pins.

The output signal frequency is proportional to the object/target speed detected in the field-of-view of the sensor. For instance, a moving target with 1Km/h speed determines an output signal with frequency equal to 44Hz, given the transmitted signal frequency to 24.125GHz.

Distance and dimension of targets in the field-of-view of the sensor directly influence on the output signal amplitude, which shows a very reduced dynamic, namely at most 300uVolt, particularly considering that this signal may be read by microcontrollers with reduced performance and computational capacity, like WSN sensor nodes, that in general exhibit low resolution ADC converter (i.e., 10bit or 12 bit resolution with voltage reference equal to the supply voltage).

Therefore, the signal output of the radar sensor can not be directly acquired/analyzed by such devices, thus an amplification stage is required.

In addition, considering the wildlife road-crossing problem, particular interest is focused on a sub-set of sensor output signal frequencies, in relation to the actual speed of the associated movement. Therefore, the output signal frequency range 154Hz-3.39KHz is filtered, thus allowing the detection and the analysis of movements in the reading field of the sensor with speed approximately ranging between 3.5Km/h and 77Km/h. This processing allows considering neither too slow movements neither too fast ones, which unlikely may belong to actual animal movements.

To this end, a specific filtering stage has been designed. This processing stage is mainly composed by two filter typologies, namely a 2nd order Butterworth high pass filter with about 3dB gain and a 2nd order Butterworth low pass filter with about 3dB gain. In particular, the filtering sequence is composed by one low pass stage followed by two high pass filters, thus enhancing the filter of low speed components. Fig. 3.4 and Fig. 3.5 show the circuitual schemes of the filters respectively.

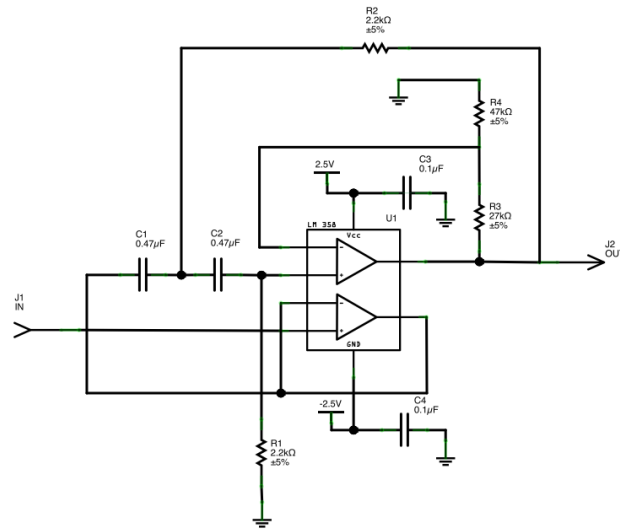


Figure 3.4: High pass filter: cut frequency 154Hz.

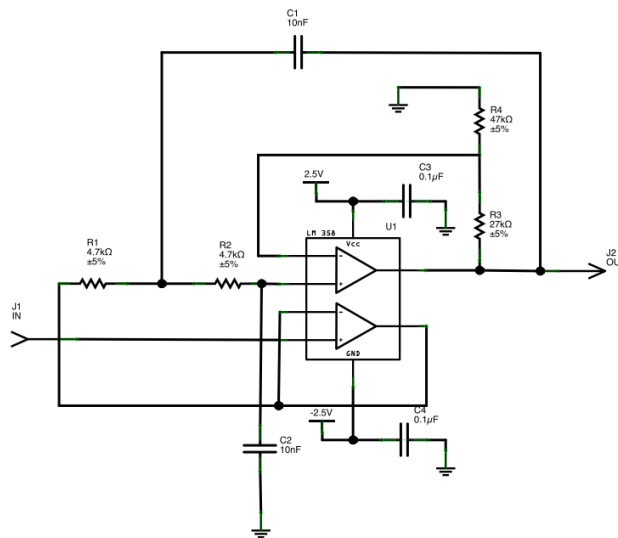


Figure 3.5: Low pass filter: cut frequency 3.39KHz.

The designed interface board integrates in the order an amplification stage, with amplification factor equal to 100, the high pass filter and two low pass filters, as described above, a double semi-wave rectifier (Fig. 3.6), thus to consider all the signal energy (i.e., not only the positive semi-wave energy), a Schmidt trigger

3.4. SENSOR PRELIMINARY SETUP AND TESTING

with hysteresis and tunable threshold (Fig. 3.7). A led is connected to the trigger, thus its blink allows determining the actual detection of movements.

Fig. 3.8 shows the interface board prototype implementation.

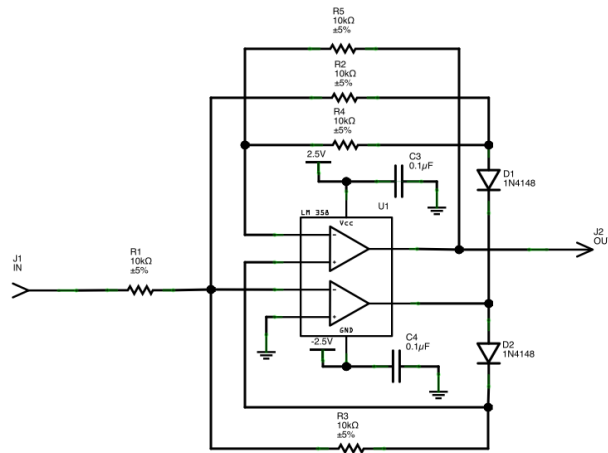


Figure 3.6: Double semi-wave rectifier.

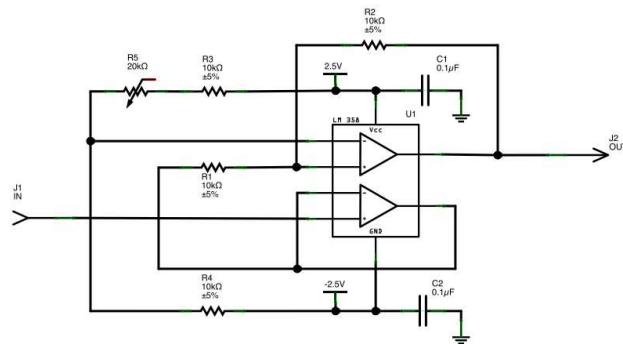


Figure 3.7: Schmitt trigger with hysteresis and tunable threshold.

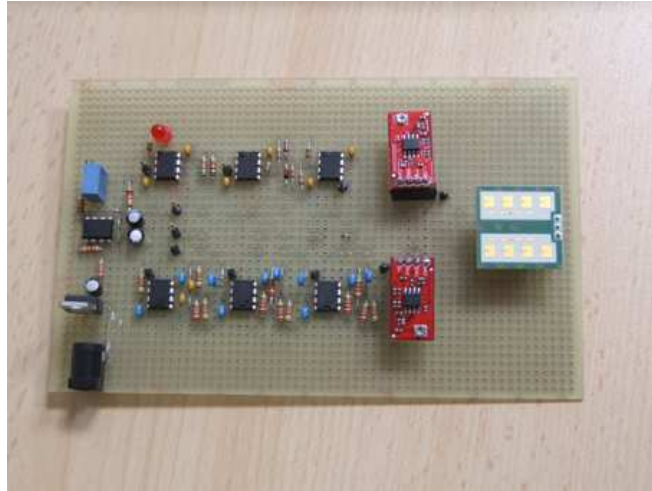


Figure 3.8: Radar sensor interface board: processing of output signal.

The radar module output signal, if processed with the designed interface board, may be acquired and analyzed also by WSN devices by using digital or analog connections, thus allowing the easy integration of the sensor with the WSN sensor node. Finally, particular attention have to be addressed to the sensor supply requirements (i.e., voltage supply), since in general this parameter differs from the WSN device voltage supply. Therefore proper voltage conversion should be applied and the sensor current drain (i.e., 30-40mA) should be taken into account in order to optimize the lifetime of the integrated device. Supply managing procedures may be considered in order to activate the radar sensor only during specific time periods, thus decreasing the overall power consumption, as a trade-off between data collection rate and detection capability.

3.4.1.2 Testing

In order to perform the validation tests, it is necessary to setup the experimental scenario thus to properly supply the interface board and the radar sensor and to correctly acquire the sensor signal output.

Therefore a stable power supply and an oscilloscope are used during the first setup in order to verify the correct functioning of each single component of the interface board and the sensor (Fig. 3.9).

3.4. SENSOR PRELIMINARY SETUP AND TESTING

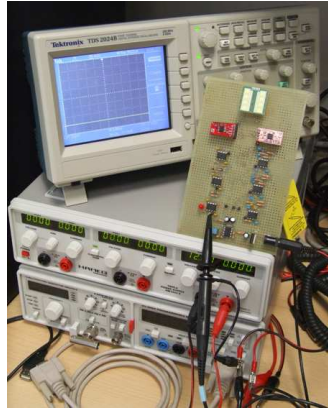


Figure 3.9: Radar sensor testing setup.

During a second step, the power supply is substituted by a lead battery and the movement detection is committed to the led on the interface board, thus major mobility is allowed to the equipment (Fig. 3.10).

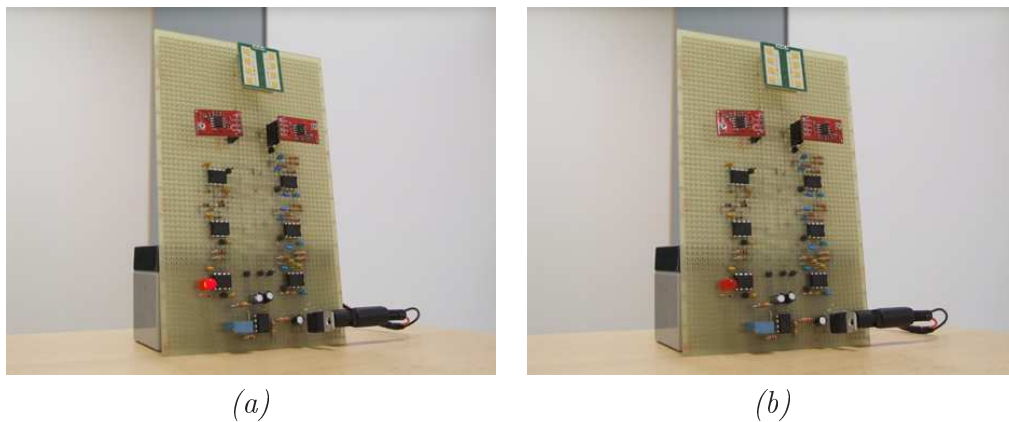


Figure 3.10: Radar sensor testing setup: (a) active LED for movement detection, (b) LED off for no movement detection.

By exploiting the first setup described above, all the equipment is continuously active and supplied, thus the actual radar sensor working can be monitored real-time throughout all the test duration. For the first test, the experimental scenario considers a target moving in the area with constant speed equal to 1Km/h. As it can be notice in Fig. 3.11, the signal output of the sensor exhibits a frequency equal to 44Hz, as expected.

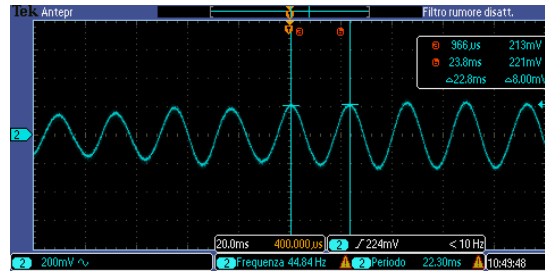


Figure 3.11: Radar sensor testing: target with constant speed 1Km/h.

Similarly to the previous test, now the target moves in the sensor field-of-view with low speed, approximately 3.5Km/h, which increases during the test up to 5Km/h. Fig. 3.12 shows the signal captured by the oscilloscope connected to the radar sensor output. The captured snapshot allows inferring the actual target speed detected by the sensor, which is about 4Km/h given the signal frequency equal to 160Hz.

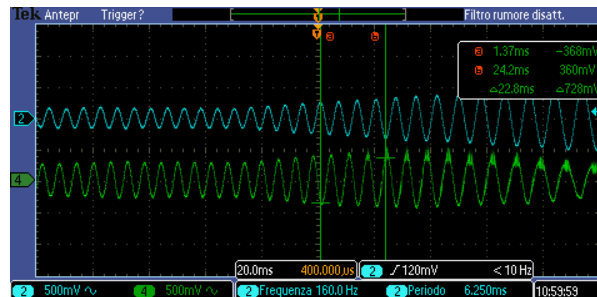


Figure 3.12: Radar sensor testing: target with speed in the range 3.5-5Km/h.

Next test regards the validation of the correct identification of leaving movements with respect to the sensor plane. Therefore the target moves away with constant speed from the radar sensor and the expected output signal behaviour is confirmed by the oscilloscope acquisition (Fig. 3.13): the signal amplitude decreases as the target is farther from the sensor, while the signal frequency is quite constant.

3.4. SENSOR PRELIMINARY SETUP AND TESTING

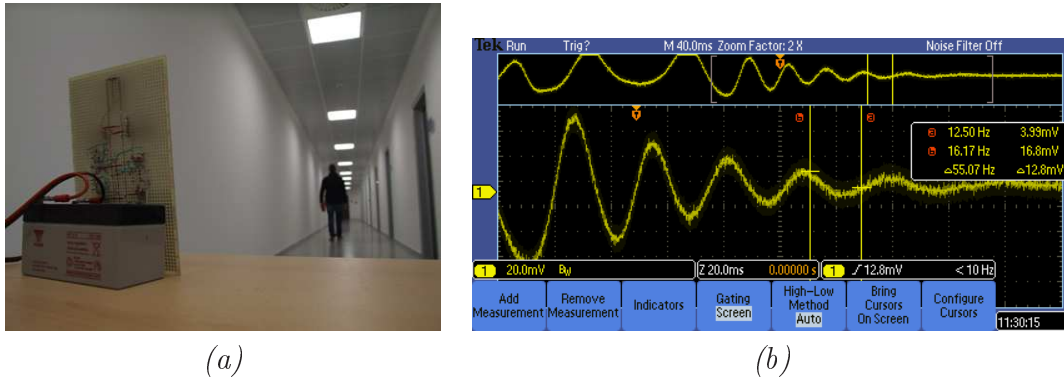


Figure 3.13: Radar sensor testing - target moves away from the sensor plane with constant speed: (a) experimental scenario, (b) radar output signal.

Contrary to the previous test, now the target approaches the sensor plane with constant speed. Therefore, similarly to the previous case, the radar output signal shows an amplitude increase throughout the test, as shown in Fig. 3.14.

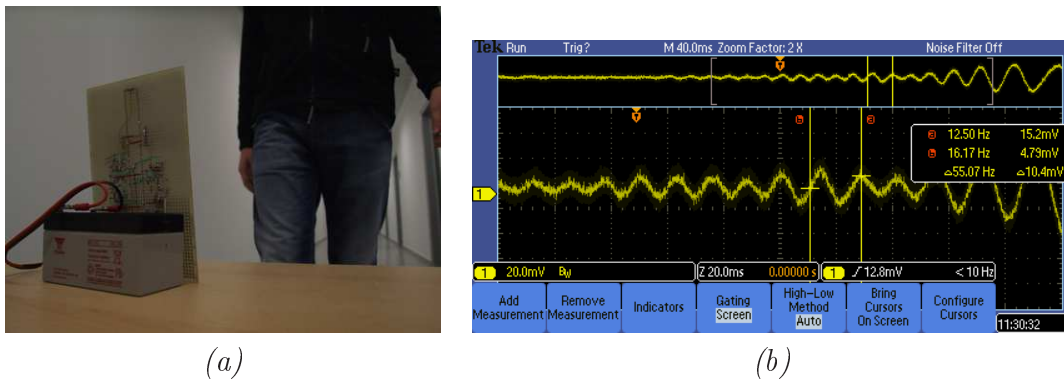


Figure 3.14: Radar sensor testing - target moves towards the sensor plane with constant speed: (a) experimental scenario, (b) radar output signal.

In addition, a test with static target has been performed, in order to validate the actual sensitivity of the sensor to this kind of scenarios. As expected the sensor do not detect this movement typology and the radar output signal appears a quite stable signal at the reference/quite value with some superimposed noise (Fig. 3.15).

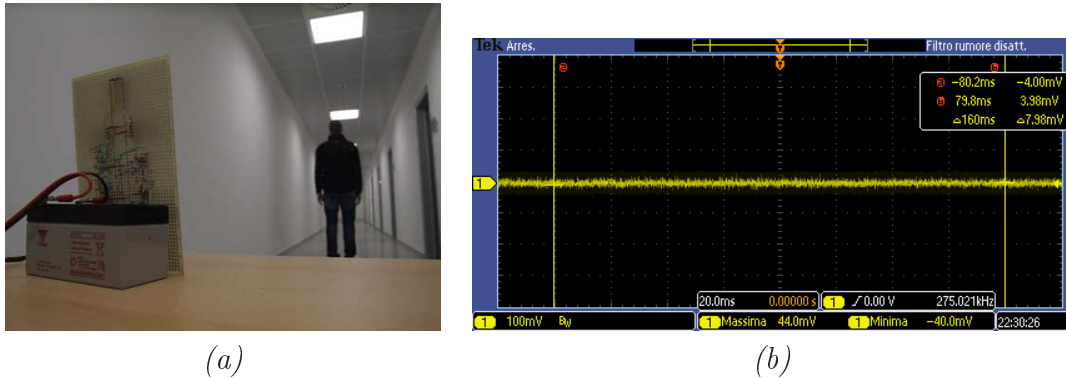


Figure 3.15: Radar sensor testing - target is still in front of the radar sensor: (a) experimental scenario, (b) radar output signal.

Finally the maximum and minimum detection distances have been validated, obtaining that the radar sensor RSM-1650 is capable to identify target movements from zero distance to the sensor plane up to about 15-20m distance from the sensor plane. Thus the sensor specifications are confirmed and its actual functioning, together with the one of the interface board, has been validated in order to integrate such sensor in the WSN sensor node.

3.4.2 Ultrasound Sensor SRF485WPR

3.4.2.1 Setup

The identified sensor, model SRF485WPR, is a waterproof sonar sensor, suitable for many outdoor applications. The sensor communication is based on RS-485 serial protocol and the total power consumption is quite reduced.

Technical parameters:

- cost: \$30.63
- voltage source: 8-14V
- current drain: 10mA
- measuring range: 0.6-5m
- aperture angle: 30°
- operating temperature: [-30,50]°C
- output signal: RS-485 protocol
- dimensions (LxWxH): 40.5x40.5x20mm

3.4. SENSOR PRELIMINARY SETUP AND TESTING

The ultrasound sensor is equipped with a 10 pin connector (Fig. 3.16(a)), divided in three groups, namely the positive voltage source, the negative voltage source and the RS-485 protocol connections (Fig. 3.16(b)). In particular the positive voltage connections (4 pins) are short-circuited and similar applied to the negative voltage pins.

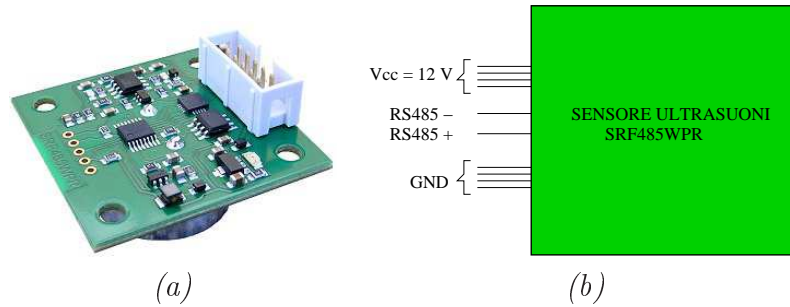


Figure 3.16: Ultrasound sensor testing setup: (a) sensor view, (b) sensor connection scheme.

As described above, the communication with the sensor is driven by the RS-485 protocol (Fig. 3.17), either for the command send to the sensor, either for the measure retrieval. This protocol is based on the voltage differential value based on voltages applied to the two protocol connections and in addition, in order to consider the communication transition as correct, the differential voltage value has to be at least 0.2Volts.

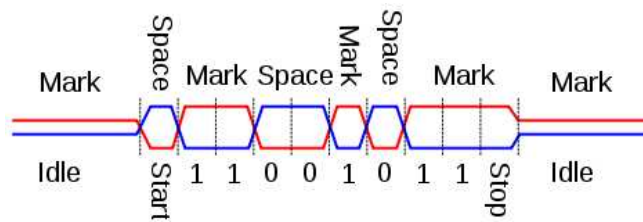


Figure 3.17: RS-485 protocol: transmission example.

In order to properly communicate with the ultrasound sensor, it has been necessary to convert the data transmitted and received by the sensor thus being RS-485 protocol compliant and at the same time allowing the data transfer with a PC via an USB serial communication. Therefore a module converter has been

adopted (Fig. 3.18) for this validation phase and thus a simple Matlab code has been used to communicate with the sensor.



Figure 3.18: Ultrasound sensor testing setup: USB-RS485 converter and SRF485WPR sensor.

The ultrasound sensor allow the measured data to be set in centimeters or inches and in addition, for both the measuring units, two working modalities are available, namely continuous reading or on demand reading.

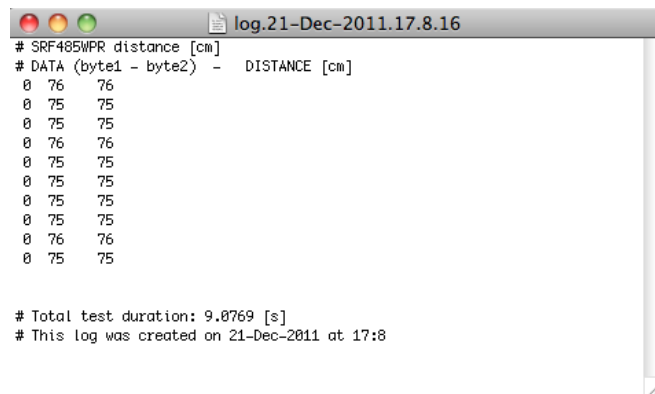
During this validation process, the continuous reading mode in centimeters has been chosen, thus allowing the real-time estimation of the sensor behaviour in the experimental scenario throughout all the test duration. Thus, in order to set this working modality the controller (i.e., PC) has to send a *break* command on the serial port to the ultrasound sensor, which consists of keeping the RS-485 connection to the low logic value per a preset period of time. This procedure allows the sensor synchronizing with the controller and interpreting in the correct way the commands that follows this first instruction. In particular, the send commands present the following structure:

break | *command* | *register* | *address (three 1byte fields)* | *data* | *checksum*

Considering the specific case of the command used during this experimental test, the command string is composed as follows:

$(0x54 \mid 0x00 \mid 0x35 \mid 0x20 \mid 0x00 \mid 0xA9)_{HEX} = (84 \mid 0 \mid 48 \mid 37 \mid 0 \mid 86)_{DEC}$

The ultrasound sensor requires about 70msec to get the measure data. Once the meaures has been get the sensor automatically sends the proper communication to the controller, which is composed by two bytes in RS-485 protocol. The



```
# SRF485WPR distance [cm]
# DATA (byte1 - byte2) - DISTANCE [cm]
0 76 76
0 75 75
0 75 75
0 76 76
0 75 75
0 75 75
0 75 75
0 75 75
0 76 76
0 75 75

# Total test duration: 9.0769 [s]
# This log was created on 21-Dec-2011 at 17:8
```

Figure 3.20: Ultrasound sensor testing: log file with the measured data.

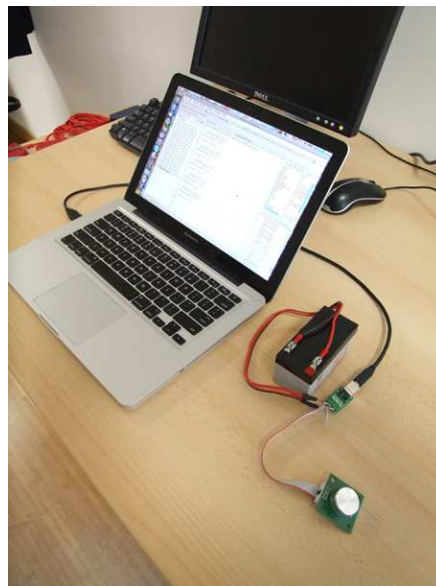


Figure 3.21: Ultrasound sensor validation setup.

Given the proper working of the testing setup (Fig. 3.21), the maximum distance measured by the sensor is validated. To this end, the sensor is installed on a support at 0.80m from the ground (Fig. 3.22) and a target moves in the sensor field-of-view from the sensor plane till the sensor is no more able to detect its correct distance.



Figure 3.22: Ultrasound sensor testing setup.

In indoor environments the sensor suffers of false positive phenomena due to multiple reflections of the sound wave on the objects present in the experimental scenario. Nevertheless, the maximum distance of 4m has been validated, against the specification of about 5m.

Analogous test has been carried out in order to determine the minimum distance measurable by the ultrasound sensor. The producer declares a minimum distance of about 0.6m, thus the target starts moving in the sensor field-of-view at the distance of 1m, approaching slowly the sensor plane. The real-time acquisition is analyzed in order to check the actual minimum distance measured by the sensor, thus the distance of 0.6-0.7m is confirmed to be the minimum detectable by the identified ultrasound sensor.

The successive test is focused on the simulation of more realistic events, thus composed by differentiated movements like leaving, staying and approaching the sensor plane. Therefore, the test starts with an empty experimental scenario, then the target moves in the sensor field-of-view leaving the sensor plane till the maximum distance, then the target comes back (Fig. 3.23(a)) till 1.60m from the sensor plane (Fig. 3.23(b)), where the target stops simulating small movements and variations, which may be compared to real environmental changes.



(a)



(b)

Figure 3.23: Ultrasound sensor testing: (a) target approaching the sensor, (b) target in steady position in front of the sensor.

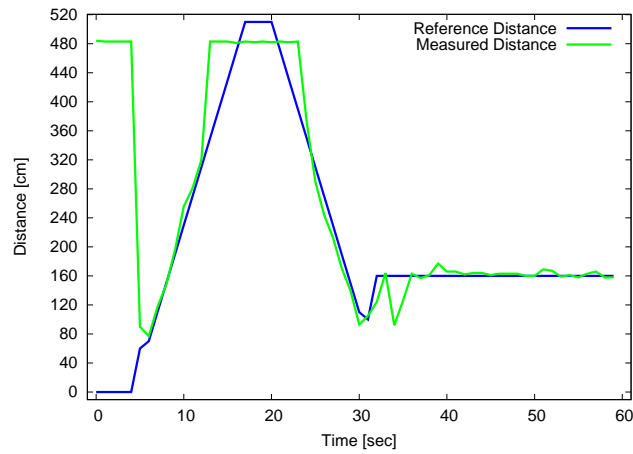


Figure 3.24: Ultrasound sensor testing setup.

Fig. 3.24 shows the experimental result obtained with the above described test. The blue line depicts the reference distance as written above, while the green line refers to the real measurements data obtained by the ultrasound sensor SRF485WPR. During the empty scenario periods the sensor returns the maximum readable distance, this is why in the first samples of the plot in Fig. 3.24 the measured distance is very high and then starts following the actual movement of the target.

The ultrasound sensor properly detects the target starting from the movement is about 0.6m from the sensor plane. The successive measurements follow quite accurately the target movement in the sensor field-of-view up to the distance of 4m. The following moving away at the distance of 5m and higher is not detected and the sensor starts again measuring the actual target distance at about 3.5m from the sensor during the approaching moving. In addition, when the target stops at 1.60m the measurements given by the sensor are quite stable and continuously detect the presence of the target in the sensor field-of-view. The perturbations introduced by the target during the still staying period are not detected by the sensor, even if its accuracy measured in real tests is of about 0.01m.

Therefore it is worth noting that the identified ultrasound sensor allows detecting still and moving targets in the sensor field-of-view, which has a maximum verified dimension of about 4-5m. In addition, reduced target perturbation do not cause relevant changes in the measured data, thus improving the sensor measurement reliability.

3.4.3 Infrared Sensor PIR-SMD

3.4.3.1 Setup

The identified infrared sensor is a compact device, suitable for several application in sensing and automation field, thanks also to the high sensitivity and the availability of double output format, namely analog and digital signals.

Technical parameters:

- reduced cost: \$27.06
- voltage source: 3-5V
- current drain: 400uA
- field-of-view: 12m
- aperture angle (H/V): 120°/60°
- operating temperature: [-20,70]°C
- output signal: analog and digital signal

- dimensions (LxWxH): 25x25x20mm

The infrared sensor connections are located on the bottom side of the sensor, as shown in Fig. 3.25. In particular, the available connections are distributed as follows:

- pin 1: analog output
- pin 2: reference voltage
- pin 3: ground connection
- pin 4: digital output
- pin 5: ground connection
- pin 6: power supply connection
- pin 7: optical resistance
- pin 8: optical resistance

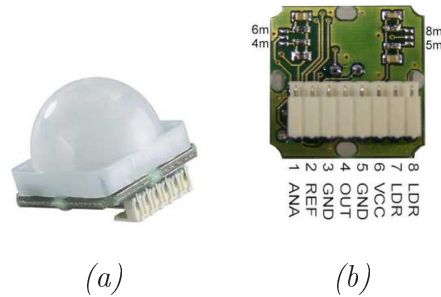


Figure 3.25: Infrared sensor: (a) front view, (b) bottom view.

In order to validate the sensor and its performance, a simple testing setup is prepared. In particular, given the availability of both analog and digital signal outputs, the analog type is chosen thus allowing the continuous analysis of the output signal by using an oscilloscope directly connected to sensor pin 1 connection. Fig. 3.26 shows the experimental setup. The stable power supply is used to power the infrared sensor, thus avoiding possible problems due to noise or instability of the supplying network during the first validation phase. This, in turn, allows concentrating the attention to the actual device working during the experimental tests.



Figure 3.26: Infrared sensor testing setup.

The use of the analog output simplifies the sensor validation, since no particular processing stages are in between the sensor internal circuitry and the acquisition device (i.e., oscilloscope). This feature is very important, since the same acquisition method may be used once integrated in the WSN sensor node, given that the WSN node platforms generally are equipped with ADC connections, to which the analog output of the sensor may be connected. On the contrary, particular attention may be addressed to the power supply level since the WSN devices are powered usually with 3-3.3Volt sources, while the sensor may be fed at 5Volt. Therefore, proper voltage conversion stages (e.g., step-down, step-up) may be considered.

3.4.3.2 Testing

The experimental tests have been performed in indoor controlled environment, in order to not introduce possible noise sources in the monitored area, thus in turn allowing a precise relation between actual movements and sensor detection on the output signal.

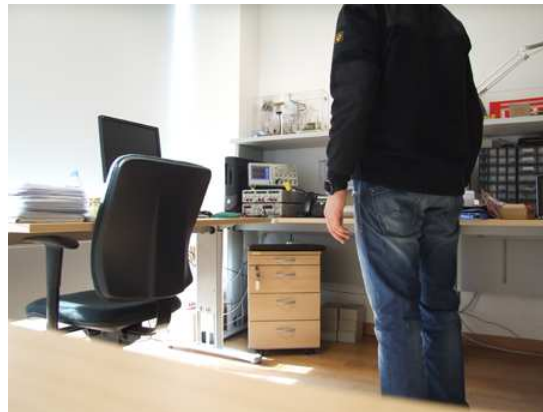
As first step, the proper working of the sensor has been validated, in particular the absence of wake up time, needed by the sensor once supplied in order to be active, has been verified. Therefore it is sufficient to feed the infrared sensor to allow the acquisition process. The steady state of the sensor corresponds to a stable output signal on the $V_{cc}/2$ value, where V_{cc} is the power supplying voltage.

When the target moves in the near field-of-view clear signal variation may be observed with respect to the steady value and, as soon as the target moves away, the output analog signal restores to $V_{cc}/2$ value. In indoor environment, due to scenario limitation, the maximum distance detected by the sensor has been about 7m. Successive tests in outdoor environments will allow determining

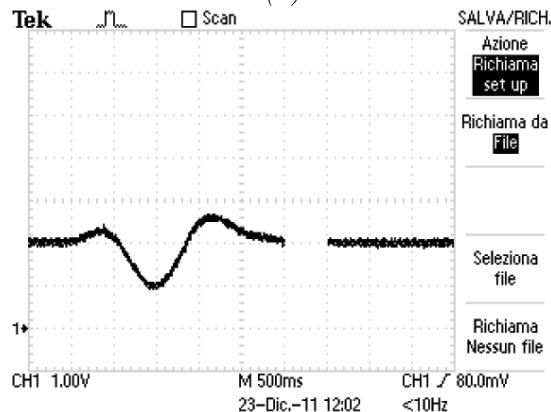
the actual maximum detectable distance.

On the contrary, the minimum dimension of the sensor field-of-view has been verified with a constant speed motion of the target, which approaches the sensor from the starting distance of 1m. The sensor is capable of detecting the target movement till the distance between the target and the sensor is nullified.

Successive tests are devoted to the validation of the actual sensor sensibility to radial movements with respect to the sensor plane. In particular these movements are performed at different distances from the sensor, but always within the known sensor field-of-view dimensions. Fig. 3.27(a) shows the target approaching the sensor from an initial distance of about 3.5m up to 2.1m. The sensor detects the presence of the moving target and the acquired output signal is shown in Fig. 3.27(b), where clearly appears the signal perturbation due to the detected movement.



(a)



(b)

Figure 3.27: Infrared sensor testing: (a) target approaching the sensor, (b) sensor output signal acquired with oscilloscope.

3.4. SENSOR PRELIMINARY SETUP AND TESTING

Similar behaviour is obtained when the target leaves the sensor plane, starting from the end position of the previous test (i.e., 2.1m) till the distance of about 3.5m, as shown in Fig. 3.28.

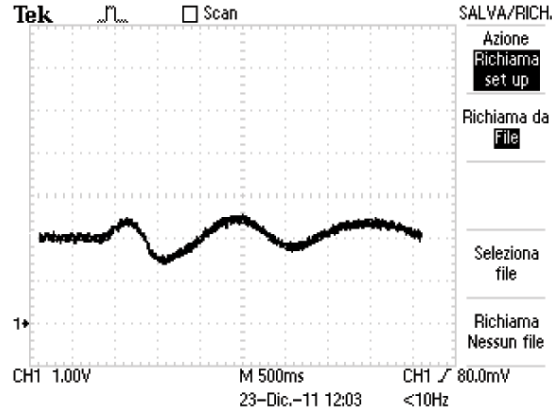


Figure 3.28: Infrared sensor testing: sensor output signal acquired with oscilloscope while target leaves the sensor plane.

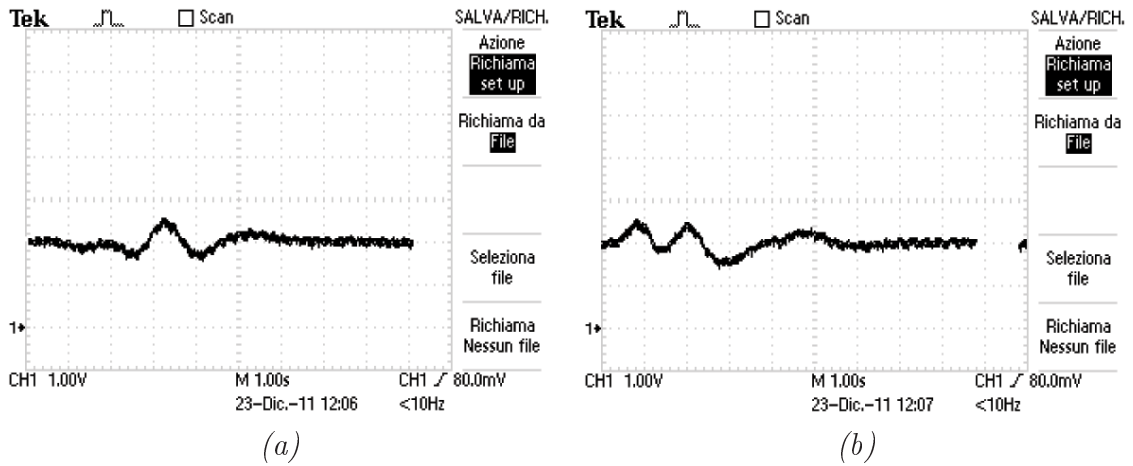
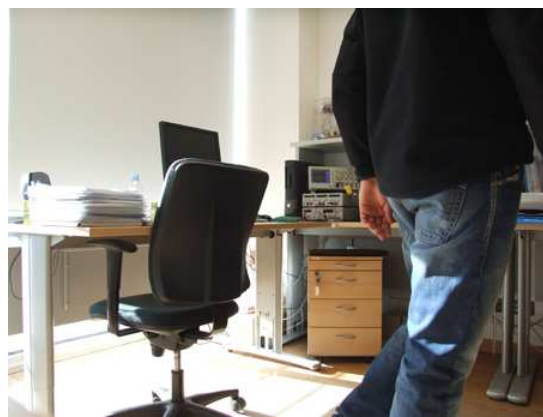


Figure 3.29: Infrared sensor testing: (a) sensor output signal acquired with oscilloscope while target approaches the sensor plane starting from 7.0m, (b) sensor output signal acquired with oscilloscope while target leaves the sensor plane from 4.5m.

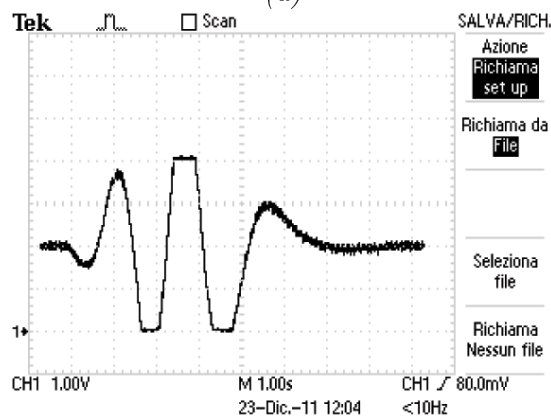
The same test is repeated increasing the distance to the sensor and similarly the sensor is capable of detecting the presence of the moving target, even if the

overall dynamic of the output signal is more reduced if compared to the previous case (Fig. 3.29).

In comparison to radial movements, successive tests are aimed at validating the sensor sensibility in case of tangential movements with respect to the sensor plane. In particular the target moves at the tangential distance of about 3.5m from left to right till exiting the sensor field-of-view. Then the target stops and repeats the test from right to the left. The same is then repeated at 7.0m distance. As it can be seen in Fig. 3.30(b) and Fig. 3.31, the sensor output signal clearly detects the target movements and it is worth noting that the signal amplitude is considerable higher than what has been obtained with the radial movement tests respectively.



(a)



(b)

Figure 3.30: Infrared sensor testing: (a) target moving tangentially in front of the sensor, (b) sensor output signal acquired with oscilloscope while the target moves tangentially at 3.5m.

3.4. SENSOR PRELIMINARY SETUP AND TESTING

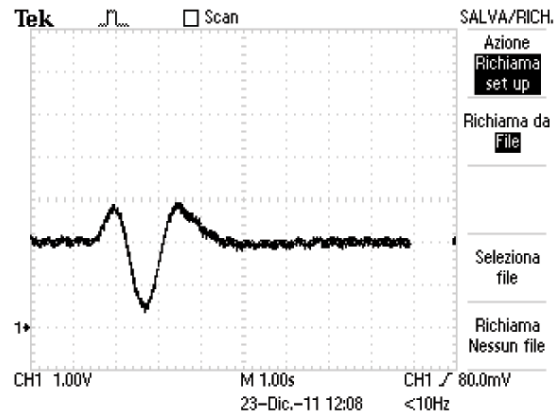


Figure 3.31: Infrared sensor testing: sensor output signal acquired with oscilloscope while the target moves tangentially at 7.0m.

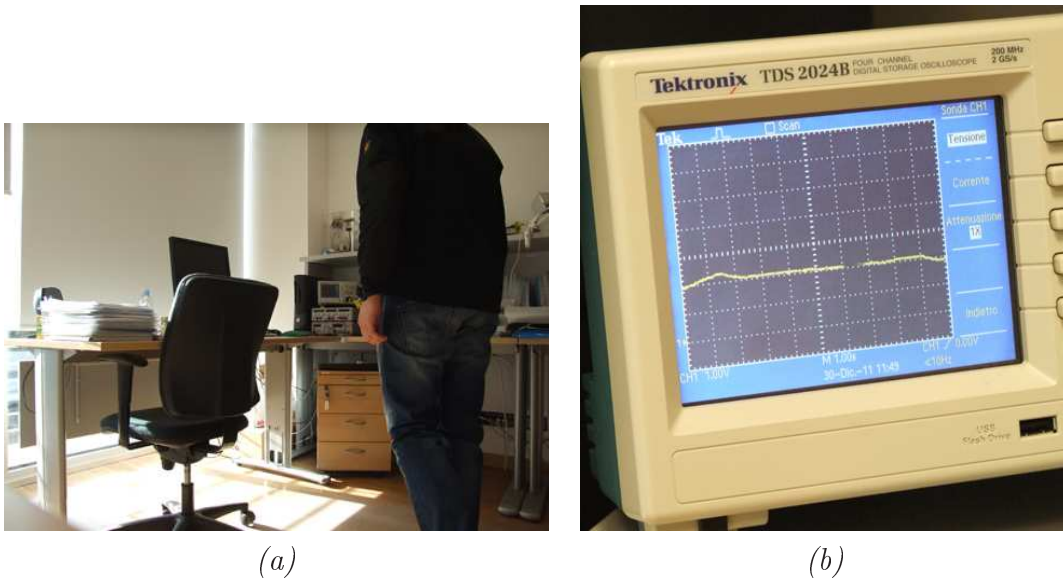


Figure 3.32: Infrared sensor testing: (a) target standing in front of the sensor, (b) sensor output signal acquired with oscilloscope while the target stands in front of the sensor at 2m distance.

Finally, considering the target still in front of the sensor at different distances, the sensor do not detect the presence of the target as expected. Fig. 3.32 shows the oscilloscope acquisition while the target is standing in front of the infrared sensor at 2.0m distance.

In conclusion, the identified infrared sensor is very sensitive to movements, which happen in its field-of-view. The experimental validation allows inferring that, as expected, this sensor typology is more sensitive to tangential movements rather than radial ones, quite the opposite to the radar sensor discussed above. Therefore the integration of such sensors may allow a sort of compensation thus being more sensitive to a larger variety of movements typologies.

3.4.4 Thermal Sensor TPA81

3.4.4.1 Setup

The TPA81 is a thermopile sensor capable of sensing the infrared radiation. It is composed by eight adjacent pixels, which acquire temperature data independently by each other.

Technical parameters:

- reduced cost: \$59.19
- voltage source: 5V
- current drain: 5mA
- measuring range: 4°C-100°C
- aperture angle (H/V): 41°/6° (8 pixels 5°/6°)
- output signal: environmental and 8 pixel temperature data via I2C protocol
- dimensions (LxWxH): 31x18x10mm

The thermal sensor is equipped with a 8 interfacing port (Fig. 3.34) and in particular the available connections are:

- V_{cc} : 5Volt power supply
- SDA : I2C protocol data connection (*serial data line*)
- SCL : I2C protocol synchronization connection (*serial clock*)
- GND : ground plane connection
- the *servo* connections are devoted to the control of a servo for module panning thus allowing the generation of a thermal image.

In order to validate the actual working of the sensor, before a possible sensor integration, a I2C-USB converter has been used, thus simplifying the communication between the sensor and the controller and gathering all the data sensed by the thermopile module.

3.4. SENSOR PRELIMINARY SETUP AND TESTING

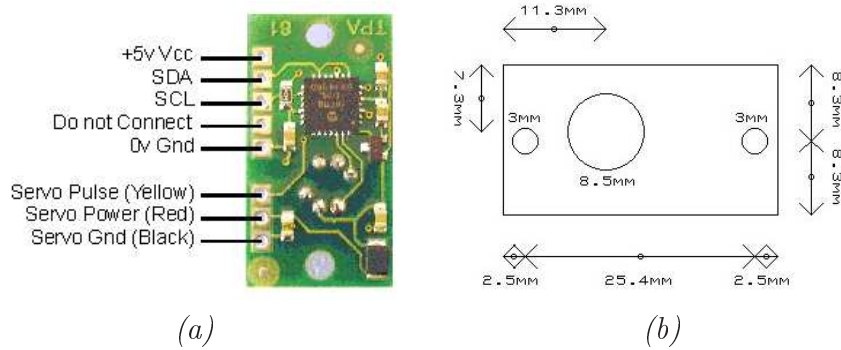


Figure 3.33: Thermal sensor TPA81: (a) connection pins, (b) sensor dimension.



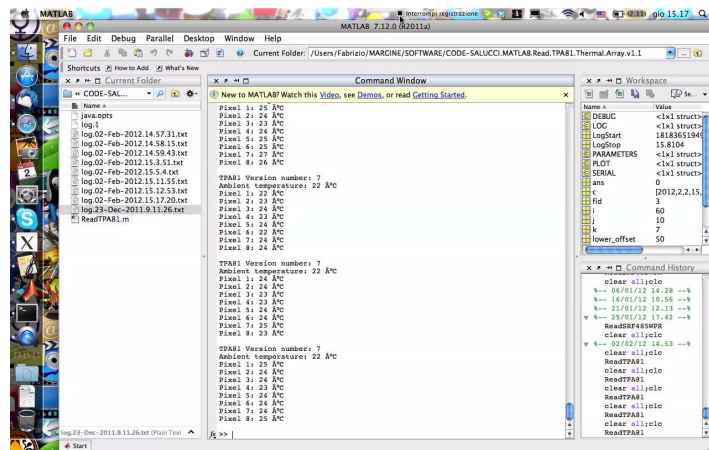
Figure 3.34: Thermal sensor TPA81 connected to the I2C-USB converter.

The data acquisition process is committed to the controller (i.e., PC) on which a simple Matlab code has been developed to this task. The developed software allows an easy management of the sensor module, sending on periodic time cycles the specific code string necessary to get the temperature data acquired by the sensor. The specific code string used, considering also the particular sensor address code, is reported below:

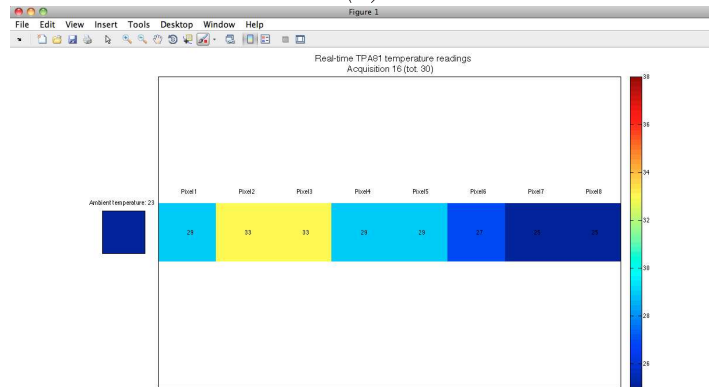
CHAPTER 3. PROPOSED SOLUTION, PROTOTYPE AND VALIDATION

$$(0x55 | 0XD1 | 0X00 | 0X0A)_{HEX} = (85 | 209 | 0 | 10)_{DEC}$$

This command allows the controller getting the data saved in a 10byte register on the sensor, where the module stores the sensed temperature data. These data are then acquired and properly processed by the Matlab routine in order to generate a real-time color map, more representative of the observed scene (Fig. 3.35).



(a)



(b)

Figure 3.35: Thermal sensor TPA81: (a) data acquisition example in Matlab workspace, (b) real-time color map generated on data acquisition.

Fig. 3.35(b) shows the color map drawn on the basis of the acquired data. In particular, the 8 pixel array is shown together with the environmental temperature measured by the sensor (i.e., the colored square on the left side of the picture).

3.4. SENSOR PRELIMINARY SETUP AND TESTING

The thermopile sensor needs to be supplied with a 5Volt source and this feature may be taken carefully into account during the possible integration process with the WSN sensor node, which instead is supplied with 3-3.3Volts. The power consumption of the thermopile sensor is quite reduced and therefore a proper power management of the integrated WSN sensor node may allow optimizing the available power source.

3.4.4.2 Testing

The experimental setup used in order to validate the sensor performance is composed by a PC with Matlab software, the thermopile sensor and the I2C to USB converter (Fig. 3.36).

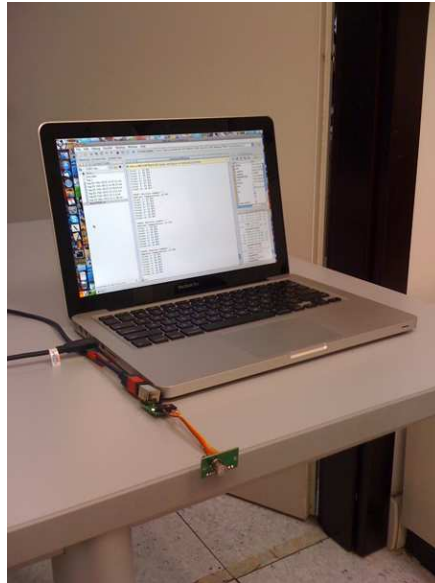


Figure 3.36: Thermal sensor TPA81 testing setup.

The first test performed is devoted to validate the actual sensor field-of-view. In particular, the sensor is installed at about 80cm from the ground and the target moves in front of the sensor, starting from the sensor position and going farther along the tangential direction till 4m distance. The target then stops and after some seconds re-start moving towards the sensor plane. The acquired data allows inferring that the sensor is capable of detecting the target presence in the scene within 1.5m range. Beyond this distance, the data acquired by the sensor are quite similar to the environmental temperature, thus the presence or movement of the target can not be identified.

CHAPTER 3. PROPOSED SOLUTION, PROTOTYPE AND VALIDATION

Therefore, given the maximum detectable distance obtained with the previous test, the target is placed at 1m distance from the sensor and starts moving from left to right and viceversa, keeping the same radial distance. Fig. 3.37 shows an example of the color map generated by the Matlab software, which allows determining the presence and relative position of a target in the sensor field-of-view. It is worth noting that the sensor is capable of detecting the presence of the target and in particular the radial movement throughout all the test duration.

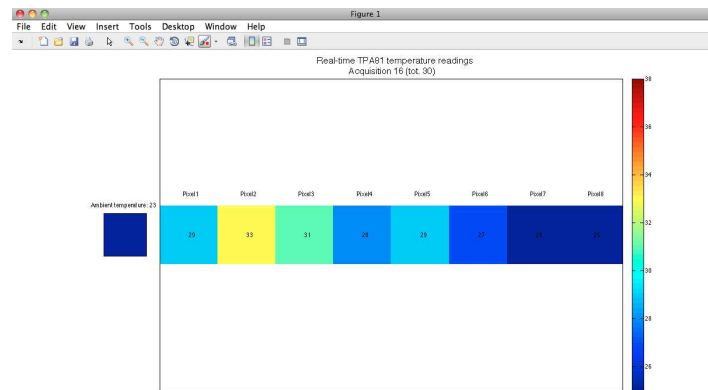


Figure 3.37: Thermal sensor TPA81: color map representative of a target placed on the left side of the sensor field-of-view.

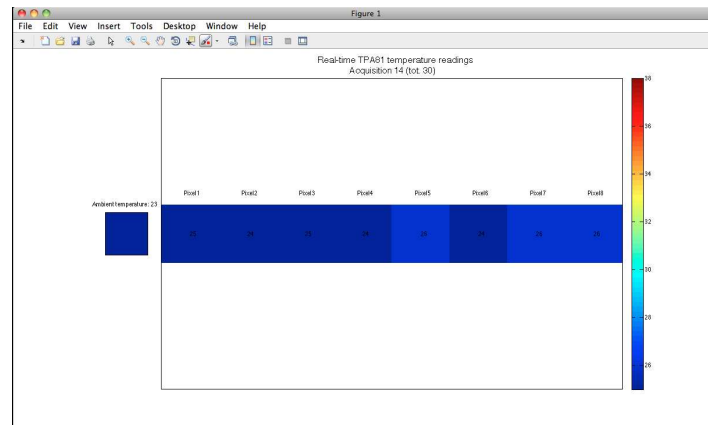


Figure 3.38: Thermal sensor TPA81: color map representative of a target moving at 2m distance from the sensor plane.

3.4. SENSOR PRELIMINARY SETUP AND TESTING

Similar to previous test, the target repeats the same movements at the distance of about 2m from the sensor plane, in order to verify and confirm the maximum detectable distance validated in the first tests. As expected, the thermopile sensor is not able to detect the presence of the moving target and the acquired data do not differ from the environmental temperature value, as shown in Fig. 3.38.

In conclusion, the thermopile sensor represents a low-cost solution, with reduced power consumption and of quite easy integration with the WSN sensor node. Nevertheless, the sensor performance are quite inadequate particularly considering the main problem objective of this thesis.

In general, the costs of such technology are quite high and the identified thermal sensor represents one low-cost off-the-shelf solution. Therefore the integration of such sensor is not valuable for the actual detection of wildlife moving in the road proximity.

3.5 WSN Node Architecture

This section is devoted to the definition of the WSN node architecture, which should manage all the sensors identified in the previous phases, communicate with them for gathering the sensed data and finally interact and cooperate with the other nodes of the wireless network and in particular, with the gateway node in charge of forwarding data to the control unit and if the case activating the actuation node.

3.5.1 WSN Node 3Mate Architecture

The 3Mate node architecture (Fig. 3.39) is a mobile platform useful for monitoring applications, thanks to the large variety of sensor technologies, which may be used with this device, like temperature, humidity, acceleration sensors. The power consumption is quite reduced and several degrees of freedom in the programming stage make of this platform a valuable device for controlling the WSN sensor node.

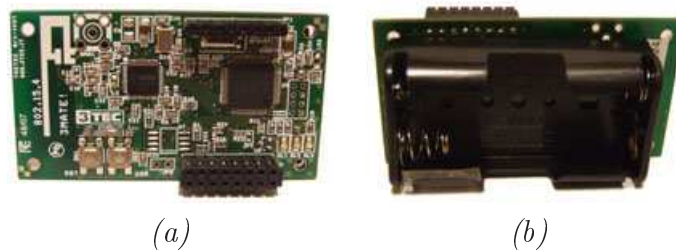


Figure 3.39: WSN node 3Mate: (a) front side, (b) back side.

The 3Mate device is IEEE 802.15.4 (2.4GHz) standard compliant and the radio transfer bitrate is quite high, up to 250kbps. The serial communication with USB connections is straightforward by using the programmer board (Fig. 3.40), which allows the direct communication between the WSN node and the control unit.

3.5. WSN NODE ARCHITECTURE

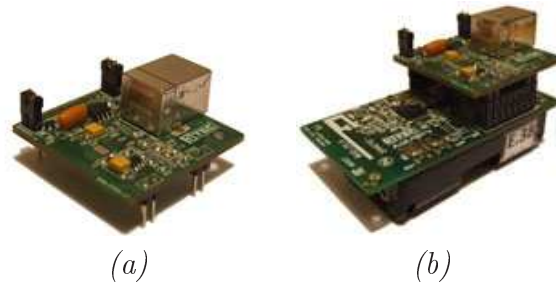


Figure 3.40: WSN node 3Mate: (a) programmer board, (b) 3Mate device with programmer board.

In addition, the 3Mate platform is equipped with two main buttons, namely:

- reset: used to reset the node
- user: it enables additional functionalities, which may be programmed by the user.

In addition, the device has on the front side three connector strips, composed by 8 pins each as shown in Fig. 3.41, which make available several connection typologies, like UART (Universal Asynchronous Receiver Transmitter) serial, ADCs and digital GIO (General Input Output) connections.

The principal component of the device is represented by its microcontroller MSP430 (Texas Instruments), which features 10KB RAM and 48KB flash memory.

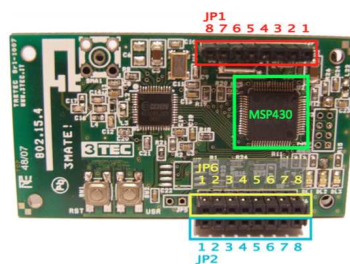


Figure 3.41: WSN node 3Mate: connection strips.

In particular, the availability of numerous connections, both analog and digital, allows interfacing all the devices identified in the technology scouting phase. Fig. 3.42 shows a connection scheme for the management of all the sensors together with the powering branch. The specific control of batteries and renewable

energy source allows monitoring the proper state of the WSN sensor node and identifying critical events for the life of the integrated device.

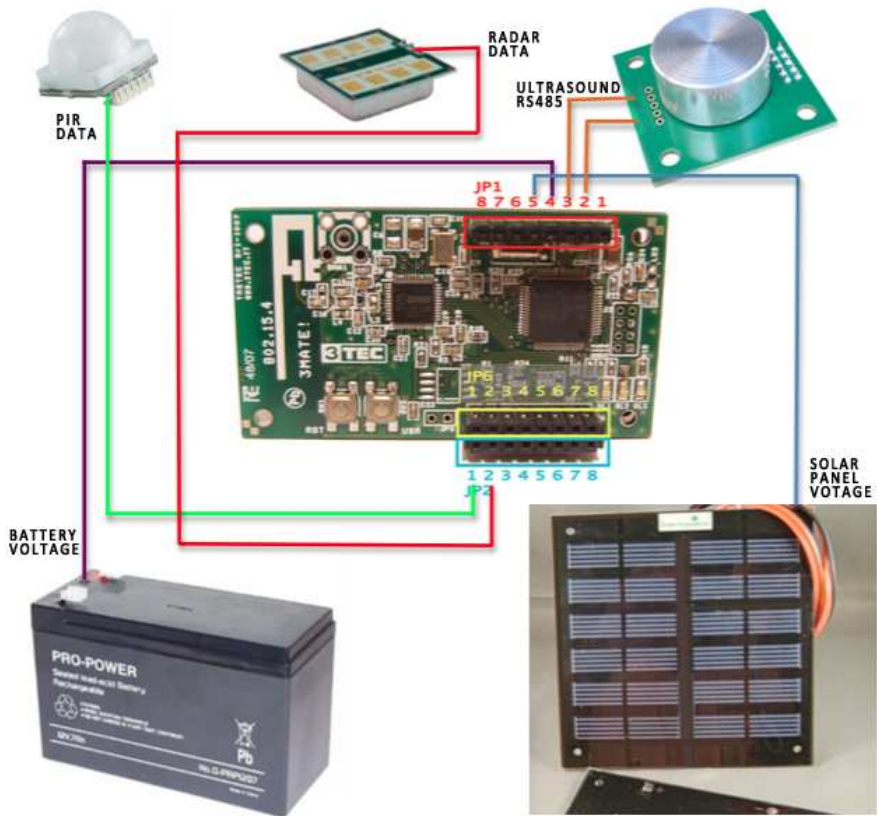


Figure 3.42: WSN node 3Mate: integration scheme.

3.5.2 Power Consumption and Management of the Integrated Solution

Considering the proposed integration scheme, shown in Fig. 3.42, which includes all the sensors discussed in the previous sections, the analysis of the power budget is discussed, in order to determine the device lifetime.

The prototype is therefore mainly composed by the following devices:

- WSN Node 3Mate
- radar sensor model RSM1650

3.5. WSN NODE ARCHITECTURE

- ultrasound sensor model SRF485WPR
- infrared sensor model PIR_STD_LP
- operational amplifiers model LMV358
- dual operational amplifiers model LM358N
- analog switch model MAX4662
- step-down converter 12Volt-5Volt model MAX1837EUT50
- step-down converte 12Volt-3.3Volt model MAX1837EUT33

3.5.2.1 Power Consumption

Table 3.5 reports the main components of the integrated sensor node, describing model, current drain during active phase I_0 , current drain during inactive phase I_S and supplying voltage supposing the use of a 12Volt battery.

#	Description	Model	Current Drain I_0	Current Drain I_S	Voltage
1	Step-down converter 3.3V	MAX1837EUT33	$25\mu A$	$25\mu A$	12.0V
1	Step-down converter 5.0V	MAX1837EUT50	$26\mu A$	0	12.0V
1	UART-RS485 converter	SP3485	$1mA$	0	3.3V
1	Analog switch	MAX4662	$5\mu A$	$5\mu A$	3.3V
8	Operational Amplifier	LM358N	$0.5mA$	0	5.0V
2	Operational Amplifier	LMV358	$210\mu A$	0	5.0V
1	WSN Node	3Mate	$23mA$	$21\mu A$	3.3V
1	Radar sensor	RSM1650	$40mA$	0	5.0V
1	Ultrasound sensor	SRF485WPR	$10mA$	0	12.0V
1	Infrared sensor	PIR_STD_LP	$400\mu A$	0	5.0V

Table 3.5: Power budget: main components of the integrated sensor node and related current consumption using 12Volt battery.

Table 3.6 reports instead the power consumption computed on the basis of data shown in Table 3.5. In Table 3.6 the term P_0 refers to the power consumption during active phase, while P_S the power consumption during inactive phase, similar to the expression used in Table 3.5.

CHAPTER 3. PROPOSED SOLUTION, PROTOTYPE AND VALIDATION

#	Description	Model	Power P_0	Power I_S
1	Step-down converter 3.3V	MAX1837EUT33	0.3mW	0.3mW
1	Step-down converter 5.0V	MAX1837EUT50	0.3mW	0
1	UART-RS485 converter	SP3485	3.3mW	0
1	Analog switch	MAX4662	0.06mW	0.06mW
8	Operational Amplifier	LM358N	2.5mW	0
2	Operational Amplifier	LMV358	1.05mW	0
1	WSN Node	3Mate	75.9mW	69.3 μ W
1	Radar sensor	RSM1650	0.2W	0
1	Ultrasound sensor	SRF485WPR	0.12W	0
1	Infrared sensor	PIR_STD_LP	2mW	0

Table 3.6: Power budget: main components of the integrated sensor node and related power consumption using 12Volt battery.

Similar analysis can be carried out considering a different power supply, namely a 6Volt battery. In this case a step-up converter has to be used in order to properly supply the ultrasound sensor, which need 12Volt power supply.

#	Description	Model	Current Drain I_0	Current Drain I_S	Voltage
1	Step-down converter 3.3V	MAX1837EUT33	25 μ A	25 μ A	6.0V
1	Step-down converter 5.0V	MAX1837EUT50	26 μ A	0	6.0V
1	Step-up converter 12.0V	MAX734ESA	2.5mA	0	6.0V
1	UART-RS485 converter	SP3485	1mA	0	3.3V
1	Analog switch	MAX4662	5 μ A	5 μ A	3.3V
8	Operational Amplifier	LM358N	0.5mA	0	5.0V
2	Operational Amplifier	LMV358	210 μ A	0	5.0V
1	WSN Node	3Mate	23mA	21 μ A	3.3V
1	Radar sensor	RSM1650	40mA	0	5.0V
1	Ultrasound sensor	SRF485WPR	10mA	0	12.0V
1	Infrared sensor	PIR_STD_LP	400 μ A	0	5.0V

Table 3.7: Power budget: main components of the integrated sensor node and related current consumption using 6Volt battery.

3.5. WSN NODE ARCHITECTURE

#	Description	Model	Power P_0	Power I_S
1	Step-down converter 3.3V	MAX1837EUT33	0.15mW	0.15mW
1	Step-down converter 5.0V	MAX1837EUT50	0.15mW	0
1	Step-up converter 12.0V	MAX734ESA	15mW	0
1	UART-RS485 converter	SP3485	3.3mW	0
1	Analog switch	MAX4662	0.03mW	0.03mW
8	Operational Amplifier	LM358N	2.5mW	0
2	Operational Amplifier	LMV358	1.05mW	0
1	WSN Node	3Mate	75.9mW	69.3 μ W
1	Radar sensor	RSM1650	0.2W	0
1	Ultrasound sensor	SRF485WPR	0.12W	0
1	Infrared sensor	PIR_STD_LP	2mW	0

Table 3.8: Power budget: main components of the integrated sensor node and related power consumption using 6Volt battery.

3.5.2.2 Prototype Lifetime

Taking into account the use of a 12Volt battery, able to supply 1.2Ah, the total consumption can be computed as follows:

$$P = \alpha \cdot P_0 + (1 - \alpha) \cdot P_S$$

where:

- P_0 is the power consumption during inactive or standby time
- P_S is the power consumption during active phase
- α is the duty-cycle (%) of the activity period.

The prototype lifetime (T_{run}) is obtained by comparing the total power consumption (P) to the actual power supplied by the used battery (P_{batt}), for instance in the case of 12Volt battery with 1.2Ah, the supplied power will be $P_{batt} = 14.4Wh$.

- System activity 100%, $\alpha = 1$

$$P = 424mW$$

$$P_{batt} = 12V \cdot 1.2Ah = 14.4Wh$$

$$T_{run} \simeq 34h \simeq 1.5days$$

- System activity 50% (30sec/min), $\alpha = 0.5$

$$P = 212mW$$

$$T_{run} \simeq 68h \simeq 3days$$

- System activity $\sim 30\%$ (20sec/min), $\alpha = 0.3$

$$P = 142mW$$

$$T_{run} \simeq 102h \simeq 4days$$

Analogous result may be obtained taking into account the use of a 6Volt battery, able to supply 4.5Ah, thus the supplied power will be $P_{batt} = 27Wh$.

- System activity 100%, $\alpha = 1$

$$P = 437.58mW$$

$$T_{run} \simeq 61.70h \simeq 2.5days$$

- System activity 50% (30sec/min), $\alpha = 0.5$

$$P = 218.82mW$$

$$T_{run} \simeq 123.39h \simeq 5days$$

- System activity $\sim 30\%$ (20sec/min), $\alpha = 0.3$

$$P = 145mW$$

$$T_{run} \simeq 185.05h \simeq 8days$$

Therefore, the only use of a battery source may not be sufficient to guarantee a valuable lifetime to the system. In particular, renewable energy sources may be exploited to extend the system lifetime. Proper analysis has to be conducted in order to identify the specific solar cells to be used, taking into account the battery source features and the system time of actual activity, which mainly impact on the power consumption.

Several types of solar cells are available as off-the-shelf products. Thus, considering a solar panel featuring 6Volt, 250mA a study on the actual prototype lifetime may be conducted. In particular, considering a day-time of 100% activity of the integrated sensor node, complete of all the sensors identified, the current drain needed to supply all the components during all the day long, is about $I_{24h} = 78mA \cdot 24h = 1.872A$.

Given this current drain, the energy apported by the solar panel has to be considered and in particular the actual current supplied by the solar cells is about $I_{solar} = 250mA \cdot 7h = 1.75A$, considering seven hours of effective solar radiation.

3.5. WSN NODE ARCHITECTURE

Therefore, it is clear that at the end of the day the power budget is in deficit of about $I_{deficit} = 122mA$.

This configuration allows extending the lifetime of the system to 37 days, which in turn means that after this time the battery have to be changed with charged ones. The solar cells, therefore, slow down the battery discharge process, but the complete recharge may not happen.

To actually extend the system lifetime two solutions may be chosen: a) change solar panels with higher performance models, b) reduce the system time of activity.

Concerning the former case, the identification process of higher performance solar panles may be not so trivial, given that not only supplying features have to be accounted, but also other characteristics such as cost and dimensions may be minimized. Therefore, the alternative to this approach is represented by the latter case described above, namely the reduction of the system time of activity. As an example, by reducing the activity time to 50sec per minute, the current consumption is in turn reduced to about $I \simeq 1.56A$, which is smaller if compared to the actual current supplied by the solar panel discussed above during a period of effective solar radiation in the range of about seven hours (i.e., $I_{solar} \simeq 1.75A$). Thus this approach do not imply neither any increase in the costs neither in the overall prototype dimensions.

Particular attention may be addressed to the effective radiation period considered in the previous discussion. In fact, considering seven hour of actual solar panel work may be too optimistic, also considering that there is no guarantee on such parameter. Therefore, for the sake of completeness, the power budget computed earlier may be reformulated considering different period of time in which solar panels are considered to properly supply energy to the system. In this view, let us consider two main examples, namely the first case with at most 3 hours of effective solar radiation and the second one with at most 5 hours of solar radiation. Thus:

- *case a) 3 hours of effective solar radiation:* similar to what have just been presented earlier in this section, the total current supplied by the solar panel may be computed as $I_{solar} \simeq 250mA \cdot 3h = 750mA$. The total current consumption during 24hours of 100% activity is about $I_{24h} \simeq 78mA \cdot 24h = 1.872A$. Therefore, it is clear that in such conditions the solar panel supply is not sufficient in order to actually extend the system lifetime. To this end, the prototype period of activity may be computed as: $I_{24h} \simeq 78mA \cdot \alpha \cdot 24h \leq 750mA$. Thus the system activity time may be reduced to 24sec per minute (i.e., $\alpha = 0.4$), thus obtaining: $I_{24h} \simeq 78mA \cdot 0.4 \cdot 24h \simeq 749mA$, which is comparable to the amount of current supplied by the solar panel.
- *case b) 5 hours of effective solar radiation:* analogously to the computation in case a), the following may be obtained: $I_{solar} \simeq 250mA \cdot 5h = 1.25A$, thus $I_{24h} \simeq 78mA \cdot \alpha \cdot 24h \leq 1.25A$, which lead to: $\alpha = 0.66$ or $I_{24h} \simeq$

$78mA \cdot 0.66 \cdot 24h \simeq 1.24A$, which means that the system may be active for about 40sec per minute.

It is worth noting, that in the above computation the current drain during inactive phases has not been considered, since this amount of current is negligible if compared to the other entities considered for the evaluation of the α term.

Therefore, in conclusion, it may be convenient to consider an automatic adjustment procedure of the system time of activity, based on the actual reading of battery and solar panel voltages. This expedient may ideally allow obtaining infinite system lifetime, given that the battery may not never be completely discharged, by reducing the system time of activity complementary to the solar panel capacity. Thus the only limitation in such condition would be represented by the actual battery life, computed as performance degradation in relation to repeated charge/discharge cycles.

3.5.3 Hardware Interface of the Integrated Sensor Node

Following the previous development stages, focused on the identification of specific technologies useful to the aim of this thesis project, the successive step regards the design of the hardware interfacing board, which should allow the proper communication among all the components, namely sensors and WSN node controller, in order to gather all the sensed information and to manage at the same time their working.

Starting from all the technologies identified and presented in Section 3.2 (i.e., radar, infrared, ultrasound and thermal technologies), as discussed above, the thermal technology has been excluded since low-cost off-the-shelf solutions do not perform sufficiently, thus implying only a current drain to the system, in turn hardening the expansion process regarding the system lifetime.

Therefore the technologies and related sensors used for the actual integration process are the following ones:

- radar technology: sensor RSM-1650
- ultrasound technology: sensor SRF485WPR
- infrared technology: sensor PIR_STD_LP

Each sensor present different characteristics in terms of input/output signals, power supply, layout and dimensions. In this view, the WSN node allows interfacing all these technologies without any particular problem, thus exploiting and managing several devices with one single controller.

As already discussed, the WSN Node 3Mate exhibit three main connection strips on which analog, digital and supplying connections are available. In particular, some of them are also of reconfigurable type, which means that, for

3.5. WSN NODE ARCHITECTURE

instance, an analog connection may be properly programmed by the end-user in order to work as a digital one.

Table 3.9 reports the main electrical and communication characteristics of the identified sensors together with the WSN node controller.

<i>Component</i>	<i>Model</i>	<i>Supplying Voltage</i>	<i>Input Signal</i>	<i>Output Signal</i>
WSN Node	3Mate	3.3V	Analog/Digital	Analog/Digital
Radar Sensor	RSM-1650	5.0V	/	Analog
Ultrasound Sensor	SRF485WPR	12.0V	RS485 String Code	RS485 String Code
Infrared Sensor	PIR_STD_LP	5.0V	/	Analog

Table 3.9: Electrical and communication characteristics of sensors and WSN node.

3.5.3.1 Supplying Voltage

Given the variety of supplying voltages, which differ from sensor to sensor, the proposed solution is composed by the use of voltage regulators, which allows using a single power source (i.e., lead battery 6Volt, 4.5Ah) instead of singular dedicated supplying sources. Fig. 3.43 shows the circuitual schematics of the voltage regulators to 3.3V, 5.0V and 12.0V respectively.

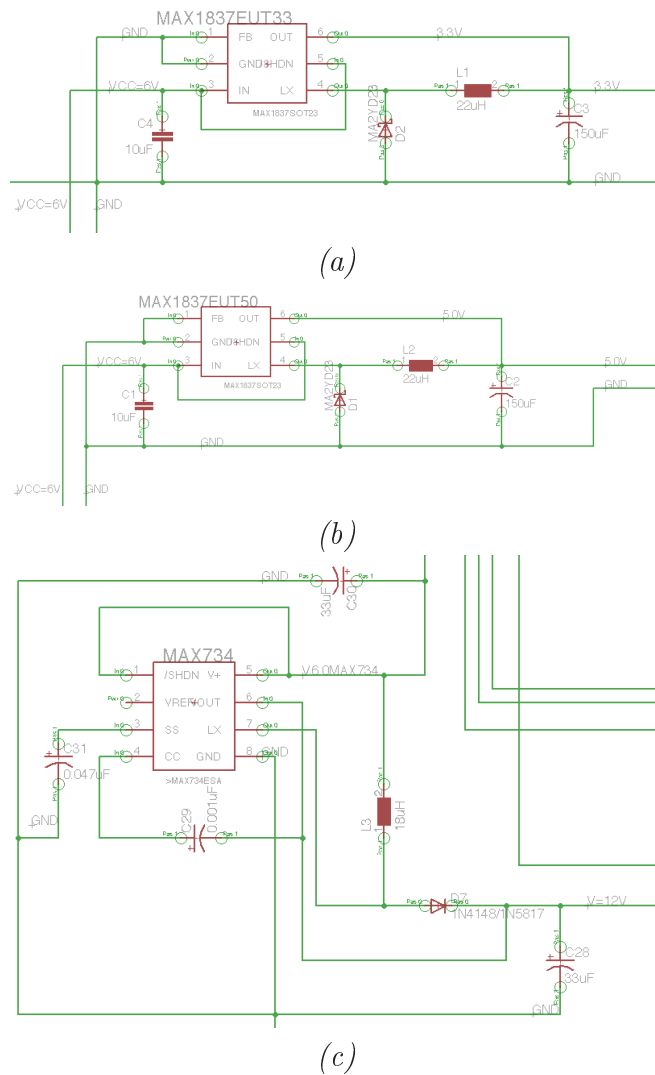


Figure 3.43: Voltage regulators circuitual scheme: (a) step-down regulator 6.0V-3.3V, (b) step-down regulator 6.0V-5.0V, (c) step-up regulator 6.0V-12.0V.

CHAPTER 3. PROPOSED SOLUTION, PROTOTYPE AND VALIDATION

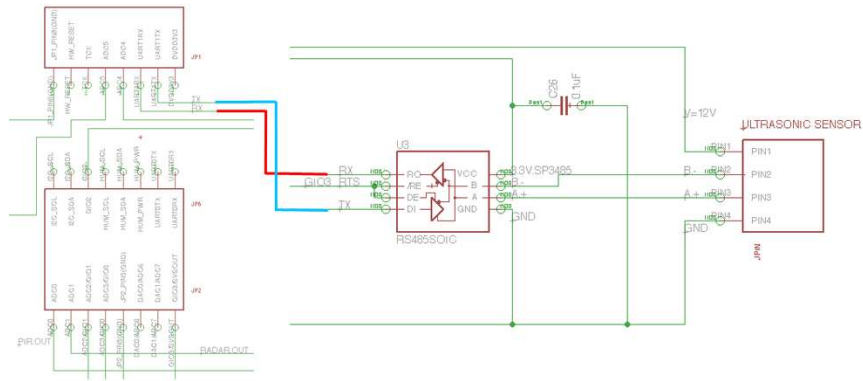


Figure 3.45: Ultrasound sensor connection to WSN node controller: circuitual scheme.

- infrared sensor*: the output signal of the infrared sensor ranges between 0Volt and the supply voltage V_{cc} . Therefore, in order to maximize the signal dynamic, the higher supply voltage accepted by the sensor is used, namely 5Volt. The problem now regards the controller and its analog connections. In fact, these ports may allow input signals lower than 2.5V. Voltages higher than this threshold are saturated. Thus, a proper signal amplitude adapter is used, which allows rescaling the infrared sensor output signal to the range accepted by the controller. The obtained signal is connected to port ADC0, pin1 connector JP2. Fig. 3.46 shows the circuitual scheme of the interfacing solution discussed.

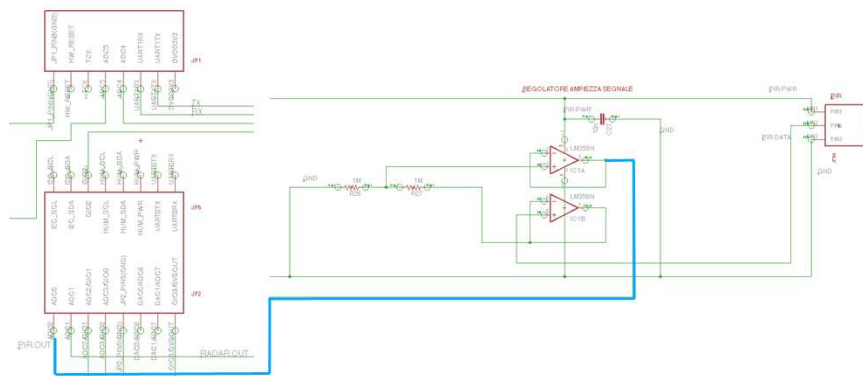


Figure 3.46: Infrared sensor connection to WSN node controller: circuitual scheme.

3.5. WSN NODE ARCHITECTURE

In addition, in order to allow the manage and in particular enabling the possibility to activate each single sensor independently, an analog switch is introduced in the interfacing board, which takes in input the different voltage supplies, regulated as described before, and the outputs are represented by the feeding branches for each sensing device. The analog switch can be controlled using digital connections of the controller, which range between high and low logic states, namely, on the base of the analog switch typology, enabling or disabling the related output respectively. Fig. 3.47 shows the circuitual scheme of the analog switch, together with input and output connection relation. Table 3.10 reports the operating signal connected to each port of the switch.

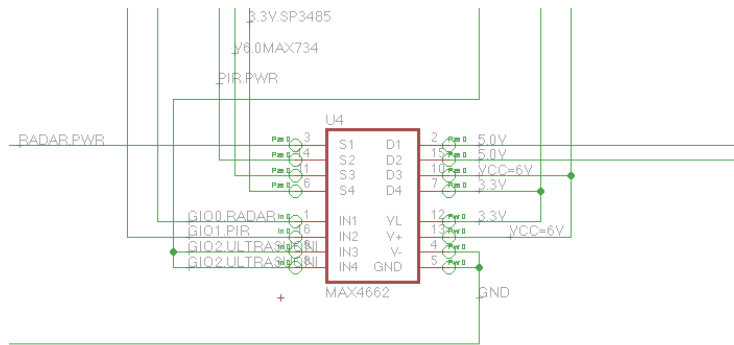


Figure 3.47: Analog switch connection to WSN node controller and sensors: circuitual scheme.

<i>Input</i>	<i>Output</i>	<i>Control Signal</i>	<i>Power Supply</i>
D1: 5.0V	radar power supply	GIO0	VL: 3.3V
D2: 5.0V	PIR power supply	GIO1	V+: 6.0V
D3: 6.0V	step-up 6-12V power supply	GIO2	V-: ground
D4: 3.3V	UART-RS485 converter power supply	GIO2	GND: ground

Table 3.10: Specific input and output connections of the analog switch for sensors management.

3.5.3.3 Supply Monitoring

As previously discussed, it is fundamental to monitor the actual state of the prototype and in particular of the energy supplies of which it is equipped. Therefore,

CHAPTER 3. PROPOSED SOLUTION, PROTOTYPE AND VALIDATION

battery and solar panel voltages are monitored as index of the actual state of the respective components. To this end, these signals have to be rescaled, as done for the infrared sensor, in order to allow the controller properly processing the information via an analog connection (for sake of completeness analog ports allow input voltages in the range 0-2.5Volt). In particular, a voltage resistive divider is designed and its output is connected to the controller on port ADC4 (pin4 connector JP1) and ADC5 (pin5 connector JP1) for battery and solar panel respectively.

Appendix A reports the complete circuitual scheme of the interfacing board, composed by all the sub-systems discussed in this section.

Fig. 3.48 shows the integrated sensor node prototype and the developed circuitual board for the sensors interfacing.

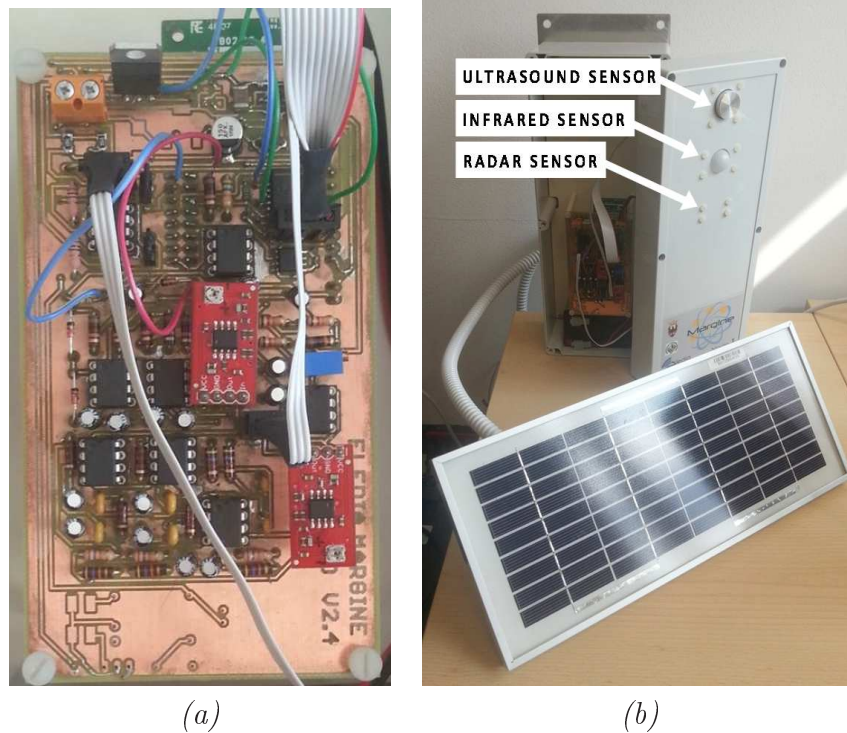


Figure 3.48: Integrated sensor node prototype: (a) circuitual board, (b) integrated device.

3.6 Wireless Network Architecture

The network architecture points out the complex structure of functions and relationships among network devices, which the system or network have to supply to the end-user. In particular, a fundamental aspect of the network architecture is represented by the actual physical structure of the network, also known as network topology.

The network topology can be also represented graphically thus highlighting all the interconnections among network devices. Therefore, it is important to carefully take into account this aspect, also considering the specific application scenario and its characteristics.

3.6.1 Linear Network Architecture

This network topology is the simplest one, since the only interconnection admitted are the uni- or bi-directional ones among pairs of devices. In particular, the network elements are placed along a linear positioning and thus one node represents the next hope for the nearest one towards the successive network node. Fig. 3.49 shows an example of such topology structure.



Figure 3.49: Linear network architecture scheme.

One of the main drawback of such architecture is represented by the fact that the network reliability is quite reduced, given that the malfunctioning of a single device imply the inability for the other nodes to communicate along the entire network, generating two different sub-networks.

3.6.2 Ring Network Architecture

The ring topology is an evolution of the linear case. In fact, it may simply be obtained by closing the linear structure, thus forming a ring or closed linear topology (Fig. 3.50).

This topology therefore solves the main drawback of the linear case, already discussed, since even considering the malfunctioning case of one network node, the remaining ones may re-organize themselves in a linear topology, thus allowing the complete communication along the network.

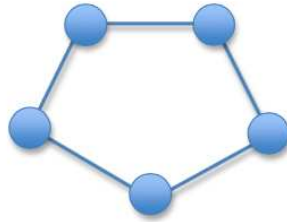


Figure 3.50: Ring network architecture scheme.

3.6.3 Star Network Architecture

The star network architecture is composed by a central node, which is in charge of directing each communication packet towards the correct destination. In such a case, each node is directly connected with the central node and no other additional links are established among the network nodes.

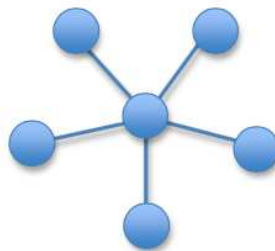


Figure 3.51: Star network architecture scheme.

The presence of a unique central node represents one main drawback, similarly to the linear topology case. In fact, if the central node do not work properly, the overall network stops communicating. Nevertheless, this particular topology allows an easy network management, both considering the addition or removal of one or more nodes in the network. Moreover, the connection among several star topology networks is quite easy since only the central nodes may be properly routed among themselves. In such a case, it is clear that the possible malfunctioning of a central node implies the interruption of all communications towards that specific sub-network, but the remaining nodes organized in sub-networks may continue the proper working.

3.6.4 Mesh Network Architecture

The mesh topology do not require any kind of central node or coordinator. The network devices are able to communicate with all the other nodes in the network thanks to dedicated links and following specific routing rules. This architecture category may further classified on the basis of the particular connections among the nodes, namely completely connected networks (in which each single node is connected with any other node in the network) and non-completely connected networks (in which some nodes are connected only with some other devices in the network).

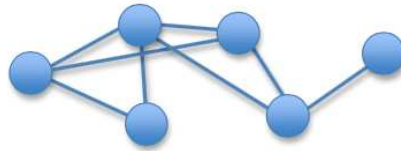


Figure 3.52: Mesh network architecture scheme.

This network topology is highly reliable, since even the malfunctioning of one or more network nodes do not imply the stop of communications among the other nodes, thanks to the multiple links among nodes.

3.6.5 Application Scenarios and Network Topology

As discusses above, the network architecture may be defined together with the knowledge of the actual application scenario and of its characteristics and the specific functionalities, which the network has to satisfy. Therefore, the following subsections take into account some examples of system application scenarios together with the definition of the network topology more suitable for the specific case.

3.6.5.1 Controlled Environment

The category controlled environment includes all those application scenarios used for experimental validation tests of the WSN sensor node prototype. In particular, these environments are characterized by the absence of “background noise”, like buildings or plants, which may limit or alter the actual field-of-view of the sensors. Therefore the benefit of such application scenarios is precisely represented by the fact that experimental test in real environments may be performed without any particular perturbation.

Let us consider two main typologies of controlled environment, classified in relation to the maximum coverage of the network node radio transceiver, namely: reduced dimension controlled environment and medium/large dimension controlled environment.

In the former case, the radio coverage is larger than the dimensions of the controlled environment, as shown in Fig. 3.53.

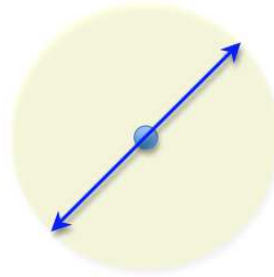


Figure 3.53: WSN node radio transceiver coverage: scheme and diameter of the covered area.

In such conditions, the network architecture, which may be used, is of the star topology. In fact, given the need of collecting the sensed data from all the nodes placed in the environment, the use of a central node directly connected to the control unit for data storage and analysis (i.e., gateway node) confirm this choice. In addition, the possibility to directly send data towards the central node allows simplifying the network routing and in turn the tasks of each network node.

The latter case, instead, includes all those scenarios with dimensions comparable or larger than the maximum coverage of the sensor node radio transceiver (Fig. 3.55). In such configuration, the suggested network topology is a hybrid one, composed as the combination of star and mesh topologies. In particular, the connection between the gateway node and a peripheral node (i.e., sensor node) is not guaranteed directly. Given the large environment dimensions, the distance between these two nodes may be larger than their respective radio coverage, thus implying the need of several hops among other nodes, in charge of receiving and forwarding data towards the destination node (i.e., gateway or peripheral node depending on the message type).

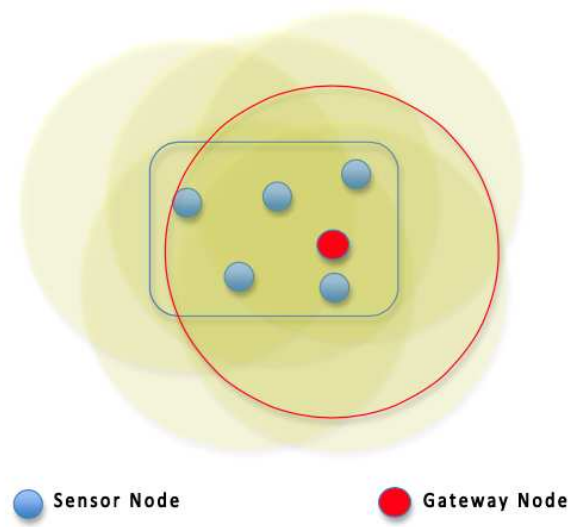


Figure 3.54: Controlled environment of reduced dimensions.

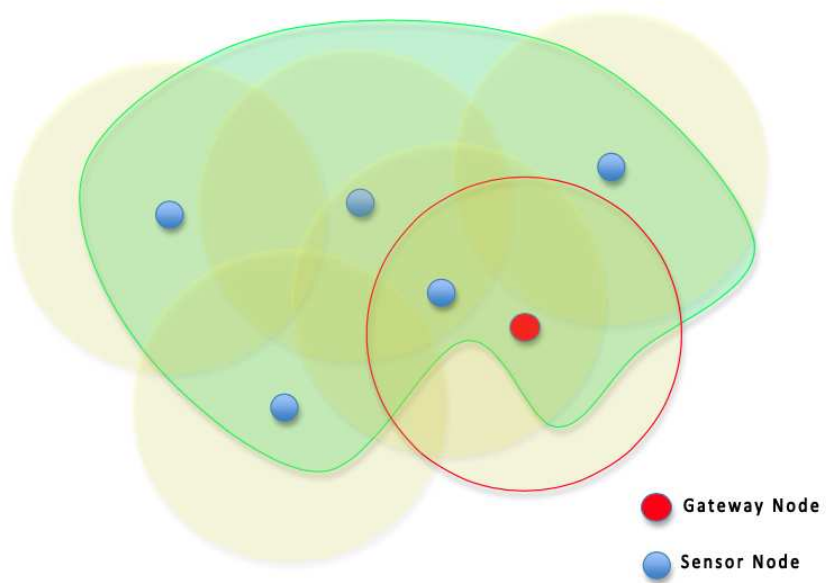


Figure 3.55: Controlled environment of medium/large dimensions.

3.6.5.2 Real Environmet: Experimental Site

Considering the analysis discussed in the previous section, it is possible to suppose the network architecture of the monitoring system composed by several sensor nodes placed along the road in order to allow the proper communication among the network.

In particular, considering the dimensions of a possible experimental test site, these will be very large compared to the maximum radio coverage. Therefore, similar to the medium/large controlled scenario, a hybrid star-mesh network topology may be used. More specifically, the network topology may be composed by four main classes of WSN nodes, each with specific fuctionalities:

- peripheral/sensor node: WSN node in charge of interfacing and managing all the sensors (i.e., radar, ultrasound, infrared);
- gateway node: WSN node in charge of receiving and forwarding the sensed data to the control unit to which it is directly connected (e.g., pc or server). It is also in charge of sending radio messages to peripheral nodes and to the actuator node when needed;
- actuator node: WSN node interfaced with the actuation device (e.g., luminous road sign);
- anchor node: WSN node in charge of directing the radio packets sent over the network towards the correct destination, in order to allow the proper communication among all the nodes, also those too far for a direct connection with the gateway node.

In addition, this network topology allows arranging the sensor nodes quite easily along the monitored road, by inserting at regular intervals anchor nodes for network extension. In this way, all the sensor nodes will be able to sense and send the acquired data, which will be properly received by the gateway node and thus by the control unit. Fig. 3.56 shows an example sketch of an exprimental test site and the possible positioning of the WSN nodes for the proper system working.

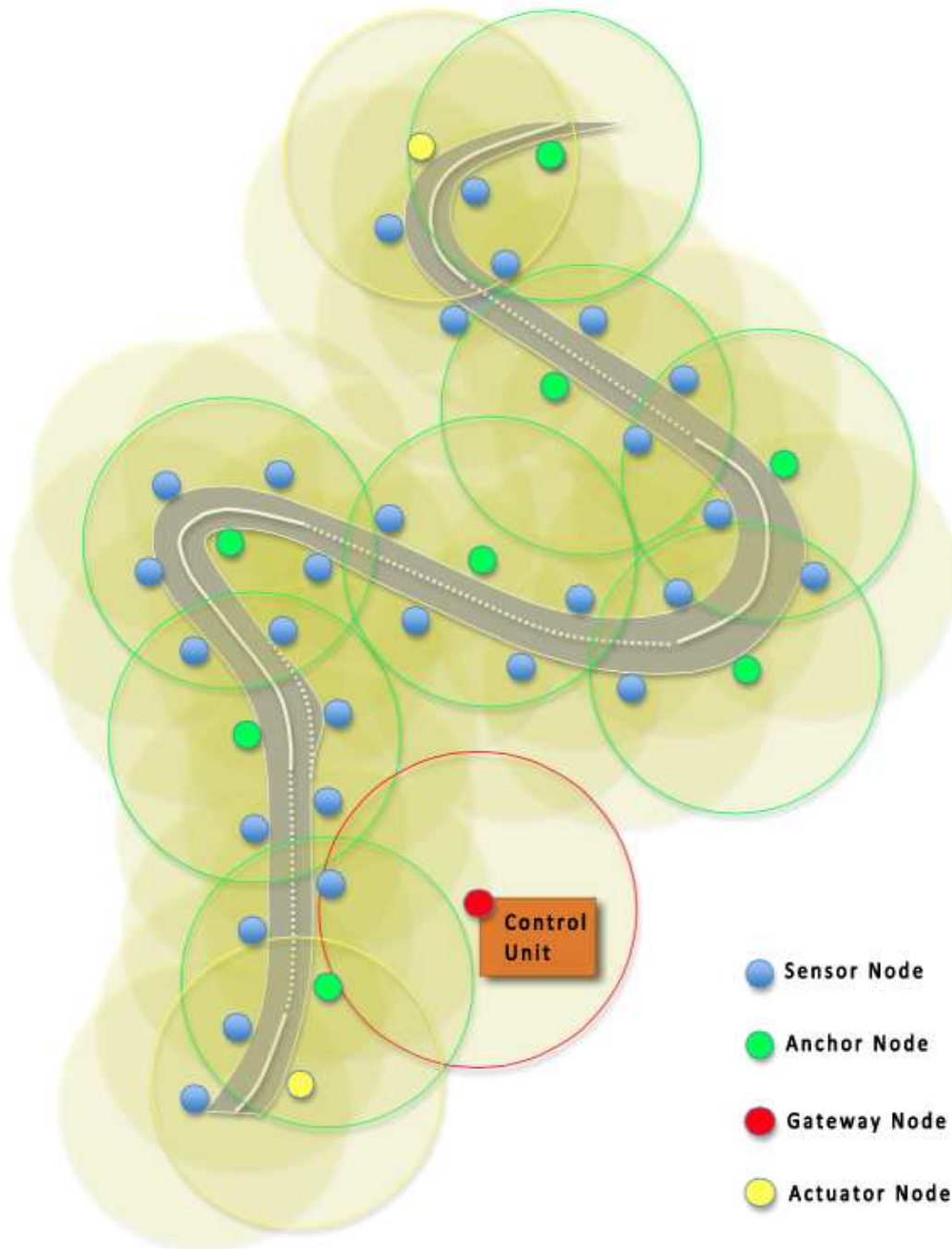


Figure 3.56: Experimental test site: network topology sketch.

3.7 Testing of the WSN Monitoring System in controlled Test-site

A small dimension WSN network has been deployed in a controlled scenario, at the “Centro Fauna Alpina A. Falzogher”, Casteller - Trento. The performed tests in such scenario exploit three WSN sensor nodes, which integrate the sensors discussed in the previous sections. Several movements have been performed in the monitored area, in order to validate the actual working of the system. As expected, approaching and leaving movements are clearly detected by radar sensors, defining an area large about 12-15m from the WSN node position in the orthogonal direction in which any movement is acquired. Fig. 3.57(a) shows the target approaching the node with id=2 and the simple graphical interface displays in red the sensors, which detect the event (Fig. 3.57(b)).

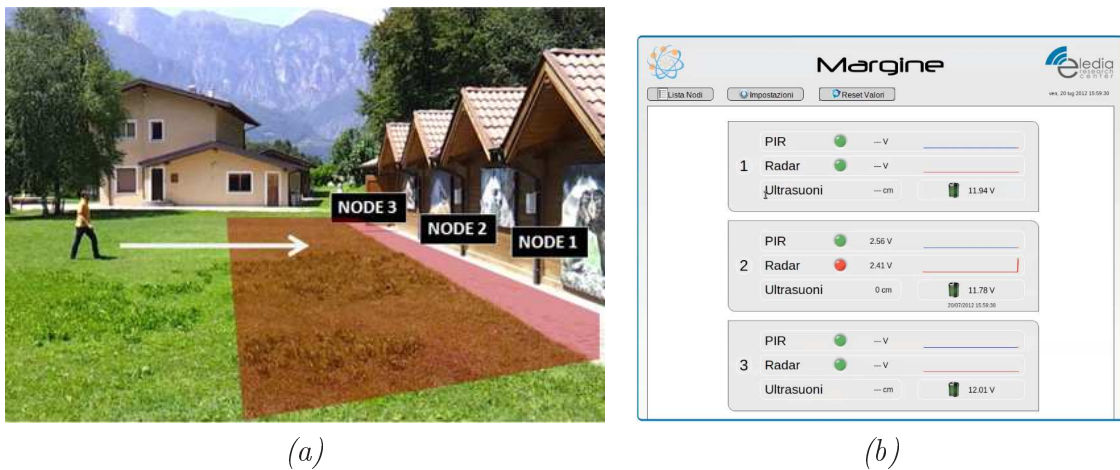


Figure 3.57: WSN monitoring system testing: (a) approaching event, (b) graphical interface showing the event detection.

Considering instead lateral movements, infrared and radar sensors allow the detection of the moving target, as shown in Fig. 3.58. In particular, the target starts its run near the position of sensor node with id=3 and then moves towards the other nodes. Ultrasound sensors, on the contrary, do not detect the presence of the target even if sometimes some measured distances are get by the sensor nodes, which do not coincide with the actual target position.

3.7. TESTING OF THE WSN MONITORING SYSTEM IN CONTROLLED TEST-SITE

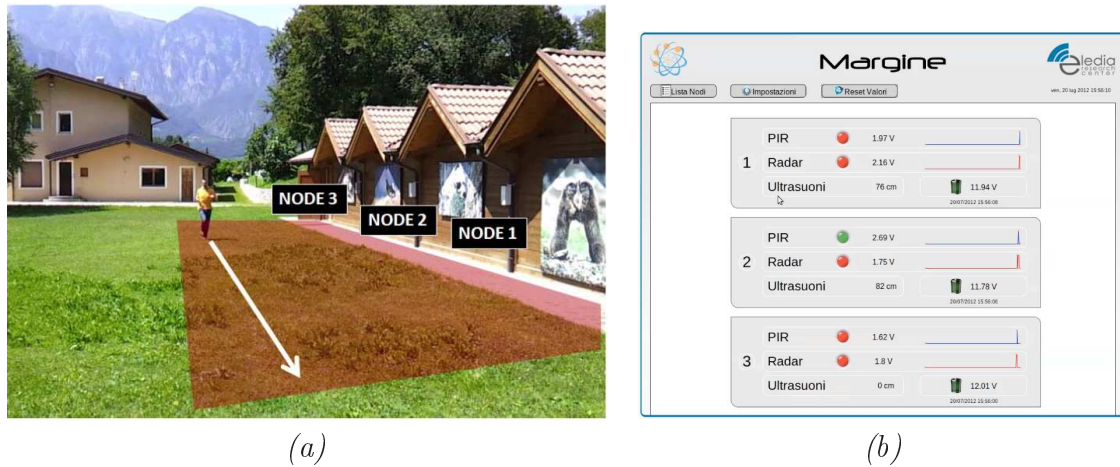


Figure 3.58: WSN monitoring system testing: (a) lateral movement, (b) graphical interface showing the event detection.

On the basis of these tests, additional ones have been performed also considering complex events as the combination of these simple cases. As expected, the outcome resemble what have been presented above and in particular radar sensors appears to be highly sensitive to actual movements with respect to the other sensors.

3.7.1 Test in Deer Fence

Thanks to the collaboration of game warden it has been possible to install the monitoring system in a deer fence at the “Centro Fauna Alpina A. Falzogher” (Casteller, Trento). The sensor nodes have been deployed on a fence near a passage where deers are usual to pass trough, as shown in Fig. 3.59.



Figure 3.59: WSN monitoring system testing: sensor node position inside the deer fence.

The deer movements have been performed in two main steps and with different typologies, which has allowed the validation of the sensors actual working in relation to the specific event occurred. In particular, at first some deers moved laterally in front of the sensor node 1, leaving then the scene near sensor node 2. Fig. 3.60 shows a picture of the movement, in particular Fig. 3.60 (a) the approaching movement lateral to node 1, while Fig. 3.60 (b) the leaving movement orthogonal to node 2.

The detected events are shown in Fig. 3.60 (c) and Fig. 3.60 (d) respectively. As expected the infrared sensor of node 1 and the radar sensor of node 2 correctly sensed the events in their field-of-view.

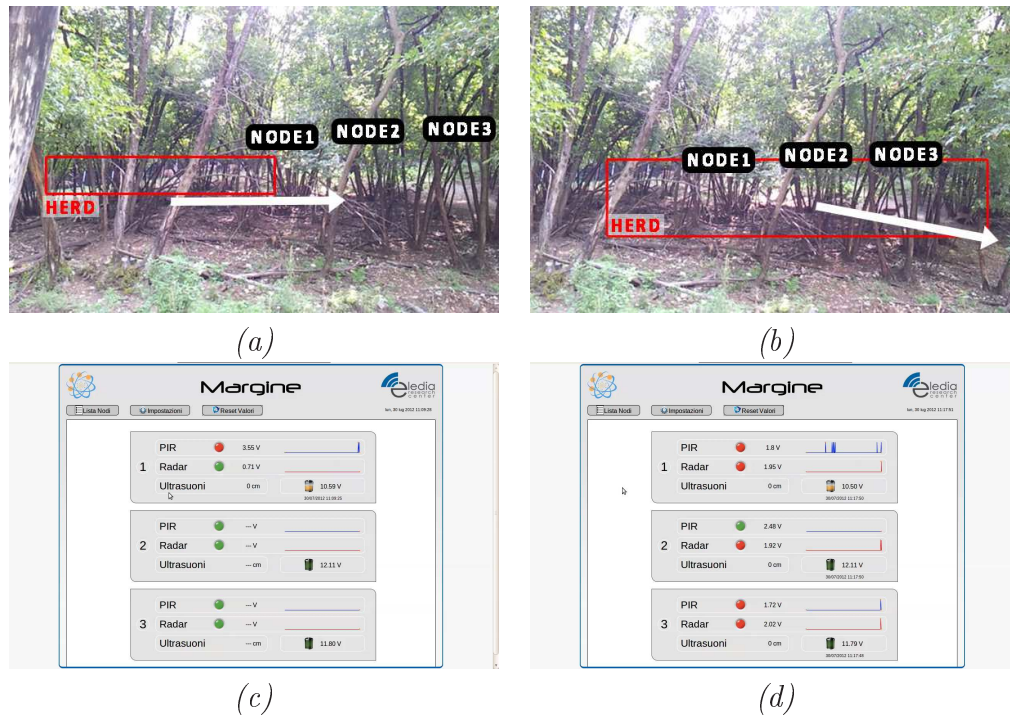
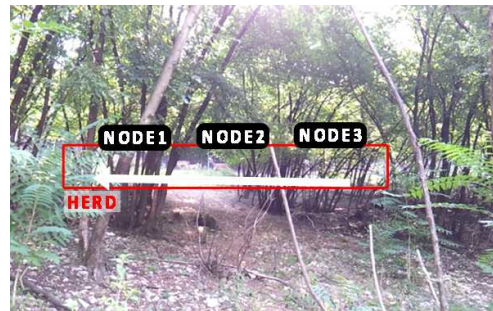


Figure 3.60: WSN monitoring system testing: (a) lateral approaching movement, (b) leaving movement, (c) graphical interface showing the approaching event detection, (d) graphical interface showing the leaving event detection.

The second motion, instead, regards a herd of deers, which moves linearly in front of sensor nodes, from node 3 to node 1. Fig. 3.61 (a) shows the herd of deers running in front of the sensors. Also in this case, the motion has been correctly detected by all three sensor nodes, as shown in Fig. 3.61 (b), which reports the graphical interface displaying all the events detected by the sensor nodes.

3.7. TESTING OF THE WSN MONITORING SYSTEM IN CONTROLLED TEST-SITE



(a)



(b)

Figure 3.61: WSN monitoring system testing: (a) deers movement, (b) graphical interface showing the event detection.

Both the events have been clearly detected by the sensor nodes, confirming the high sensitivity of each sensor to specific movement typology. In particular:

- the radar sensor allows detecting moving targets within 10-15m from the sensor plane and specifically orthogonal movements are more sensitive to this sensor technology. In addition, such sensor is quite robust for this application, considering also the possibility to protect the sensor itself with a dielectric box, which may not alter its radiation performance.
- the infrared sensor is more sensitive to lateral movements, allowing the detection of moving targets within about 6m from the sensor plane. The sensor is quite robust, but the main disadvantage for this technology is the need to open a hole in the sensor node enclosure, thus allowing the sensor having a view of the monitored scenario.
- the ultrasound sensor does not allow the distinct detection of movements in its field-of-view during the performed tests. In particular, this is mainly due to the actual installation position of such sensor. In fact, additional tests have proven that by varying the sensor height from the ground to about 1.5m, the precise ranging is given to the controller. In addition, as

CHAPTER 3. PROPOSED SOLUTION, PROTOTYPE AND VALIDATION

for the infrared sensor, also in this case a hole in the sensor node enclosure is needed, thus allowing the proper sensor functioning.

Therefore, Table 3.11 resumes the test outcomes and the judgement, which has been deduced considering four main parameters, namely: physical robustness, integration with sensor node enclosure, field-of-view dimension, measuring reliability. In particular, good, medium or bad judgments are used.

<i>Technology</i>	<i>Robustness</i>	<i>Integration</i>	<i>Measuring Range</i>	<i>Reliability</i>
<i>Radar</i>	good	good	good	good
<i>Infrared</i>	medium	medium	bad	medium
<i>Ultrasound</i>	bad	medium	bad	bad

Table 3.11: Sensors evaluation on the basis of four main parameters given by the experimental tests outcome and specific technology features.

3.7. TESTING OF THE WSN MONITORING SYSTEM IN CONTROLLED TEST-SITE

Chapter 4

Engineering and Pilot Site Extension

This chapter describes the engineering process performed on the basis of the validation conducted and described in the previous sections. In particular, the Doppler radar identified as off-the-shelf technology is kept as unique technology on the WSN sensor node, since it allows gathering more useful information from the monitored area. Therefore the final prototype of the sensor node is defined, together with the engineering process aimed at optimizing power consumption, dimensions and performance.

4.1 Doppler Radar

The proposed monitoring system is mainly based on the use of Doppler radar sensors. As well known, the physical phenomenon behind the device functioning is the Doppler effect, for which a moving target implies the frequency shift of the backscattered signal with respect to the signal transmitted by the sensor itself. Therefore, particular attention should be given to the surface characteristics on which the signal impinges, since different effects on the electromagnetic wave may be experimented, such as different reflections and scattering phenomena.

More in detail, the Doppler effect describes the capacity of a moving target of producing a frequency shift of the reflected electromagnetic wave, from which useful information may be retrieved. One of the principal application of such effect is represented by the Doppler radar sensors, which are able to estimate the target velocity by exploiting the frequency shift between the backscattered and the transmitted signals. Typical example of such phenomenon is given by an ambulance moving with respect to a stationary observer. The sound emitted by the vehicle alarm, which is specifically emitted at a certain frequency, will be perceived by the observer in different ways as the ambulance approaches or leaves the observer. In particular, in the former case the frequency shift will allow the observer hearing an higher frequency alarm and viceversa when the vehicle leaves the observer, the perceived alarm frequency will be lower than the actual one.

Therefore, considering the scheme shown in Fig. 4.1, the Doppler shift may be computed as follows:

$$f_{shift} = 2v \frac{f_{tx}}{c} \cos(\theta)$$

where:

- f_{shift} represents the frequency Doppler shift of the radar transmitted signal, expressed in Hz;
- v is the actual target speed, expressed in m/s;
- f_{tx} is the radar emitted signal, expressed in Hz;
- θ is the angle between the target motion trajectory and the orthogonal direction to the radar sensor, expressed in radians.

For instance, the use of the described equation allows the easy computation of the target speed, given the working frequency, θ and the Doppler shift. Nevertheless, two particular cases may be defined, namely considering θ equal to 0° or 90° . Such conditions, in fact, are particular scenarios in which the target moves orthogonally with respect to the radar or it performs lateral/tangential movements with respect to the sensor plane respectively. Therefore the following may be defined:

- if $\theta = 0^\circ$ the maximum Doppler shift is obtained, given that: $f_{shift} = 2v \frac{f_{tx}}{c} \cos(0^\circ) = 2v \frac{f_{tx}}{c}$
- if $\theta = 90^\circ$ the minimum Doppler shift is obtained, given that: $f_{shift} = 2v \frac{f_{tx}}{c} \cos(90^\circ) = 0$

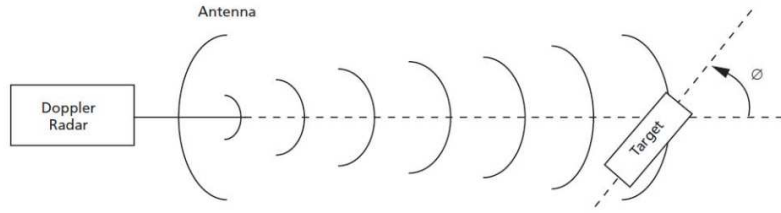


Figure 4.1: Doppler effect scheme.

During the design of such systems, the analysis of the ratio between transmitted and received power is a very important parameter, mainly related to system and target characteristics [64, 65]. In detail, the following relation allows computing the received power back in a radar system, by considering several parameters as described after:

$$P_{rx} = \frac{P_{tx} G^2 \lambda^2 A \sigma_0}{(4\pi)^3 R^4 L}$$

where:

- P_{tx} is transmitted power, expressed in Watts
- G is the antenna gain in dB unit
- λ is the wavelength of the radar transmitted signal, expressed in meters
- A is the area illuminated by the radar, measured in m^2
- R is the distance between radar and target, expressed in meters
- σ_0 is the target normalized Radar Cross Section (RCS)
- L represents the system losses

As it can be noticed, several parameters are involved in the computation of the received power and particular attention may be given to the RCS parameter, which allows measuring how much a target may be detected by the radar system,

4.1. DOPPLER RADAR

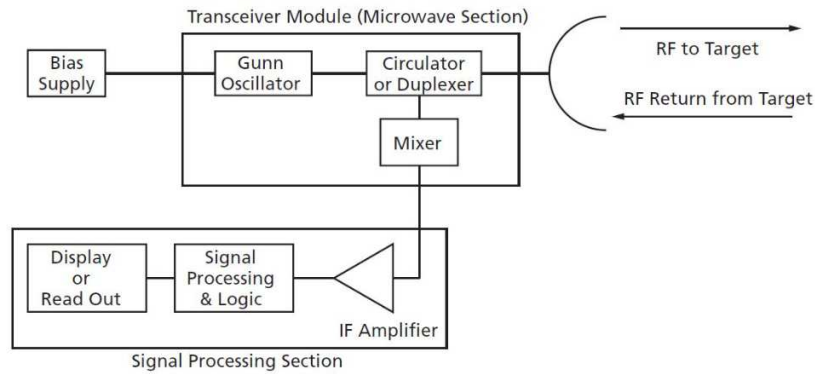


Figure 4.2: Doppler radar scheme.

namely higher RCS values state for highly detectable target and theoretically larger received power and viceversa.

Fig. 4.2 illustrated a simplified block scheme of a Doppler radar. In detail, the gunn diode, properly excited by the external power supply, generates electromagnetic waves at a given frequency, which are passed to the circulator or duplexer. The circulator is a microwave component generally composed by three or more ports and characterized by a direction of rotation. A typical application of such component is for signal decoupling and reception, since one port may be connected to the signal source, another port to the antenna element and from the last port the signal received on the antenna decoupled with respect to the source signal may be retrieved. Therefore, thanks to the use of such component, a continuous wave radar may be designed, which allows the simultaneous transmission and reception on the antenna.

The next component is represented by the mixer, which is used in order to shift the received signal to lower frequencies. In fact, let us consider the transmission signal frequency to be f_{tx} . The received signal frequency will be related to the transmitted one and to the Doppler effect, considering the presence of a moving target. Therefore, $f_{rx} = f_{tx} + \Delta f$ will be the frequency of the signal reflected by the target towards the antenna. At this point, the received signal will pass through the circulator and then to the mixer, where the signal multiplication with the one generated by the gunn diode will allow shifting to lower frequencies the received signal and specifically to the value of Δf . Thus the signal may be filtered and amplified for next processing stages.

In particular, thanks to the technological progress, all these components are integrated in a single one called transceiver, which only needs of a power supply and a radiating element.

Radar technology is widely used nowadays for several applications, which may range among space applications as described by authors in [66, 67], or weather applications, bird migration surveillance for wind energy systems, airborne radar, hydrology monitoring and many others. More in detail, for instance, [68] presents the development of an innovative tool for atmospheric storms observation based on Doppler radar, operating in the X-band frequency range and mounted on an airplane. In particular, considering this scenario, the radar is used in order to provide accurate measurements of air motion and rainfall related to large storms, which in general are too far and/or too large for being observable by ground radar systems [69, 70].

Another relevant field of application of the radar technology is related to surveillance systems and as an example monitoring wind turbine plants for bird migration phenomena [71]. Wind energy is very attractive and the number of deployed plants is growing a lot, thanks to the possibility of harvesting such energy wherever there are strong winds. The main problem concerning the turbine structures is related to birds and bats mortality mainly due to collision, displacement due to disturbance, barrier effect and habitat loss [72, 73]. Therefore, the authors propose the use of weather radar for providing quantification data regarding bird migration patterns, thus limiting the negative effect of this green, free and renewable energy. Doppler radar may also be exploited for wind observation analysis and in particular several methodologies have been developed, such as a multi-grid analysis of 3D Doppler radar radial velocity [74, 75].

Always in the environmental monitoring, radar has been used in order to map and monitor wetlands and forests, which are very important for water quality and aquatic habitat. Therefore hydrology studies may be conducted on synthetic aperture radar data used for such application as described in [76].

Additional studies have also been focused on the analysis of real-time estimation and compensation methodologies of airborne radar platform movements [77]. Airborne radars are nowadays essential devices for many applications, but due to the natural movements of the aerial platform, Doppler shift may be affected by this phenomenon. Therefore, accurate real-time estimation and compensation of such motions may be considered in order to properly allow moving target detection. To this end several studies have been performed, which may try to compensate the shift by adjusting the frequency of the oscillator, or by inserting a phase shift thus cancelling the unwanted effect [78, 79, 80, 81].

Different from the above application examples, [82] presents the application of Doppler radar for monitoring and analysis of respiration pattern in an unobtrusive manner. In particular, the identification of abnormal breathing pattern represents an important task very useful for improve knowledge about respiratory disorders and at the same time refining diagnostic procedures. Doppler radars have been largely used for health care monitoring systems and several works have been reported in literature [83, 84, 85, 86, 87], but as the authors of [82] declare, no specific studies have been focused on the identification of breathing patterns,

4.1. DOPPLER RADAR

thus allowing to capture different types of respiratory trends.

4.2 WSN Sensor Node Engineering

Considering the outcomes reported in Table 3.11, showing the judgment of the several technologies used during the previous phases of the project thesis, the doppler radar model RSM-1650 is the unique technology, which performs at a sufficient level for the aim of the monitoring system. Therefore, by using only this technology, the key idea is to exploit two radar sensors, thus doubling the WSN sensor node field-of-view. In particular, a sketch of this idea is shown in Fig. 4.3.

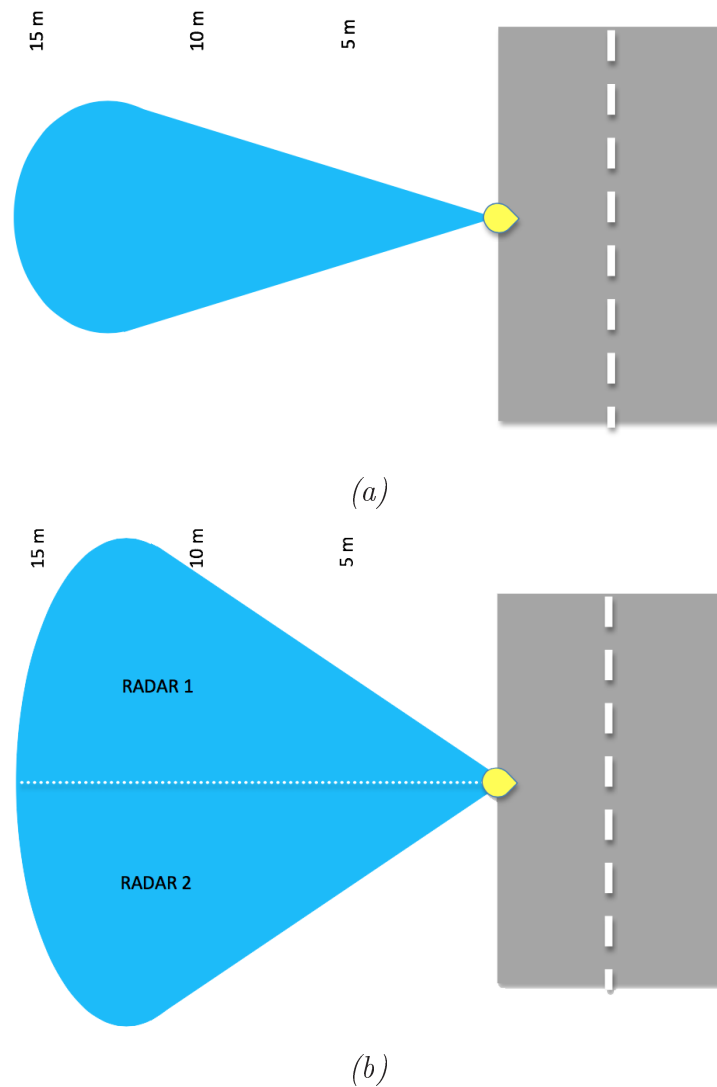


Figure 4.3: WSN sensor node field-of-view: (a) single radar module, (b) double radar module.

Therefore, given the second radar module, a change in the sensor node circuitual schematic is necessary and in particular an innovative solution is introduced in order to limit power consumption and to optimize the available resources. In this view, a multiplexer is introduced thus allowing the use of a single conditioning stage for the radar signal, being of the first or second radar module. Fig. 4.4 shows the block diagram of the proposed solution. The radar signals are multiplexed according to a specific logic in charge of the controller and thus programmed via its firmware.

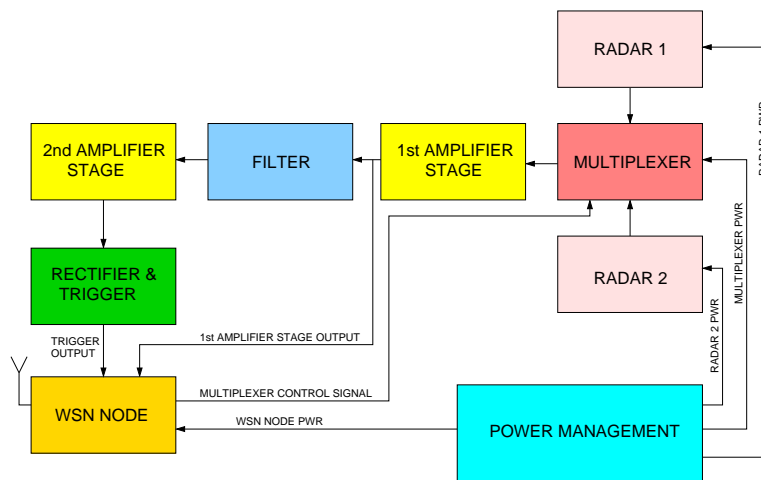
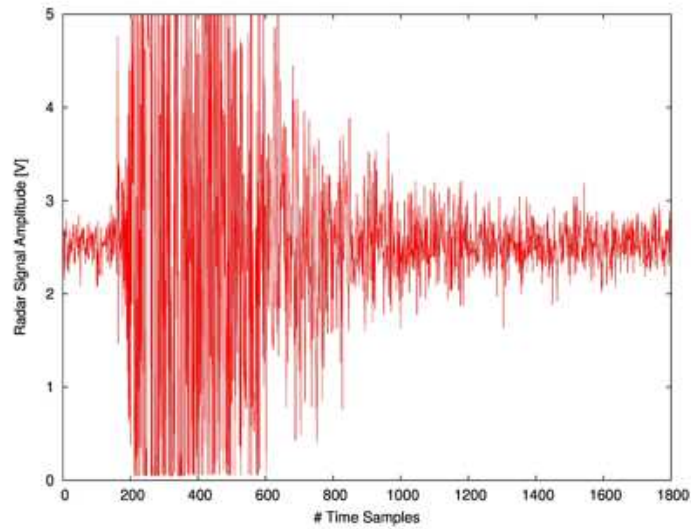


Figure 4.4: Block diagram of the conditioning stage in case of double radar module.

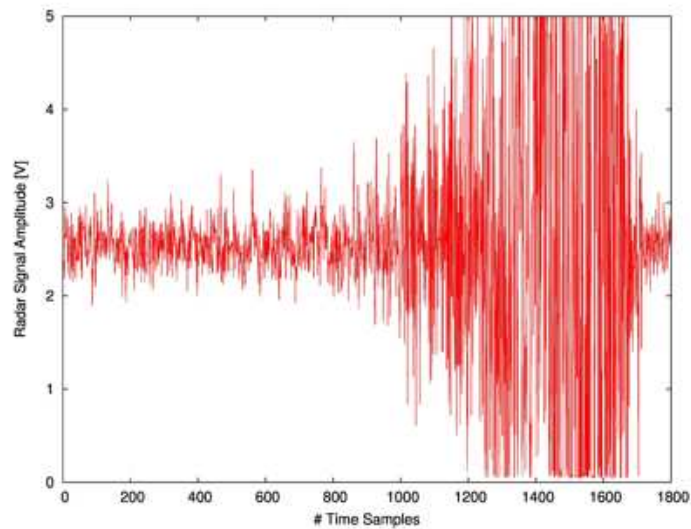
Additional information may be obtained by the radar sensors, thanks to the direct connection to the controller of the output of the first amplification stage. This allows the acquisition of a raw signal, which is highly informative with respect to the actual event occurred in the sensor field-of-view. This signal then continues the processing phase through the filtering stages, in order to neglect undesired signal components, and the rectifier, thus collecting the larger amount of the signal energy. The combination of such signals, namely raw and processed, may allow better event detection and analysis, thus improving the system performance. As an example, the processed signal may be used as trigger for starting the acquisition and processing of the raw signal. In this way higher computation demand is required only when actual movements are detected and in such cases more information are obtained by the combination and analysis of multiple versions of the radar signal.

Fig. 4.5(a) reports an example of the raw signal, output of the first amplifier stage, and relative to a leaving movement from the sensor plane. The signal stops

when the target has reached about 15m from the radar module. As expected the signal decreases progressively as the target move away. Similar case is shown in Fig. 4.5(b) in case of an approaching event. In this case, the target moves towards the sensor plane and the detection starts when the target is at about 14m from the sensor plane. Opposite to the previous case, the signal amplitude increases as the target approaches the radar sensor.



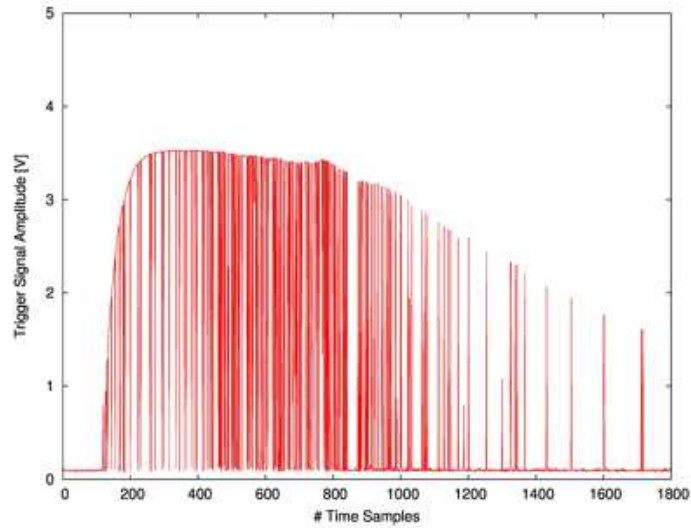
(a)



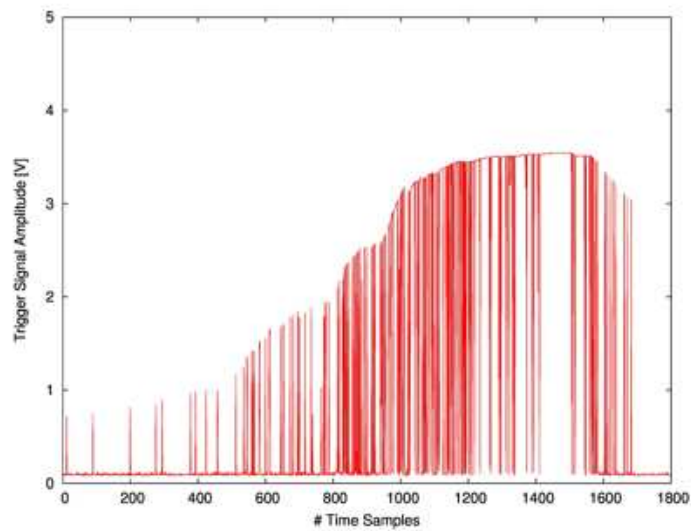
(b)

Figure 4.5: Radar signal output of the first amplifier stage: (a) leaving movement, (b) approaching movement.

Fig. 4.6 reports instead the processed signal, after the filtering and rectifier stages, corresponding to the same tests performed and shown in Fig. 4.5.



(a)



(b)

Figure 4.6: Radar signal output of the complete conditioning stage: (a) leaving movement, (b) approaching movement.

As it can be seen there is clear correspondence among the results and in particular it is worth noting that the processed radar signal, output of the complete

conditioning stage, allows the detection of the moving target at higher distances, specifically 20-22m from the sensor plane during leaving events and 17m during approaching events.

Therefore by comparing these results, it may be noticed like the processed signal may be exploited for the first event detection, which allows triggering the acquisition of the raw radar signal from which additional information may be retrieved (i.e., direction, speed, etc.).

4.2.1 WSN Node Platforms

Several technologies are available considering the WSN node platform, which represents the controller section of the WSN sensor node described in this document. Each of the devices presented hereafter are characterized by specific features, which may be advantages or disadvantages considering the specific scenario in which the platform has to be used. Therefore, the precise analysis of these components is a crucial aspect, in particular regarding the specific work the platform will have to perform.

A first classification of the WSN node platforms may be conducted on the basis of the radio module working frequency, namely 868MHz and 2.4GHz. In fact, these are the main working frequency adopted by such modules and it is a fundamental aspect for their definition since, as well known, the operating frequency of the radio module is directly related to the actual communication distance. In addition, for the sake of completeness, the following recall the inverse relation between frequency f and wavelength λ , given by: $\lambda = c/f$, where c is the light speed in meters/seconds [m/s], f is the working frequency measured in Hertz [Hz] and λ is the signal wavelength expressed in meters [m]. Thus the actual relation between wavelength and coverage distance allows determining that higher frequencies implies theoretically smaller communication ranges and viceversa considering lower frequencies. Nevertheless, such parameters may not be considered in absence of the actual radiation power, namely even radio modules operating at higher frequencies may perform larger communication ranges thanks to higher power transmission levels.

In the following, the main WSN platforms used nowadays are presented with a brief resume of their specifications:

- 3Mate platform
 - working frequency: 2.4GHz
 - IEEE802.15.4 standard compliant
 - transmitting power: [-25dBm, 0dBm]
 - printed antenna and external antenna connector predisposition
 - 16-bit microprocessor, 48KB flash memory, 10KB RAM

4.2. WSN SENSOR NODE ENGINEERING

- 12-bit analog-to-digital converter, with adjustable voltage reference (max 3.0Volt)
- power supply 3.3Volt
- dimensions: 70x40x15mm
- cost: ~\$140.00



Figure 4.7: WSN node platforms: 3Mate device.

- TinyNode platform
 - working frequency: 868MHz
 - transmitting power: [-3dBm, 12dBm]
 - wire antenna and external antenna connector predisposition
 - 16-bit microprocessor, 48KB flash memory, 10KB RAM
 - 12-bit analog-to-digital converter, with adjustable voltage reference (max 3.0Volt)
 - power supply 3.3Volt
 - dimensions: 30x40x10mm
 - cost: ~\$120.00



Figure 4.8: WSN node platforms: TinyNode device.

- Flyport platform
 - working frequency: 2.45GHz
 - Wi-Fi 802.11 standard compliant
 - transmitting power: 16dBm
 - printed antenna and external antenna connector predisposition
 - 16-bit microprocessor, 256KB flash memory, 16KB RAM
 - 10-bit analog-to-digital converter, with voltage reference (max 2.048Volt)
 - power supply 3.3Volt or 5.0Volt
 - dimensions: 35x48x15mm
 - cost: ~\$43.00



Figure 4.9: WSN node platforms: Flyport device.

- Arduino and XBee platforms
 - working frequency: 868MHz or 2.4GHz
 - transmitting power: 10dBm for 2.4GHz, [0dBm, 25dBm] for 868MHz
 - printed antenna and external antenna connector predisposition
 - 8-bit microprocessor, 32KB flash memory, 2KB RAM
 - 10-bit analog-to-digital converter, with voltage reference (max 5.0Volt)
 - power supply 3.3Volt
 - dimensions: 65x30x13mm
 - costs:
 - * Arduino FIO: ~\$25.00
 - * XBee Pro 2.4GHz Radio Module: ~\$38.00
 - * XBee Pro 868MHz Radio Module: ~\$82.00

4.2. WSN SENSOR NODE ENGINEERING



Figure 4.10: WSN node platforms: Arduino and XBee devices.

In order to validate the actual platforms communication coverage, an experimental scenario in road proximity has been identified, thus resembling as much as possible the actual working conditions of the WSN platform once integrated in the sensor node of the monitoring system. In particular, the tests have been performed along Via Sommarive and Via alla Cascata, Povo, Trento as shown in Fig. 4.11 together with the altitude measurements at some points along the stretches of road.

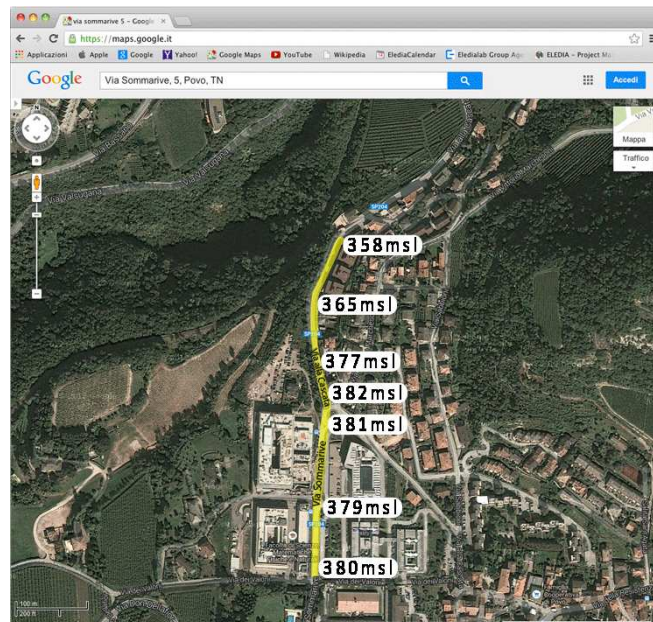


Figure 4.11: WSN node platforms testing: experimental test scenario map and altitude measurements.

In the experimental scenario the perfect line-of-sight is not guaranteed, given vehicles and pedestrian passages, which interfere with the actual radio communication. In addition, the stretches of road identified are not ideally linear and in particular two small curves are present, thus introducing some challenge in the experimental validation, together with different altitudes, which brings the communicating modules at different heights, in turn hardening the communication between them.

The performed tests imply the use of a couple of WSN node platforms of the same typology each time and therefore specific platform management firmware is implemented to periodically send data from one node to the other, with proper counter used to verify the actual packet-loss of the communication. The test is interrupted when no data is received anymore by the receiver node or when the actual packet-loss is too high, thus strongly degrading the communication between the nodes. In addition, the two nodes are respectively a transmitter and a receiver node. The receiver is kept still at one side of the experimental scenario, while the transmitting one moves farther as the communication works. Fig. 4.12 shows the actual WSN platform setup during the experimental validation.

In addition, the WSN node platforms are placed in a plastic case in order to allow the experimental validation being as much similar as possible to the actual application scenario of the monitoring system, thus validating the actual communication range with antennas installed inside the sensor node enclosure.

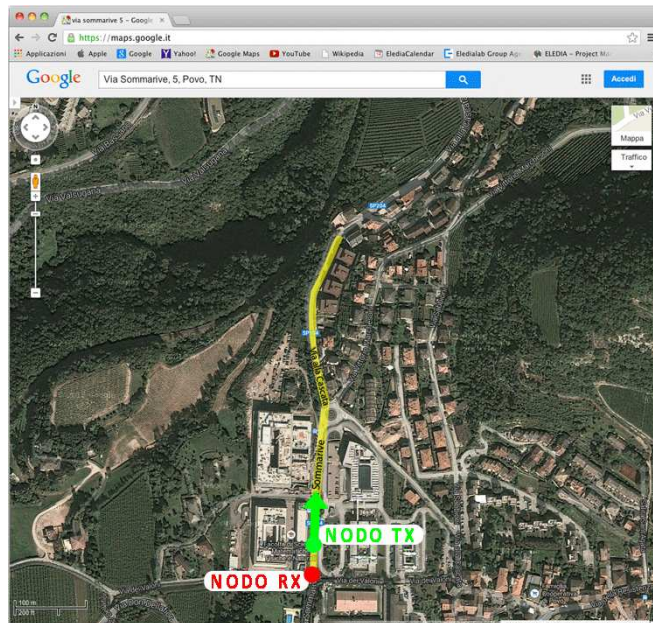


Figure 4.12: WSN node platforms testing: experimental setup and nodes position.

The following resumes the actual experimental outcomes obtained in terms of maximum communication distance between couple of same typology nodes:

- 3Mate platform:
 - maximum coverage: 280m
- TinyNode platform:
 - maximum coverage: 180m
- Flyport platform:
 - maximum coverage: 300m
- Arduino and XBee platforms:
 - maximum coverage: 400m for 2.4GHz
 - maximum coverage: 450m for 868MHz

Therefore, considering the tests outcomes, the WSN platform performing better than the other ones is represented by the Arduino and XBee combination platform and specifically considering the 868MHz radio module. Nevertheless, such solution is not cost-effective particularly considering the XBee module operating at such frequency. Thus, similar results have been obtained by the use of Arduino and XBee 2.4GHz modules. Such configuration, in fact, is more cost-effective and the actual maximum communication coverage resembles the previous one. The other technological solutions are not convenient for the monitoring system, considering costs and radio module performance.

4.2.2 Prototype Layout Optimization

Starting from the prototype developed and described in the previous sections, an optimization procedure has been performed in order to improve components positioning and implementing some circuital changes, which allow enhancing the prototype performance.

The circuital layout may be classified in three main sections, namely the power supply branch, the WSN node or controller, the radar signal conditioning stage. In particular, regarding the supply network and considering the final choice of the sensors used, namely the absence of ultrasound and infrared sensors, the possibility to exploit 12Volt battery is no more needed, thus the battery performing 6Volt, 4.5Ah is selected as definitive power supply of the WSN sensor node. Therefore, given this components selection, a first change of the circuital

scheme precisely regards the feeding network and the voltage regulators used. In fact, by using the 6Volt battery and the Arduino platform for the controller section, a single 5Volt voltage regulator with low drop-out (i.e., differential voltage computed as difference of the regulated output and the minimum input voltage needed by the component to properly regulate the output supply) is needed to supply internal circuitry and radar sensors, given that the WSN device is capable of efficiently convert the supply voltage to a stable 3.3Volt output for its own functioning. In addition, the 3.3Volt regulated output may be used for external supply or reference if needed, by exploiting the proper connections available on the WSN device. One major benefit of such change is related to the stability of the radar signal, directly at the output of the sensors, and the avoidance/reduction of noise introduced by the conditioning stages. Therefore the overall monitoring system takes advantage of the aforesaid stability, which means acquiring a more stable and more informative signal.

In addition, still regarding the supply network, a specific voltage regulator has been designed to properly manage the solar panel energy for the battery charge. Even if the lead battery charging process is less critical than the case of lithium batteries, particular attention may be addressed to such component in order to extend the system lifetime and to avoid possible malfunctionings. Indeed it is necessary to implement controlled charge-discharge cycles, arranging the regulator circuit in order to imply voltage and current limits towards the battery unit, thus avoiding possible excessive exposition to anomalous voltages and currents over the properly safe charging limits. Therefore, given the use of 6Volt 4.5Ah battery, the maximum allowed voltage is set to 7.5Volt with maximum current flow of 500mA, which is approximately the 10% of the actual battery capacity. In this way, the battery may be charged during a period of about 8 hours, considering the presence of clear solar radiation for all this time.

An additional advantage of such circuitry is given by the increased degree of freedom in the solar panel selection phase, ensuring in any case some minimal requirements needed for the proper work of the entire prototype, namely minimum solar panel voltage to be higher than battery voltage and solar panel effective current comparable and higher than the 10% of the actual battery capacity. All values over such conditions are filtered by the regulator designed.

Another relevant change, introduced in the optimized prototype, is related to the conditioning stage of the radar signal. In particular, the low pass and high pass filters, described in Section 3.4.1.1, are substituted by a band-pass filter composed by a Butterworth 2nd order low pass filter and a Butterworth 2nd order high pass filter, both with gain about 9dB. This allows filtering the radar signal with higher precision and a more stable transfer function, with respect to the previous solution namely composed by one low pass and two high pass filters, and with an higher gain, which allows improving the detection procedure applied after. In addition, the actual cut-off frequencies are respectively 100Hz and 1900Hz, which correspond to speed range of about 3-43Km/h.

An additional change regards also the amplification stages useful for enhancing the radar signal dynamic. In particular, the amplifiers are now designed on-board, thus improving the processing quality and the noise reduction. In the previous version, in fact, the amplifier modules used were off-the-shelf products and mounted on external breakout. This choice was very convenient during the prototype development, since tuning and setup procedures may be applied easily to the components. Nevertheless, the use of connectors and tunable electrical components may introduce noise and signal instability, which in turn appear during the conditioning stages. Therefore, once the desired setup is defined, the on-board design and implementation guarantee a larger reliability of the amplifier stages, thus improving the system performance.

Finally, considering the choice of exploiting two radar sensors, in view of optimizing the available resources a single conditioning stage is designed, thus a multiplexer is needed to allow periodically change of the analysed radar signal. In addition, in order to limit power consumption, the radar sensor is powered off during periods of non signal processing. Therefore, a specific dual load switch with controlled turn-on is used to this end. In particular, two digital connections of the WSN node are used to control such component.

Fig. 4.13 shows the circuitual schematic of the optimized solution, which integrates all the changes described in this section.

The final step regarding the optimization of the interfacing board is related to the design of the actual board layout, by defining the maximum dimensions of the printed circuit and the position of each circuitual component on it. Therefore particular attention have been put in this design process, defining as maximum amount of space the area 210x70mm. This area is defined by considering the actual dimensions of the road delimiters, which are particular plastic structures large about 85mm. The board layout is shown in CAD sketch in Fig. 4.14. As it may be noticed, the principal components of the interfacing board are grouped following the aforementioned classification and distributed on the board thus avoiding possible interferences among circuitual strips. The two centered holes are provided in order to install the radar sensors support, while the decenterd one in the lower section is dedicated to the installation of the radio module antenna.

Particular attention has been focused on the radio module radiating element and its positioning inside the sensor node case, by considering the actual installation position of the devices along the road. In fact, given the vertical orientation of the device enclosure and the gateway node position, which may be at higher level with respect to ground, thus having better radiation to and from the sensor nodes, the antenna component has been placed such to be at the higher position allowed by the device case. The proposed solution of installing the antenna inside the case is mainly due to better protection and camouflage effect.

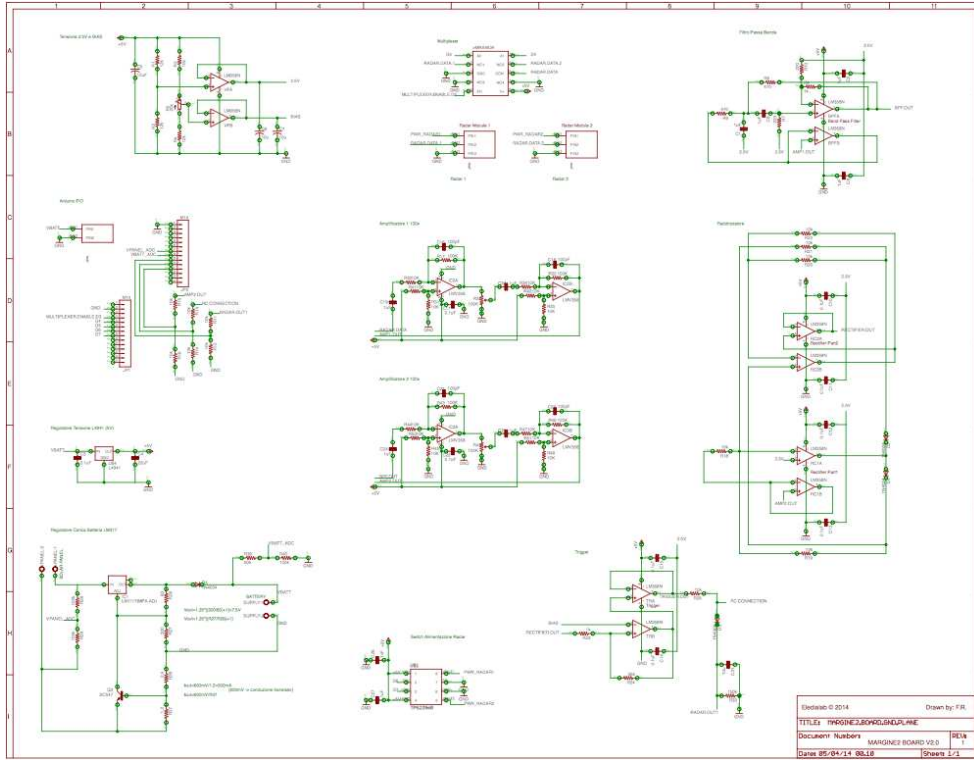


Figure 4.13: WSN sensor node prototype optimization: circuitual scheme.

The four corner holes are designed for board installation on the support of the case as described in the following.

The optimization and engineering steps described allow also the reduction in total power consumption, thus obtaining a mean current drain of 50mA considering normal prototype functioning. Therefore, a simple power budget may be computed, similar to what has been done for the non optimized sensor node. Considering the 6Volt 4.5Ah battery and the mean current consumption of 50mA, the prototype lifetime with the only battery as power supply is given by:

$$T_{life} = 4.5Ah/50mA \simeq 90h \simeq 4 \text{ days}$$

In order to allow system extended lifetime, the activity periods of some components may be properly managed, thus decreasing the overall consumption. In particular, radar modules are the most energy consuming devices together with the radio module of the WSN node. Therefore the introduction of small sleeping periods for the sensors and the use of the radio module only when specifically needed allow enhancing the prototype performance, reaching increased lifetime periods (e.g., 8-10 days) to be evaluated in relation to the actual period of clear solar radiation for battery charge.

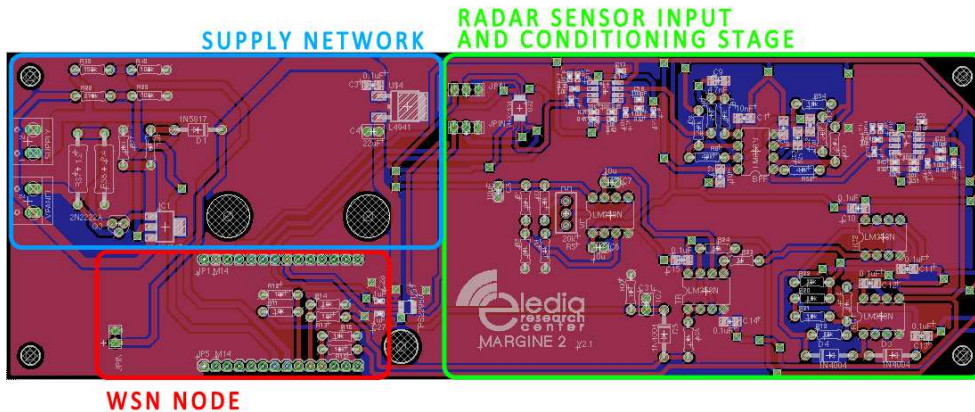


Figure 4.14: WSN sensor node prototype optimization: board layout.

4.2.3 Radar Sensor Support

The choice of using two radar modules, implies the need of specific supports able to steer the sensor field-of-view in the desired direction. In particular, for sake of completeness, the radar sensor presents a radiation pattern of 80° in the horizontal plane and 32° in the vertical plane. Therefore, for instance, steering such sensors of about 20° on the horizontal plane, may allow defining the complete sensor node field-of-view as an angular sector with radius the maximum distance at which the target can be detected, namely 15-20m from the sensor plane, and aperture angle of about 120° .

In addition, the need of steering the radar module is also dictated by the ability to conformly adapt to the different scenarios in which the sensor node may be installed, namely avoiding obstacles in the monitored area or overcome natural obstructions or slopes by tilting the sensors in the vertical plane.

Therefore, given the need of horizontal and vertical angular adjustment, an angular joint has been identified as support for the installation of the radar sensors. Fig. 4.15 show a view of the component. The extremities of the joint are threaded, thus allowing on one side the easy installation of the joint on the circuitual board and on the other the prompt fixing of the radar enclosure on it. In fact, in order to physically protect and to shield the radar modules from possible reflections or noisy signals coming from behind the sensor field-of-view, the modules are placed inside a small metallic box with a small perforated lateral section useful for the fixing on the axial joint. This setup is shown in Fig. 4.16.

The axial joint is mainly composed by two sections: the base with rotation sphere housing and the steering pivot. Both components are made of plastic material, thus the direct contact with the circuitual board do not represent any problem from the electrical point of view, avoiding additional isolating layers.

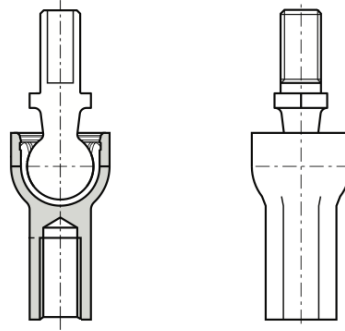


Figure 4.15: WSN sensor node prototype optimization: radar sensor axial joint.

The angular joint dimensions are about 45x20mm and its compact size allows the integration in the optimized sensor node. In particular the maximum steering angle is about 25° , which in turns imply that the maximum inclination angle of the radar sensor is 25° . This setup, therefore, allows obtaining a complete field-of-view of about 130° - 140° per 15-20m distance.

It is worth noting that each sensor is mounted on a separate support, thus higher degree of freedom are ensured by this solution. Therefore, the adaptability of the sensor node to the actual installation scenario improves the overall system performance.

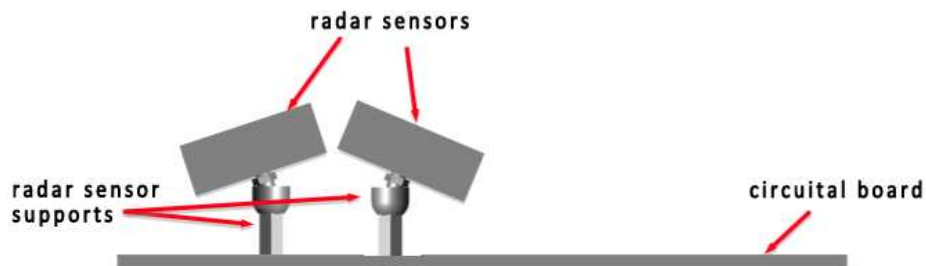


Figure 4.16: WSN sensor node prototype optimization: radar sensors and supports.

4.2.4 Optimal Case Definition

Several analysis have been conducted in order to define the optimal case for the WSN sensor node in its engineered and optimized version. In particular, the definition of the actual total dimensions to properly fit each component has been investigated, with particular attention to battery positioning mainly for security reasons. Additional investigated parameters are waterproof, mechanical robustness, easy integration on road delimiters. The maximum size of the packaging is defined in relation to the dimensions of road delimiters, which are about 100x100x1300mm, width, depth and height respectively. In addition, dimensions have to be carefully taken into account in order to allow the installation of solar panels for battery charge task. To this end, ad-hoc solar cells have been realized on the basis of electrical characteristics needed for the actual battery maintenance and the actual size of the case under definition.

Nevertheless, given the absence of low-cost solutions available off-the-shelf, able to satisfy all the imposed requirements, in particular considering reduced size and easy integration of the WSN sensor node components, an ad-hoc case has been designed and realized. The first version of such case is shown in Fig. 4.17, with maximum dimensions 90x90x300mm. The case is composed by methacrylate material properly modeled and soldered to guarantee waterproof feature, given also the unique aperture in the lower side closed by a joint screwed in cap.

This design allows furthermore a separated access to the two main components of the sensor node, namely the battery and the interfacing board on which sensors, controller and circuitry are installed. The battery unit is installed on the lower cap and in this way it is the first component to which the operator may have access to. Only by properly unlocking the interfacing board, this can be extracted from the case for maintenance activities. The key idea is that no particular interventions should be performed regarding the electronic board or the controller and sensors. Considering the normal device activity, the main maintenance should be related to battery replacement once its life-cycle is terminated. Therefore even non expert operators may perform the substitution having access to the only needed WSN sensor node section.

The fixing method to road delimiters is based on four main holes for metal rivets or screws symmetrically placed in the top and bottom areas of the case back side, as shown in Fig. 4.17(b). Additional slots are present in order to allow different fixing by using metallic or plastic strips.

The case inside is completely free and a simple sliding profile is used to properly position the electrical board of the sensor node. In particular, the four corner holes present on the electrical board are used to fix it on the sliding profile with plastic screws and thus by only moving this component, all the circuitry of the sensor node may be extracted or inserted in the correct position. In addition, small plastic guides are present in order to drive the movement of the

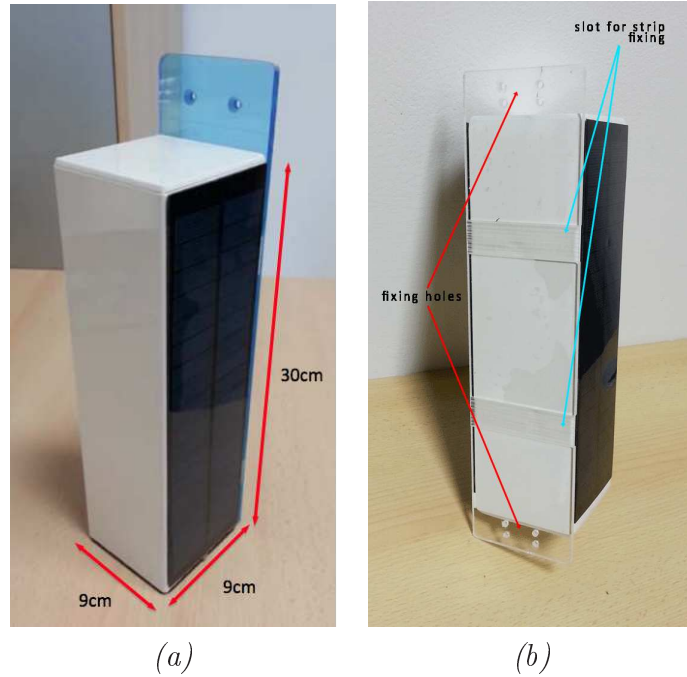


Figure 4.17: Optimal case definition: (a) front view and dimensions, (b) back view and fixing holes.

sliding profile inside the case. A lock is wedged in between the case back and the sliding profile thus avoiding the last to move when the lower cap of the case is open. Fig. 4.18(a) shows the circuit board installed on the sliding profile, while Fig. 4.18(b) is a snapshot of the installed sliding profile with a view of the lock and the guides for profile insertion.

An additional optimization regards the battery installation support, which is attached to the case cap. In particular, as it may be shown in Fig. 4.18(a), the battery unit may be laid on the vertical support, which allows fixing the battery with plastic strip or alternative solution, thus avoiding any possible contact between the battery and the internal circuitry especially during opening and closing case procedures.

4.2.5 Integration Testing

On the basis of the optimization changes discussed in previous sections, an analysis of the actual prototype working is performed. In particular, regarding the power supply network and power consumption, the use of specific equipment to monitor the effective power consumption allowed determining that the engineered board actually requires 7-8mA current against the estimated 10mA. Similar re-

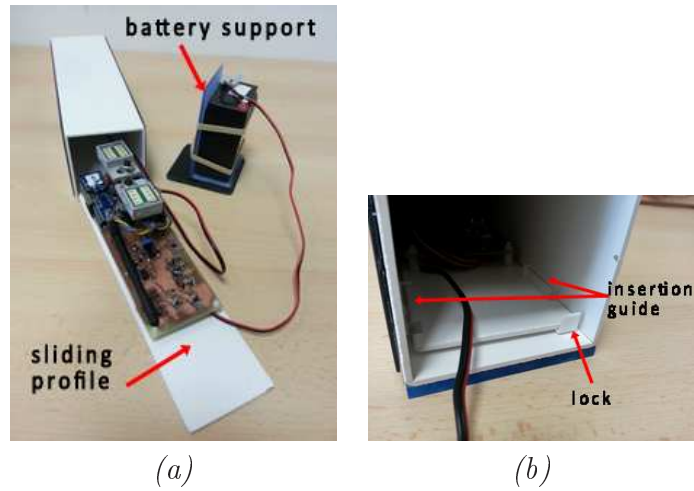


Figure 4.18: Optimal case definition: (a) sliding profile for board insertion, (b) insertion guide and lock.

sult is also obtained by considering the actual radar sensor working, which draws 32mA over the 40mA declared on its datasheet. Therefore these results allow observing an improvement of the sensor node lifetime based on the computation performed above.

In addition, regarding the conditioning stage, the filtering circuit is accurately analysed in order to validate its proper functioning. The use of signal generator and the evaluation with the radar signal allow confirming the filtering capabilities, with cut-off frequencies centered at about 100Hz and 1900Hz, which correspond to desired movement with speed in the range 3-43Km/h. The gain in the pass-band is quite constant at 18dB level as designed.

The radar sensors are also validated in particular considering the proper working and stability with the new voltage regulator and validating the actual detection range given the presence of the sensor node enclosure. Therefore, by using oscilloscope the radar signal output is validated and the voltage regulator benefits may be easily observed by looking the direct sensor output. In particular, in still condition the output signal is very steady and no relevant noise may be observed. Regarding the maximum detection range, instead, a small reduction is observed considering the presence of the sensor node case. In detail, without any obstacle the radar sensor is capable of detecting targets at the maximum distance of about 16-18m, while if the radar modules are installed inside the enclosure this maximum distance is shortened to about 14-15m.

Similar result is obtained by evaluating the total coverage of the controller radio module. In particular, by installing the module antenna outside the case, the maximum communication distance is about 450-500m, while installing the antenna inside the enclosure the distance 400-450m is reached at maximum.

Therefore it is clear that the enclosure presence impacts on the actual perfor-

mance of the sensor node, but it is worth noting that the degradations induced are not relevant to the aim and actual working of the monitoring system.

4.2.6 Controller Firmware

4.2.6.1 Sensor Node Firmware

The general functioning of the sensor node is, as already said, managed by the controller unit represented by the Arduino FIO platform. Therefore proper firmware has to be developed in order to allow the correct working of each single component thus in turn achieving the monitoring system objective.

Simpler version of the controller firmware have been written for the testing procedures, but in such cases particular attention may be given to specific part of the sensor node (e.g., radar sensor, amplifier stages, power management, etc.), thus the complete management of the device was not addressed. Therefore, custom management firmware has been developed, able to properly direct all the sensor node components together with a proper network management logic, given the large number of devices, which should be part of the network.

Therefore, particular attention is given to the control of the radar sensor, as well as the conditioning stage and the amplifiers used. Indeed, the proper management of these and all the other sensor node components allow the development of check and update procedures for the state information of the sensor node, which are very useful in order to monitor the actual working of each single device in the network. These information may be periodically sent to the control unit for data analysis and statistics. In addition, an optimal management of the available resources, namely both components, sensors and energy sources, allows improving the device lifetime and thus the overall system lifetime.

In code development, the use of parametric variables simplifies the firmware structure in relation to the specific installation, allowing in turn changing or correcting some parameters in an easy way, for instance coherently with the actual functioning of the other devices in the network.

Fig. 4.19 shows the flux diagram of the firmware developed for the sensor nodes. As it can be seen, the principal state is the *idle* one, which the controller cyclically executes and after which several firmware states may follow in relation to some state checks performed. In detail, the controller starts for the first time by sending to the gateway node a periodic info packet, in which some state information are written together with its identification code and its epoch time. Once this message has been sent, the controller enters in the *sync* state, in which attending the gateway node to send the correct epoch time for synchronization purposes. This operation may be executed within a parametrized period of time, after which the sensor node continues its operations even if the synchronization step do not successful. In the firmware flux the next operation regards the state check, specifically aimed at verifying the actual battery voltage to determine if the sensor node may operate or not. If it is the case, then the node actually

4.2. WSN SENSOR NODE ENGINEERING

starts the monitoring procedure, by periodically power on/off a radar sensor at a time and processing its output signal through the conditioning stage. Now, if an event is detected, the sensor node immediately power on the radio module for transmitting the processed data to the gateway node and to the control unit. After data is sent, the radio module is powered off and the overall flux starts again from the *idle* state. Nevertheless, if the battery voltage is too low for correct operation, the sensor node goes in a stand-by modality in which radar sensors and radio module are powered off, in order to allow the battery recharge thanks to the solar energy. Up to this is achieved the sensor node may not work. In particular, on the base of the actual battery voltage, three main possibilities are available:

- if battery voltage is high, then the device continues the normal functioning;
- if battery voltage is at a medium state, then the device may introduce a short sleep period in which main components are powerd off thus allowing the battery to recharge;
- if battery voltage is low, then the device powers off radar sensors and radio module, waiting for the battery to completely recharge.

The battery voltage levels described before in high, medium and low are specific parametric variable defined in the firmware, allowing prompt adjustment if needed. Fig. 4.20 illustrates the described options.

In addition, during the *idle* state, as said before, some opertions may be performed on a periodic time schedule. In detail:

- periodic state information may be transmitted periodically to the gateway node. The amount of time between successive sending is parametrized and set as default to 1 hour;
- synchronization step may be performed periodically in order to allow each single sensor node to be on time with respect to the others, thus allowing the implementation of specific logics for power on/off of the devices, for instance during daily hours the sensor nodes may be powered off since the wildlife road crossing risk is quite low. To this end, it is therefore necessary that all the nodes are on time for the correct working of the monitoring system.

In addition, after both the radars have been read, a small period of sleep may be introduced in order to extend the device lifetime. In particular, as default settings, the periodic change between radars happens every 250msec with 500msec of sleep period after both sensor have been acquired. It is worth noting that

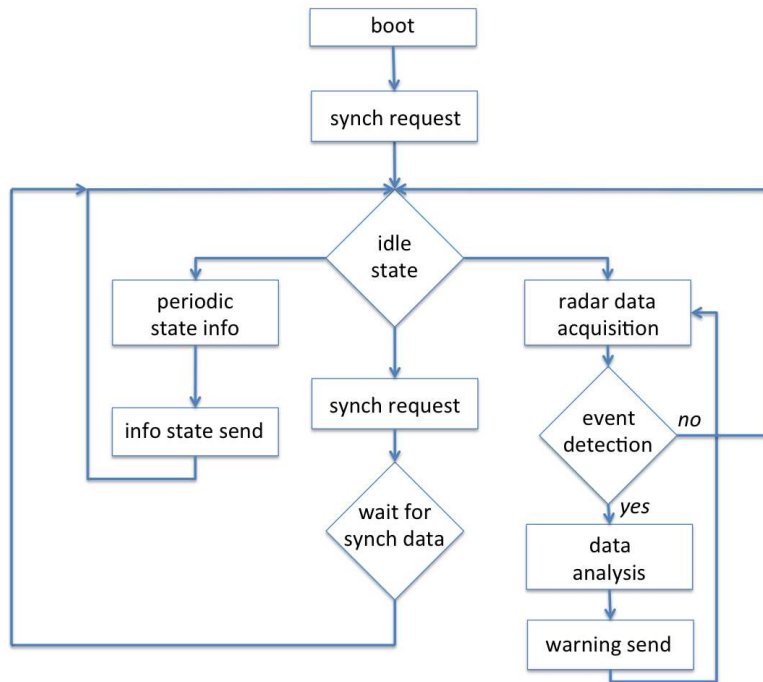


Figure 4.19: Controller firmware flux diagram.

the sleep period is executed only if no events have been detected by the radar modules, otherwise the firmware is programmed in order to keep the acquisition on the radar, which is detecting the event for total 500msec, after which the reading is turned on the other radar module in order to have a complete view of the monitored scenario. Therefore, in such condition, the radars are never powered off and no sleeping periods are introduced. Only when no radars detect an event in their respective field-of-view, then the normal functioning is restored.

4.2.6.2 Gateway Node Firmware

The gateway node requires the development of dedicated firmware able to interact with the operations ongoing on the sensor nodes. Therefore, two main activities are executed:

- data reception over the wireless link and forward towards the control unit;
- epoch time conversion from control unit time, which has to be sent to sensor nodes when required.

To this end, two serial communication are implemented, each dedicated to one of the tasks above-mentioned. In particular, regarding data reception coming

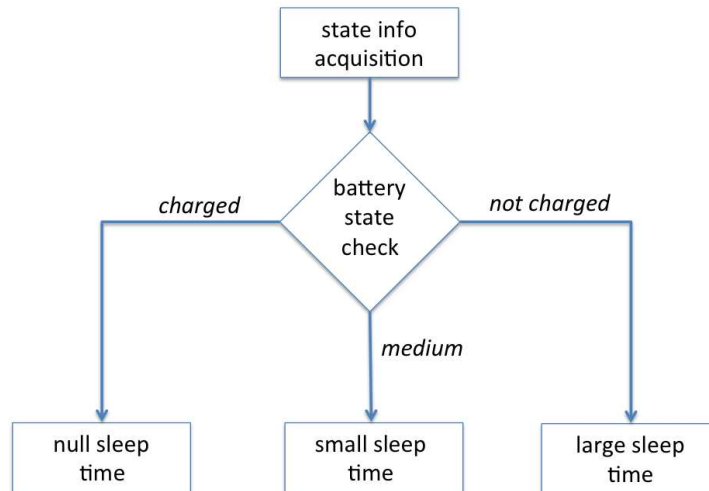


Figure 4.20: Controller firmware flux diagram: battery voltage check and adaptive sensor node activity regulation.

from sensor nodes, the serial communication used is the standard one available on Arduino platforms, which is easily redirected to the serial communication towards the control unit in charge of storing data.

Considering instead the second task, namely epoch time conversion for synchronization among WSN nodes, a specific serial communication has been implemented, by using digital connections of the Arduino platform, thus generating the so called software-serial communication. This allows having two distinct serial communications towards and from the gateway node, thus separating specific tasks which may be performed asynchronously.

Therefore, the gateway node firmware is mainly composed by a single loop in which both serial communications are continuously analyzed waiting for respective data. In fact, the synchronization is periodically given by the control unit, which sends its time to the gateway node. When this happens, the gateway node converts the time in epoch format and this value is sent to the asking sensor nodes when needed.

4.2.6.3 Validation Test

Experimental validation in controlled environment has been performed in order to actually verify the proper working of the firmware described in the previous section. In particular, some sensor nodes have been used for the tests, each located at different distances from the gateway node. This setup, in addition, has allowed the validation of the transmission quality of the radio packets among nodes, by observing the packet loss index.

In particular, the proper working of the firmware has been validated on all

the sensor nodes used, particularly considering the battery managements logics described above. In addition, regarding the wireless communication quality, in the worst case the amount of packet loss has been registered at about 10% of the total transmissions, with 1% packet loss considering periodic information packets.

4.2.7 Event Detection Methodologies

The development of event detection methodologies for Doppler radar systems may require complex computational load, also in relation to the actual signal to be processed, namely raw or pre-processed data.

Therefore, two main categories for data analysis and event detection may be defined:

- software based methodologies applied to the sensors signal output;
- hardware based methodologies in charge of pre-processing the sensors signal output for successive analysis.

The main distinction between these two categories may be focused on the actual computational capacity the microcontroller in charge of it have and on the hardware complexity needed to process the raw signal.

Considering the first case, specific methodologies have been largely investigated in literature. For instance [88, 89, 90, 91] exploit several methodologies for the analysis of radar signal, without any filtering or de-noising process. In this context, two methodologies are mainly used based on frequency transform methods, by using the Time Discrete Fourier Transform, or on auto-correlation methods.

Both these analysis may allow achieving accurate results in terms of resolution of the processed data, nevertheless the computational burden required may be carefully evaluated in relation to the actual performance of the controller platform available. One of the main advantages of such software methodologies is related to the huge number of information available after the processing, such as speed, movement direction, etc.

Considering, instead, hardware based methodologies, the pre-processing procedures may appear very complex and expensive in terms of circuital components, but they may allow lightening the software/firmware complexity and in turn the computational burden required by software methodologies. This may also be expressed as a considerable energy saving, fundamental aspect for low-energy devices, thus extending the device lifetime.

Therefore, the engineering development of the sensor node exploits both these methodologies, namely hardware and software, in order to take advantage of both of them. In particular, as already described, the pre-processing of the radar signal is performed thanks to the hardware conditioning stage implemented on the

4.2. WSN SENSOR NODE ENGINEERING

circuitual board of the sensor node, thus allowing reduced complexity in firmware development and node management. As already described in the previous sections, the use of filtering and amplification stages allow improving the radar signal quality, limiting noisy components and emphasizing the signal components related to occurred events, which have been detected by the radar sensors. For instance, the event speed filter in the range 3-43Km/h may simplify successive analysis since this parameter has already been detected, thus concentrating to other informative parameters. The successive stages of the processing allow rectifying the analysed signal, thus evaluating the event entity directly from the energy content of the processed signal. After this step, an additional section simplifies the detection capability of the controller platform, since the RC circuit designed allows a sort of delay in the signal dynamic, thus the controller can sample this signal even at lower frequency.

Fig. 4.21 shows an example of radar signal acquired by the controller platform and processed with the hardware pre-processing methodology. In particular, the signal represented in the plot is related to a real event occurred in the sensor field-of-view, lasting about 1sec with the target approaching and leaving the scenario at the minimum distance of about 6m.

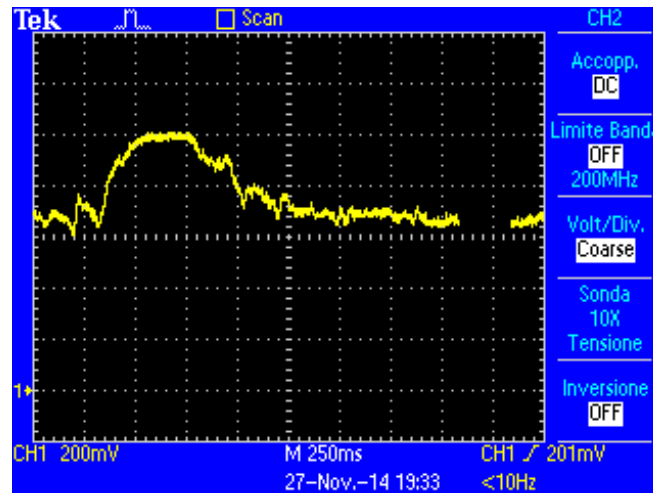


Figure 4.21: Movement event: radar signal output of the hardware pre-processing methodology.

Therefore, the detection may be allowed with simple threshold mechanisms, thus detecting the time instants in which the processed signal goes beyond the set threshold value or stays in a specific range validated experimentally, or more complex procedures. In addition, the experimental validation has allowed an accurate calibration of the processing and detection methodology, allowing good performance adequate to the monitoring system objective.

This pre-processed signal can be used to start the detection of raw radar signal, acquired and processed only in relation to event detection, from which additional information regarding the occurred event may be retrieved. Thus, the proposed methodology allows combining a first detection phase, very easy from the software point of view, and in turn with low computational burden, with a second detection phase, more complex and aimed at extracting additional information from the raw radar signal, thus improving the knowledge of the event occurred in the sensor node field-of-view and the related risk level for incoming drivers. It is worth noting that the second detection phase is activated only if the first one has detected an event, otherwise no additional processing is performed.

4.3 Experimental Validation

Given the previous integration and validation tests, mainly devoted at evaluating the proper working of the main components introduced with the optimization and engineering processes on one side and the firmware correctness on the other, an additional testing campaign has been performed, in order to validate the overall system in real controlled scenario, by investigating parameters such as radio coverage, system robustness in event detection, and warning capability.

Therefore, a real scenario resembling pilot test features is identified to perform the experimental validation. In particular an empty area sufficiently wide to allow the maximum radar sensor coverage (i.e., at least 15m) is discovered, thus allowing movement generation inside and outside the sensor nodes field-of-view.

The sensor nodes used during this process have been installed on specific tripod supports, allowing their deployment in conditions as similar as possible to the actual final installation on road sides. In particular five nodes have been used. Fig. 4.22 shows a picture of the installed sensor nodes, placed at the height of about 1m, which is the installation position the sensor will have on the road delimiters.

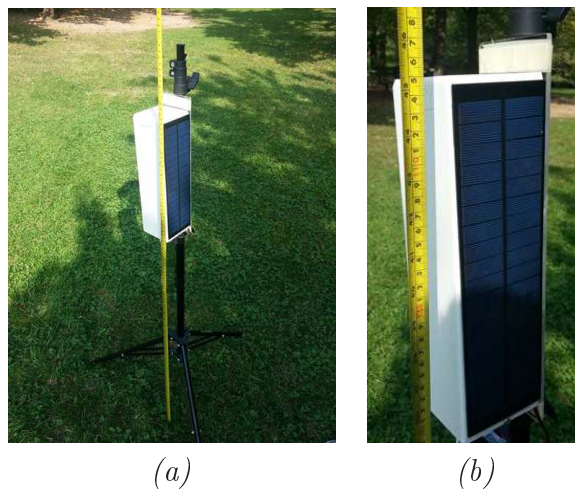


Figure 4.22: Experimental testing: (a) sensor node installation support, (b) sensor node installation height.

In addition, the sensor nodes used during these tests have been deployed at about 20m from each other (Fig. 4.23), similarly to the road delimiters position along the stretches of road.



Figure 4.23: Experimental testing sensor node installation distance.

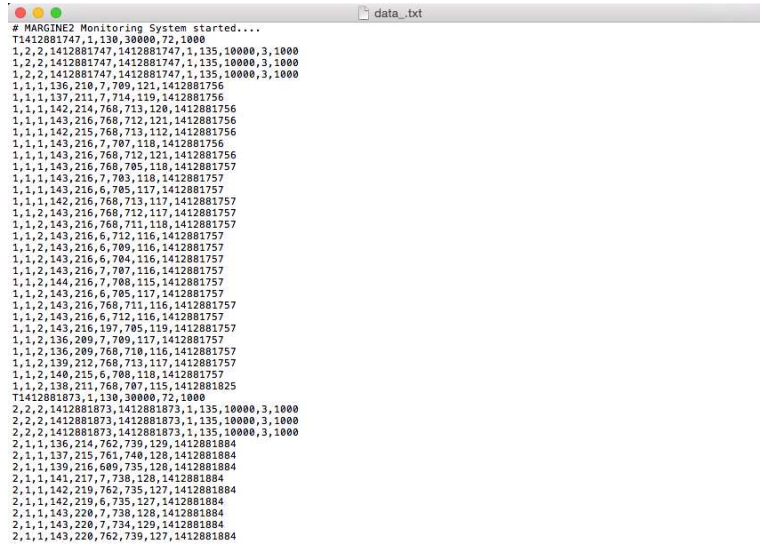
The performed tests in the identified scenario, with the setup described above, are mainly characterized by movements and events in the sensor nodes field-of-view. In detail the movement typologies may be resumed as follows:

- lateral movement to the sensors plane;
- orthogonal movement to the sensor plane (i.e., approaching or leaving movements);
- circular movement in the sensor field-of-view.

In addition to such events, movements in between near sensor nodes have been performed in order to validate the absence of shadow zones in which events may not be detected by the monitoring system.

The sensor nodes used for the tests are equipped with the firmware described in section 4.2.6. Therefore, as described, when a sensor node is powered on a specific procedure is activated before the device starts its normal functioning. The use of several sensor nodes during the experimental tests have allowed verifying the correct working of the controller firmware and Fig. 4.24 shows an example of radio packet messages received by the gateway node at the powering on of nodes 1 and 2. In particular, as it may be seen, the sensor nodes send the synchronization request to which the gateway node reply with its epoch time. Then the sensor node replies again with some functional parameters and its new working time, which corresponds with the gateway node time. The successive messages are related to movements of the operator, which is working of the specific device.

4.3. EXPERIMENTAL VALIDATION



```
# MARGINE2 Monitoring System started...
T1412881747,1,130,30000,72,1000
1,2,2,1412881747,1412881747,1,135,10000,3,1000
1,2,2,1412881747,1412881747,1,135,10000,3,1000
1,2,2,1412881747,1412881747,1,135,10000,3,1000
1,1,1,136,210,7,709,121,1412881756
1,1,1,137,211,7,714,119,1412881756
1,1,1,142,214,768,713,120,1412881756
1,1,1,143,216,768,712,121,1412881756
1,1,1,142,215,758,713,112,1412881756
1,1,1,143,216,7,707,118,1412881756
1,1,1,143,216,768,712,121,1412881756
1,1,1,143,216,768,705,118,1412881757
1,1,1,143,216,7,703,118,1412881757
1,1,1,143,216,6,705,117,1412881757
1,1,1,142,216,768,713,117,1412881757
1,1,2,143,216,768,712,117,1412881757
1,1,2,143,216,768,711,118,1412881757
1,1,2,143,216,6,712,116,1412881757
1,1,2,143,216,6,709,116,1412881757
1,1,2,143,216,6,704,116,1412881757
1,1,2,143,216,7,707,116,1412881757
1,1,2,144,216,7,708,115,1412881757
1,1,2,143,216,6,705,117,1412881757
1,1,2,143,216,768,711,116,1412881757
1,1,2,143,216,6,712,116,1412881757
1,1,2,143,216,197,705,119,1412881757
1,1,2,136,209,7,709,117,1412881757
1,1,2,136,209,768,710,116,1412881757
1,1,2,139,212,768,713,117,1412881757
1,1,2,140,215,6,708,118,1412881757
1,1,2,138,211,768,707,115,1412881825
T1412881873,1,130,30000,72,1000
2,2,2,1412881873,1412881873,1,135,10000,3,1000
2,2,2,1412881873,1412881873,1,135,10000,3,1000
2,2,2,1412881873,1412881873,1,135,10000,3,1000
2,1,1,136,214,762,739,129,1412881884
2,1,1,137,215,761,740,128,1412881884
2,1,1,139,216,609,735,126,1412881884
2,1,1,141,217,7,738,128,1412881884
2,1,1,142,219,762,735,127,1412881884
2,1,1,142,219,6,735,127,1412881884
2,1,1,143,220,7,738,128,1412881884
2,1,1,143,220,7,734,129,1412881884
2,1,1,143,220,762,739,127,1412881884
```

Figure 4.24: Experimental testing: data log file.

Fig. 4.25 shows an example of the performed lateral movements in front of the installed sensor nodes. The target moves along the red trace drawn, which is about 12-15m from the sensors. Additional tests have been performed by varying the gateway node position, thus allowing the validation of the maximum radio coverage.

The large majority of the performed tests have been correctly detected by the sensor nodes and the respective alarm signals have been received by the gateway node. Also considering lateral movements in the sensor nodes field-of-view, the correct sequence of alarms generated by the sensor nodes has always been evaluated in the correct order as the motion has been performed. In addition, the possibility to steer the radar sensor has allowed avoiding shadow regions in which events may not be detected. Thus the events repetition on statistical base has allowed determining the system performance in a real controlled scenario, which may be resumed as follows:

- sensor node distance: 18-20m
- maximum detection distance from sensors: 15m
- maximum radio coverage: 400-450m



Figure 4.25: Experimental testing: lateral movement in sensor nodes field-of-view.

4.4 Pilot Site Identification and Sensor Node Installation

The experimental pilot site has been identified around the Predazzo and Ziano localities on the SS48 road in the Val di Fiemme, Province of Trento, Trentino Alto-Adige Region, Italy, for about 500m stretch of road. Fig. 4.26 (a) shows the map of the pilot site location. Fig. 4.26 (b), instead, shows a graphical sketch of the sensor node installation along the road, together with the monitored area, called security area.

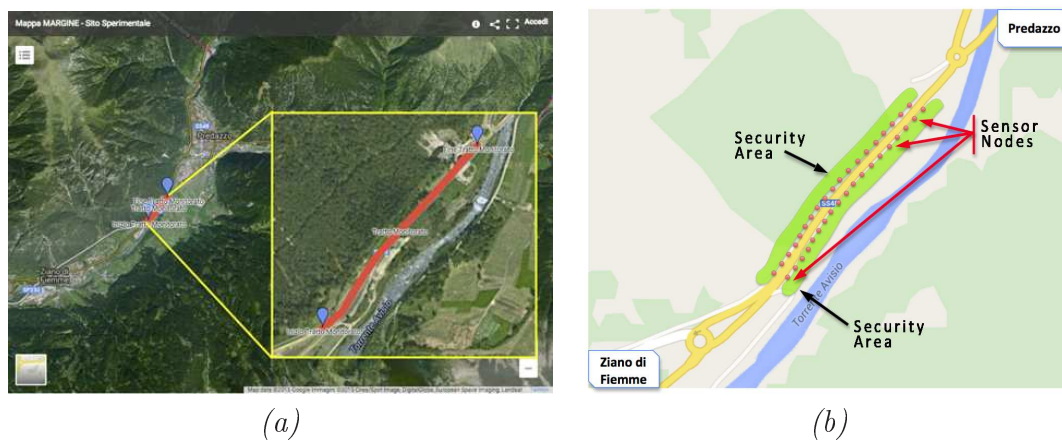


Figure 4.26: Pilot site: (a) map location, (b) node installation sketch.

The pilot site has been identified in collaboration with the 'Servizio Gestione Strade' of the Province of Trento and by considering some parameters particularly related to wildlife road crossing risk, namely actual incidents and crossing events registered in the last years. In addition, the presence of a dense wood on a side and the river on the other increases the probability of actual wildlife passages looking for good forage areas.

Fig. 4.27 depicts the actual system working. In detail, given the security area defined on the basis of the sensor devices field-of-view, shown in figure with the red box, the presence of events occurring inside such area determines their detection and the proper data transmission towards the control unit of the system. As already described, data are stored for successive processing and statistics.

Therefore, given the design and production of the sensor nodes as already described (Fig. 4.28 shows some sensor nodes under construction), the successive

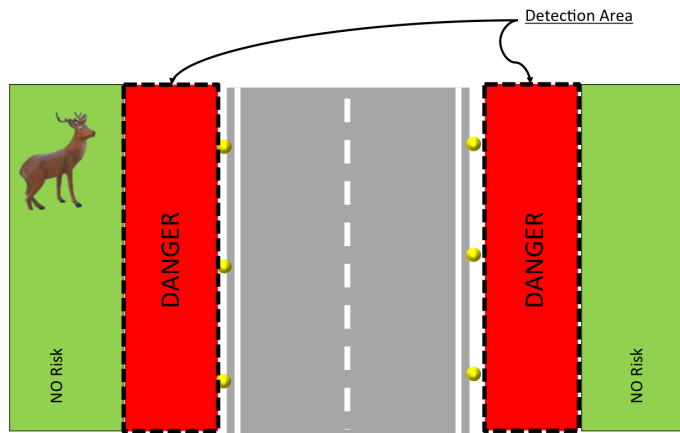


Figure 4.27: Wildlife road crossing monitoring system: risk definition scheme.

step has regarded the devices installation along the identified road. Thanks to the collaboration of the 'Servizio Gestione Strade' of the Province of Trento, the road delimiters have been accurately positioned at the reciprocal distance of 20m from each other throughout all the test site. This has allowed deploying the sensing devices with regular displacement between single pairs, thus avoiding shadowing areas in the security zone depicted by the sensors field-of-view.



Figure 4.28: Sensor nodes under construction.

4.4. PILOT SITE IDENTIFICATION AND SENSOR NODE INSTALLATION

The actual installation of the sensor nodes have been performed by exploiting the anchoring holes prefabricated in the case back and metal rivets have been used, thus ensuring a strong attachment to the road delimiter. Fig. 4.29 reports the fixing procedure of a sensor node on a road delimiter.



Figure 4.29: Sensor nodes installation on the pilot site.

Regarding the gateway node, given the presence of the variable message panel structure (Fig. 4.30 (a)- (b)), this component of the WSN network has been properly installed in a waterproof box directly attached to the metal railing of the structure 4.30 (c). Nevertheless, the presence of a huge metal structure near the antenna of the gateway node have implied the experimentation of radiation performance degradation, thus not allowing the system communicating over long ranges as expected. To solve this problem, a Yagi antenna has been used, thus improving the gain and radiation pattern of the gateway radio module 4.30 (d). This solution, in fact, allows restoring the radio system performance already validated in previous tests. Therefore all the sensor nodes installed in the pilot site should correctly communicate with the gateway node in a single hop.

In addition, the gateway node, as already explained, has to be directly connected to the control unit for data forwarding and storing. Therefore, the control unit, composed by a reduced size pc (i.e., Intel NUC) has been installed in the variable message panel rack, mainly for protection issues.

The monitoring system, as defined and implemented, do not consider any kind of verification system to validate its actual working in relation to real wildlife crossing or detected events, namely defining the amount of false positive and/or

false negative detections. To this end, a digital video recorder system with infrared camera has been installed on the pilot site, thus acquiring the so called ground truth of the monitored scenario h24 and allowing the comparison among registered data (4.30 (b)).

4.4. PILOT SITE IDENTIFICATION AND SENSOR NODE INSTALLATION



Figure 4.30: Pilot site: (a) variable message panel and position of some sensor nodes signed by red marker, (b) variable message panel and position of gateway node signed by yellow marker, (c) gateway node installation, (d) gateway node Yagi antenna and verification system.

4.4.1 Experimental Testing

Several tests have been performed by exploiting the deployed sensor nodes, in order to validate the proper working of the monitoring system in the real installation scenario, by performing different movements, which may resemble the actual events determined by wildlife road crossing. In addition, repeated motion typologies have been implemented, thus evaluating the monitoring system working on a statistical base.

Fig. 4.31 shows the movements typologies performed in front of the sensor nodes. In detail, the sketch shows the position of some sensor nodes, displayed with the yellow circle along the road, the single device field-of-view, drawn as the angular sector in orange, and the total security area determined by the detection range of all the nodes deployed in the test site. Such area, is defined as the zone in which events may be detected by the monitoring system, such that every target approaching the road from any of the two road sides is promptly detected by the relative sensor node installed in the proximity of the occurring event.

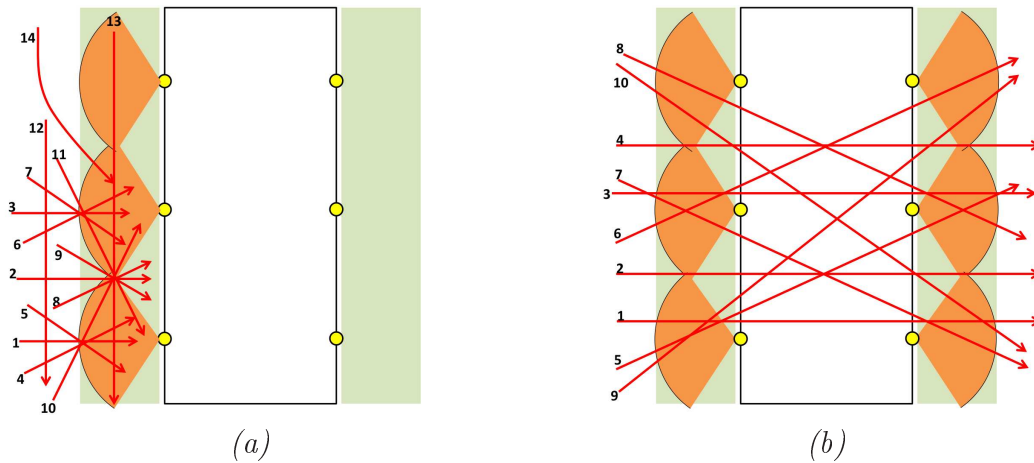


Figure 4.31: Pilot site experimental testing: (a) approaching, leaving and lateral movements, (b) road crossing movements.

In particular, Fig. 4.31(a) reports the approaching, leaving or lateral movements category, while Fig. 4.31(b) reports the road crossing events one. Such tests has allowed validating the proper working of the monitoring system installed on the pilot site, with particular attention to some parameter such as actual security area size, proper work of the devices and event detection capability according to the tested events typologies.

4.4. PILOT SITE IDENTIFICATION AND SENSOR NODE INSTALLATION

Therefore, Fig. 4.33 and Fig. 4.34 show the results obtained by performing approaching events to sensor nodes installed. Similarly, Fig. 4.35 reports some tests result by performing lateral movements both in and out the security area, such validating the proper detection only if the movements happen in the road proximity. Fig. 4.36 and Fig. 4.37, instead, show the results obtained by performing some crossing events of different type. As it may be noticed, given the occurring event, the sensor node in front of which the target moves correctly detects the motion with good accuracy. In particular, approaching and leaving events may be clearly identified by looking the processed radar signal envelope, as detailed in Fig. 4.32. In case of approaching event, the signal envelope gradually increases from low values up to its maximum dynamic, in relation to motion speed and target dimension. Analogous result is obtained for leaving events, for which, instead, the signal dynamic starts with high values which decreases as the target moves away from the sensor node.

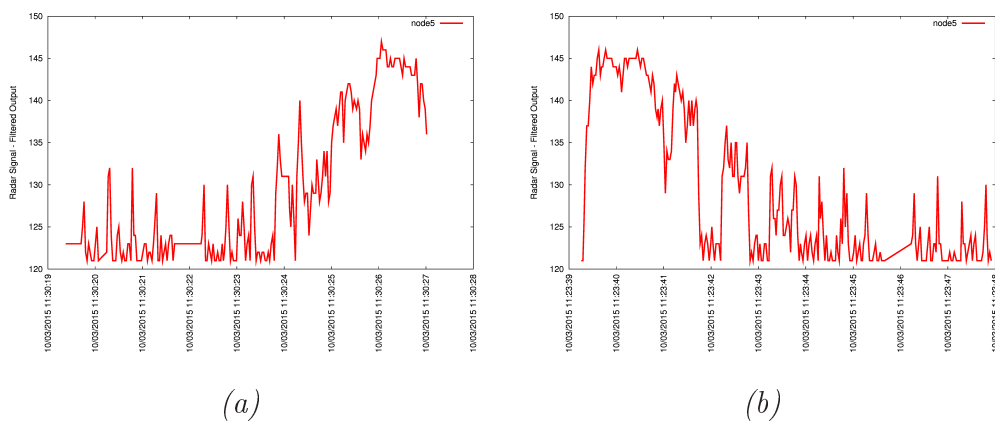


Figure 4.32: Experimental testing: (a) processed radar signal during approaching event, (b) processed radar signal during leaving event.

CHAPTER 4. ENGINEERING AND PILOT SITE EXTENSION

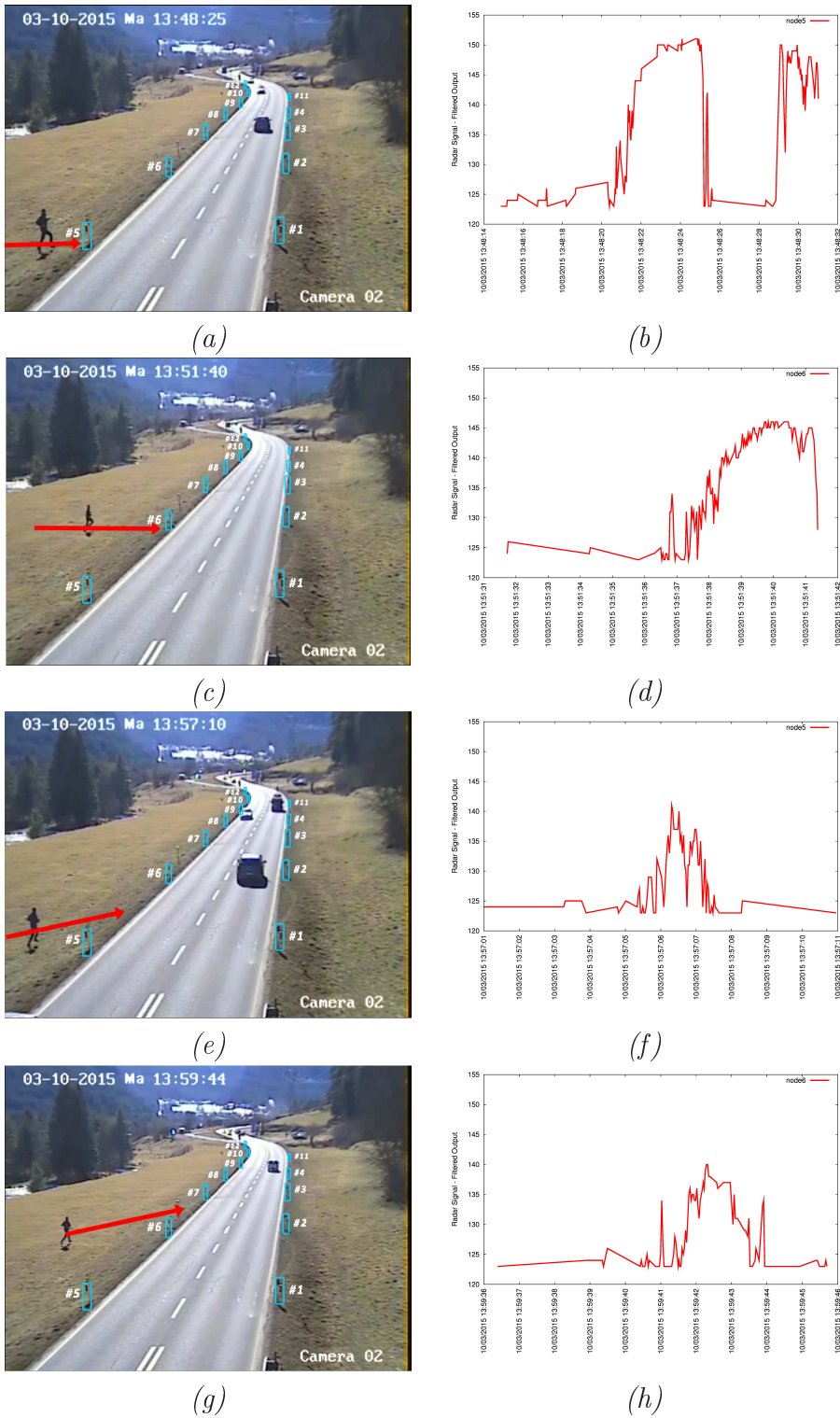


Figure 4.33: Pilot site experimental movement tests: (a)-(b) orthogonal to node #5 and processed radar signal, (c)-(d) orthogonal to node #6 and processed radar signal, (e)-(f) lateral to node #5 and processed radar signal, (g)-(h) lateral to node #6 and processed radar signal.

4.4. PILOT SITE IDENTIFICATION AND SENSOR NODE INSTALLATION

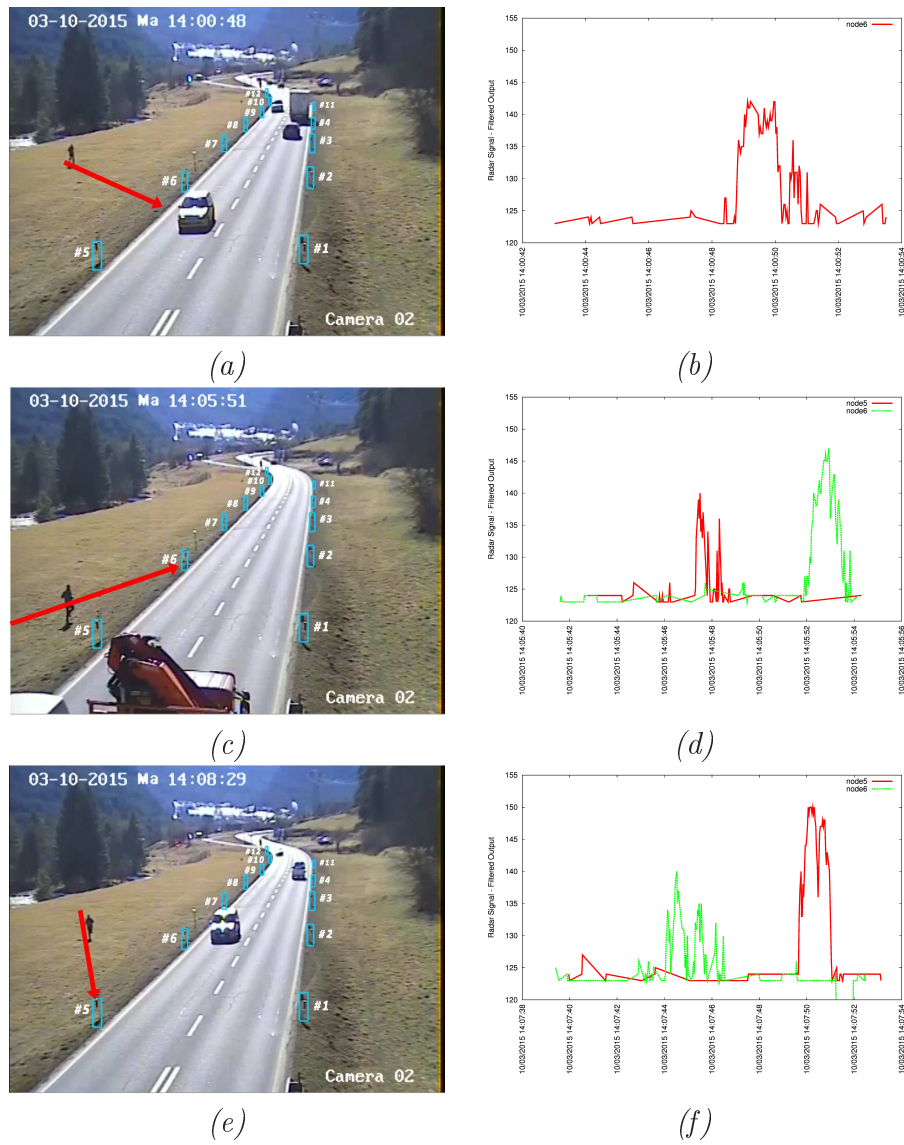


Figure 4.34: Pilot site experimental movement tests: (a)-(b) lateral to node #6 and processed radar signal, (c)-(d) lateral to nodes #5 and #6 and processed radar signal, (e)-(f) lateral approach to nodes #6 and #5 and processed radar signal.

CHAPTER 4. ENGINEERING AND PILOT SITE EXTENSION

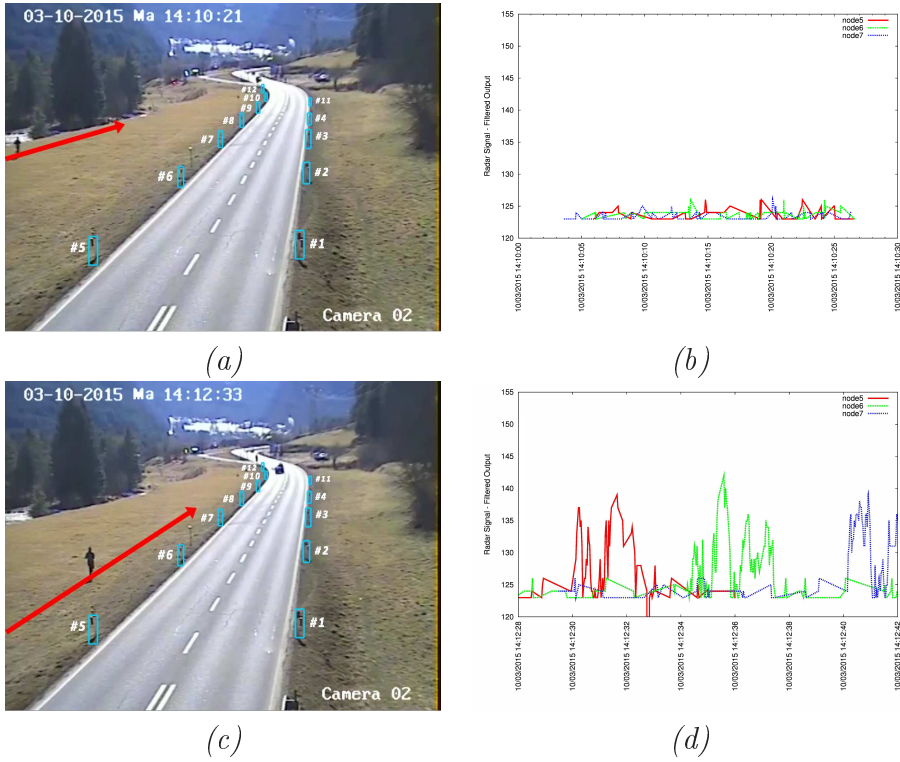


Figure 4.35: Pilot site experimental tests: (a) target moving out of the security area, (b) processed radar signal when target moving out of the security area, (c) target moving inside the security area, (d) processed radar signal when target moving inside the security area.

4.4. PILOT SITE IDENTIFICATION AND SENSOR NODE INSTALLATION

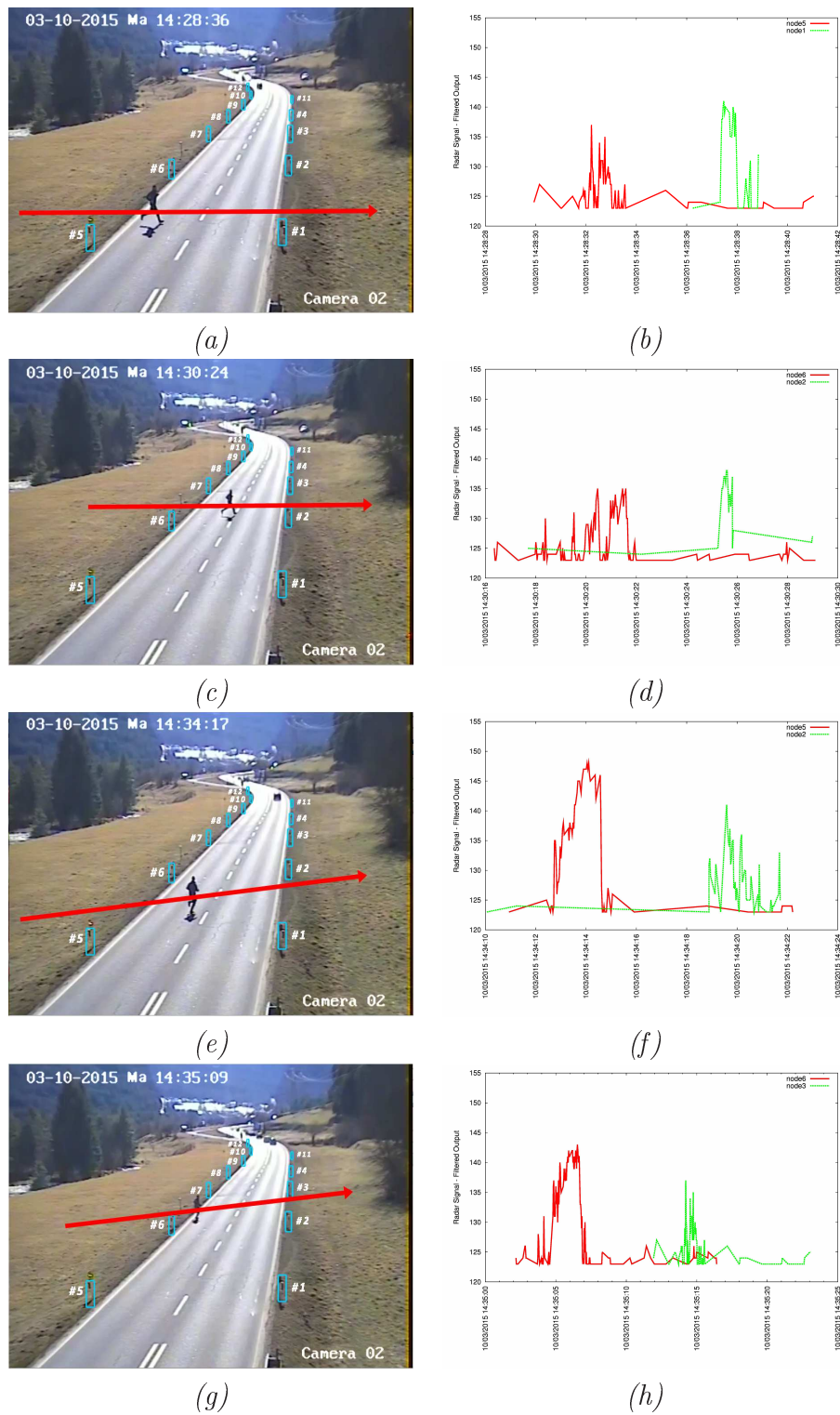


Figure 4.36: Pilot site experimental tests: (a)-(b) road crossing near nodes #5 and #1 and processed radar signal, (c)-(d) road crossing near nodes #6 and #2 and processed radar signal, (e)-(f) road crossing near nodes #5 and #2 and processed radar signal, (g)-(h) road crossing near nodes #6 and #3 and processed radar signal.

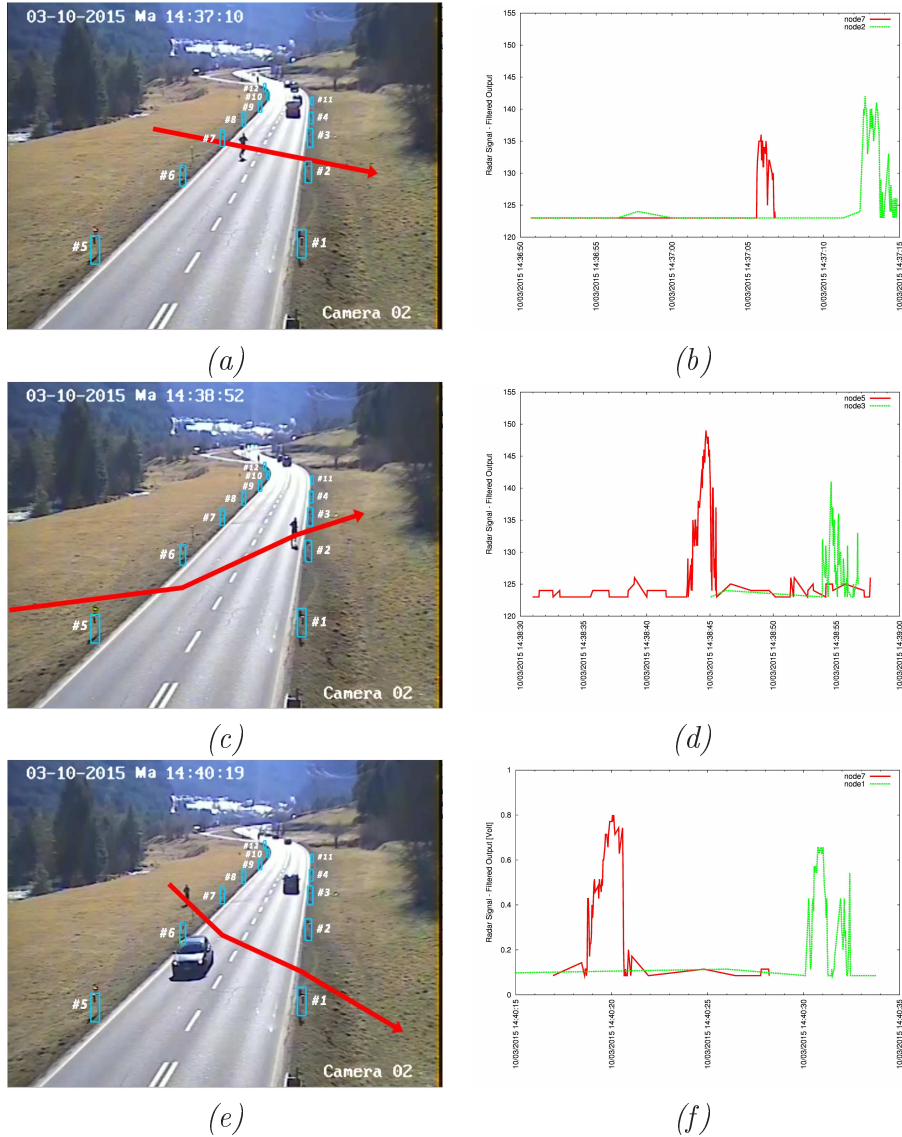


Figure 4.37: Pilot site experimental tests: (a)-(b) road crossing near nodes #7 and #2 and processed radar signal, (c)-(d) road crossing near nodes #5 and #3 and processed radar signal, (e)-(f) road crossing near nodes #7 and #1 and processed radar signal.

4.4. PILOT SITE IDENTIFICATION AND SENSOR NODE INSTALLATION

An additional result regards the system lifetime and specifically of the sensor nodes deployed. In fact, the combination of battery used as power supply, solar panel energy and the controller firmware setup allows extending the actual device lifetime ideally to infinite. In particular, it has been verified that in complete absence of solar radiation, the battery unit is capable of sustaining the sensor node working for about 14 days, considering day and night working. In case of discharged battery, as expected, the solar cells are able to recharge the battery unit within 8-10hours, given the effective solar radiation (these tests, in fact, have been performed during winter season, during which the solar radiation has less power efficiency). The plot shown in Fig. 4.38 exemplifies 10 days of device operation, starting with non completely charge battery, which is progressively recharged. It is worth noting that the daily battery voltage may not represent its actual capacity, since the electrical parallel charge circuit with solar panels implies a voltage increase, which instead can be effectively read during night periods.

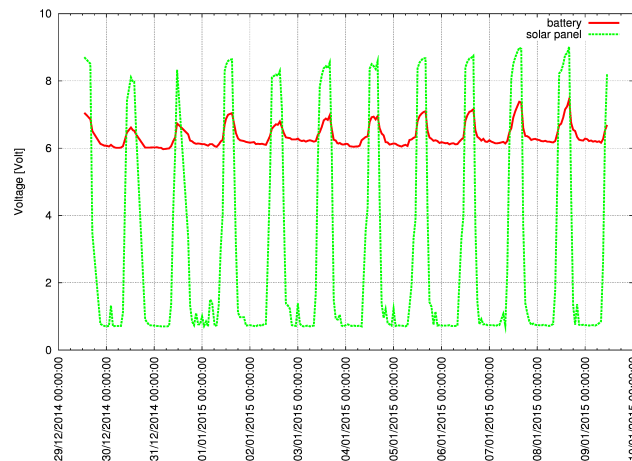


Figure 4.38: Pilot site: battery recharge.

Regarding actual wildlife road-crossing events, Fig. 4.39 shows an example of detected event. In particular, some screenshots of the actual event captured thanks to the installed verification system are reported, together with the processed radar signal regarding the roe-deer crossing. As it may be seen, the sensor nodes interested in the event correctly detect the wildlife, in particular the radar signals acquired by the two sensor nodes exhibit the patterns described above, given the movement typology occurred.

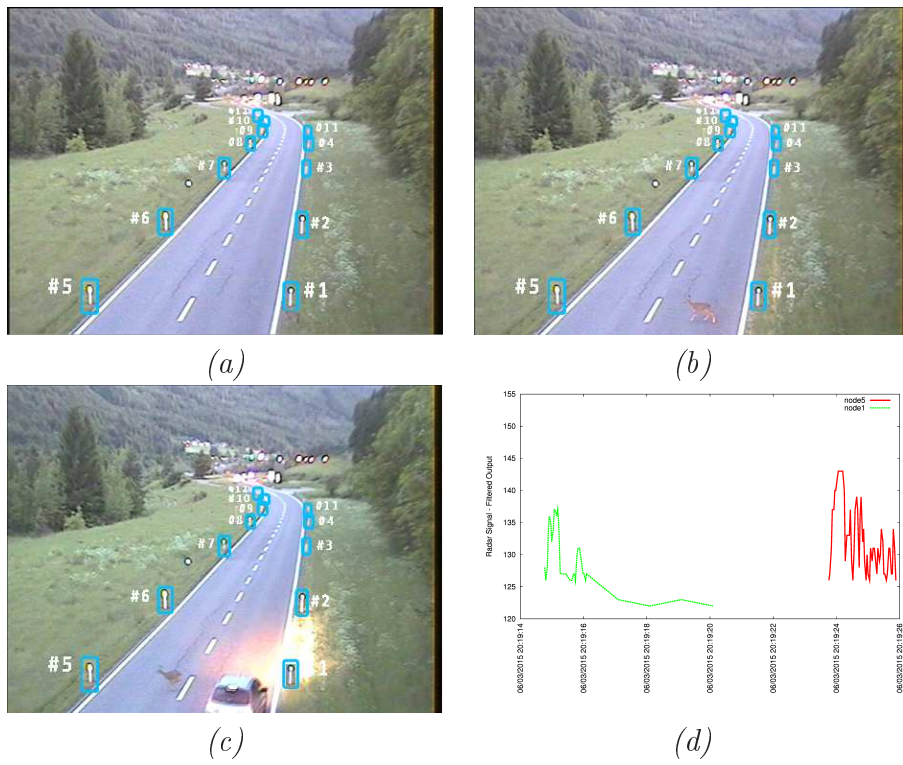


Figure 4.39: Pilot site: (a)-(b)-(c) roe-deer road crossing event, successive time instants, (d) processed radar signal acquired for the roe-deer road crossing event.

4.4. PILOT SITE IDENTIFICATION AND SENSOR NODE INSTALLATION

Chapter 5

Conclusions

In this chapter, conclusions and future developments regarding the proposed wildlife road crossing monitoring system are presented. In particular, additional considerations are given concerning the actual value of such system in order to limit fauna-vehicle incidents by preventing these events to happen.

5.1 Conclusion and Future Development

Wildlife road crossing represents a real problem to which actual solutions have not yet been defined. In particular, as already described in section 2.2, state-of-the-art solutions are mainly based on active systems, thus implying wildlife to wear specific devices, which allow them cooperating in the detection mechanism, or alternatively on road infrastructures used to limit fauna access to the roads.

Nevertheless, such solutions are characterized by some drawbacks, in detail regarding the former case, the use of devices to be worn by animals actually limits the use of such system since it may not be generalized to every fauna species, in particular those ones arranged in large herds of animals and which may not be easily captured for device equipping. In addition, another challenge regards the actual transmission of information, which should take place wirelessly, thus implying proper radio infrastructures. Moreover, also the power supply may represent a main drawback of the system, since replacing batteries used for device supply may not be actually an easy operation, as described above.

Regarding the latter case, instead, the solution of properly infrastructuring roads interested in the wildlife road crossing problem is a valuable solution, since it does not imply the use of any kind of device for the effective fauna monitoring, thus reducing the maintenance interventions by operators. In fact, once installed, these infrastructures should guarantee an higher security level on near roads and few periodic inspections may be performed in order to validate their actual state. As already described, the main used infrastructures are of the underpass, overpass and fencing typologies. Nevertheless, the main drawbacks of such structures regard costs and actual impact on the environment, which may alter both the ecosystem and the roads mobility.

Therefore, also considering the above considerations, the proposed monitoring system may be an actual solution to the problem, since, regarding the above drawbacks, it can be classified as a passive system, since wildlife do not need to wear any kind of device for their detection, and in addition the actual system cost has been kept very low, even during the prototyping process.

The engineered sensor nodes exploit the Doppler radar technology, which allows gathering useful information from the detected events, such as speed and direction of the moving target. A security area is defined along the road direction of size about 10-12m from the road margin. Therefore all the events occurring inside this area are identified by the monitoring system and they may be used in order to properly warn incoming drivers. In fact, in order to close the system operation cycle, an actuator node of the wireless network may be implemented, thus allowing the actual warn of drivers in relation to detected events. Actually a prototype of such device has been developed in order to propose and validate the complete monitoring system working. Fig. 5.1(a) shows a picture of the actuator node prototype. Of course the final actuator device will have to comply with road and security legislations in force, thus the solution may be identified in the

wildlife road sign properly equipped with warning leds, which may be triggered with different effects on the basis of the actual detected event. For instance, no leds if no events are occurring, blinking leds in low risky conditions and steady active leds in case of wildlife movements representing a very dangerous scenario for incoming drivers.

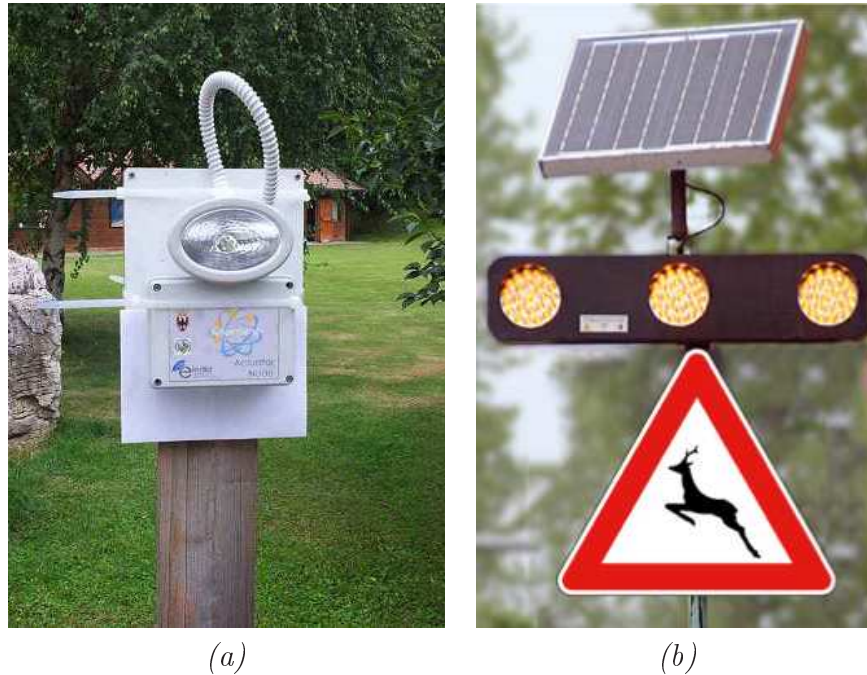


Figure 5.1: Actuator node of the monitoring system: (a) developed prototype, (b) proposed final solution.

Moreover, the relation between the radar signal and the target characteristics is very complex and a learning by example (LBE) strategy could be exploited in order to estimate it. In fact, the signal acquired by the radar modules depends on the target characteristics and it contains information on the scenario useful to determine the position, the direction and the velocity of the unknown moving target.

Towards this end, a set of targets (i.e., different positions, movements and velocities) could be defined and the problem of target identification recast as the definition of the probability of belonging to a specific class of target. According with the similarity to the known training data acquired in controlled scenarios, this approach should reduce the false positive and false negative detections. Moreover, even if a target will be identified inside the security zones, the classifier will label the event as true only when the movement characteristics will belong

5.1. CONCLUSION AND FUTURE DEVELOPMENT

to a specific class, thus avoiding the signaling of static targets or targets moving parallel to the road, which may represent lower risk conditions for road security.

Bibliography

- [1] R.T. Forman, "Road Ecology: Science and Solutions," *Island Press*, Washington, D.C., USA, 2003.
- [2] Z. He et al., "Energy-aware portable video communication system design for wildlife activity monitoring," *IEEE Circuits and Systems Mag.*, vol. 8, no. 2, pp. 25-37, 2008.
- [3] B. Wietrzyk and M. Radenkovic, "Energy efficiency in the mobile ad hoc networking approach to monitoring farm animals," *IEEE Int. Conf. on Networking and Services*, July 19-21, Silicon Valley, CA, USA, 2006.
- [4] M. Rutishauser, V.V. Petkov, T. Williams, C. Wilmers, J. Boice, K. Obraczka, and P. Mantey, "CARNIVORE: A disruption-tolerant system for studying wildlife," in *Proc. of 19th Int. Conf. on Computer Communications and Networks*, pp. 1-8, 2010.
- [5] J-H. Huang, Y-Y. Chen, Y-T. Huang, P-Y. Lin, Y-C. Chen, Y-F. Lin, S- C. Yen, P. Huang, and L-J. Chen, "Rapid prototyping for wildlife and ecological monitoring," *IEEE Systems Journal*, vol. 4, no. 2, pp. 198-209, 2010.
- [6] F. Viani, P. Rocca, G. Oliveri, and A. Massa, "Pervasive remote sensing through WSNs," *European Conf. on Antennas and Propagation*, (EuCAP 2012), Prague, Czech Republic, March 26-30, 2012.
- [7] M. Benedetti, L. Ioriatti, M. Martinelli, and F. Viani, "Wireless sensor network: a pervasive technology for earth observation", *IEEE Journal of Selected Topic in Applied Earth Observation and Remote Sensing*, vol.3, no. 4, pp. 488-496, 2010.
- [8] M. Martinelli et al., "A WSN-based solution for precision farm purposes", *Proc. 2009 IEEE Int. Geosci. Remote Sens. Symp. (IGARSS 2009)*, Cape Town, 13-17 July 2009, vol. 5, pp. 469-473.
- [9] L. Ioriatti, M. Martinelli, F. Viani, M. Benedetti, and A. Massa, "Real-time distributed monitoring of electromagnetic pollution in urban environment," in *Proc. 2009 IEEE International Symposium on Geoscience and Remote Sensing*, Cape Town, South Africa, July 13-17, 2009.

BIBLIOGRAPHY

- [10] F. Viani, M. Donelli, D. Trincherò, G. Oliveri, and A. Massa, "A WSN-based system for real-time electromagnetic monitoring," *Proc. 2011 IEEE AP-S International Symposium*, Spokane, Washington, USA, pp. 3129-3132, July 3-8, 2011.
- [11] F. Viani, M. Salucci, P. Rocca, G. Oliveri, and A. Massa, "A multi-sensor WSN backbone for museum monitoring and surveillance," *European Conf. on Antennas and Propagation, (EuCAP 2012)*, Prague, Czech Republic, March 26-30, 2012.
- [12] F. Viani, P. Rocca, M. Benedetti, G. Oliveri, and A. Massa, "Electromagnetic passive localization and tracking of moving targets in a WSN-structured environment," *Inverse Problems - Special Issue on Electromagnetic Inverse Problems: Emerging Methods and Novel Applications*, vol. 26, pp.1-15, 2010.
- [13] F. Viani, M. Donelli, P. Rocca, G. Oliveri, D. Trincherò, and A. Massa, "Localization, tracking and imaging of targets in wireless sensor networks," *Radio Science*, Vol. 46, No. 5, 2011.
- [14] F. Viani, L. Lizzi, P. Rocca, M. Benedetti, M. Donelli, and A. Massa, "Object tracking through RSSI measurements in wireless sensor networks," *Electronic Letters*, vol. 44, no. 10, pp. 653-654, May 2008.
- [15] F. Viani, G. Oliveri, and A. Massa, "Real-time tracking of transceiver-free objects for homeland security," *39th European Microwave Conference 2009 (EuMC2009)*, Rome, Italy, pp. 1892-1895, September 28 October 2, 2009.
- [16] F. Viani, M. Donelli, M. Salucci, P. Rocca, and A. Massa, "Opportunistic exploitation of wireless infrastructures for homeland security," *Proc. 2011 IEEE AP - S International Symposium*, Spokane, Washington, USA, pp. 3062-3065, July 3-8, 2011.
- [17] F. Viani, M. Donelli, G. Oliveri, and A. Massa, "A mobile wireless sensor network for collaborative tasks achievement by means autonomous robot robot swarm," *Proc. 2010 IEEE AP-S International Symposium*, Toronto, ON, Canada, July 11-17, 2010.
- [18] F. Viani et al., "Electromagnetic passive localization and tracking of moving targets in a WSN structured environment," *Inverse Problems*, vol. 26, pp. 1-15, 2010.
- [19] F. Viani, M. Martinelli, L. Ioriatti, L. Lizzi, G. Oliveri, P. Rocca, and A. Massa, "Real-time indoor localization and tracking of passive targets by means of wireless sensor networks," *Proc. 2009 IEEE AP-S International Symposium*, Charleston, SC, USA, June 1-5, 2009.

- [20] F. Viani, M. Martinelli, L. Ioriatti, M. Benedetti, and A. Massa, "Passive real-time localization through wireless sensor networks," *Proc. 2009 IEEE International Symposium on Geoscience and Remote Sensing*, Cape Town, South Africa, July 13-17, 2009.
- [21] F. Viani, G. Oliveri, M. Donelli, L. Lizzi, P. Rocca, and A. Massa, "WSN-based solutions for security and surveillance," *40th European Microwave Conference 2010 (EuMC2010) (2010 EuMA)*, Paris, France, September 26 October 1, 2010.
- [22] F. Viani, P. Rocca, G. Oliveri, and A. Massa, "Electromagnetic tracking of transceiver-free targets in wireless networked environments," *Proc. 2011 European Conference on Antennas and Propagation (EuCAP2011)*, Rome, Italy, April 11-15, 2011.
- [23] F. Viani, P. Rocca, M. Donelli, D. Trincherro, and A. Massa, "Exploiting inverse scattering theory for real-time tracking in homeland security applications," *Proc. 2011 Progress in Electromagnetics Research Symp. (PIERS 2011)*, Marrakesh, Morocco, March 20-23, 2011.
- [24] F. Viani, P. Rocca, L. Lizzi, and A. Massa, "WSN-based early alert system for preventing wildlife-vehicle collisions in alps regions," *International Conference on Electromagnetics in Advanced Applications (ICEAA2011)*, Turin, Italy, September 12-16, 2011.
- [25] J. Anand, A. Jones, T.K. Sandhya, and K. Besna, "Preserving national animal using wireless sensor network based hotspot algorithm," *IEEE International Conference on Green High Performance Computing (ICGHPC)*, pp.1-6, 14-15 March 2013.
- [26] A. Tovar, T. Friesen, K. Ferens, and B. McLeod, "A DTN wireless sensor network for wildlife habitat monitoring," *23rd Canadian Conference on Electrical and Computer Engineering (CCECE)*, pp.1-5, 2-5 May 2010.
- [27] V. Dyo, S.A. Ellwood, D.W. Macdonald, A. Markham, C. Mascolo, B. Pasztor, S. Scellato, N. Trigoni, R. Wohlers, and K. Yousef, "Evolution and sustainability of a wildlife monitoring sensor network," in *Proceedings of the 8th ACM Conference on Embedded Networked Sensor Systems*, pp. 127-140, 2010.
- [28] C. Mascolo, "Wildlife Social Life Monitoring through Sensor Network for a Better Planet," *Ubiquitous Computing at a Crossroads Workshop*, London, January 6-7, 2009.
- [29] Science and the Environment Bulletin, "Wildlife Tracking Technologies," [Online], http://www.ec.gc.ca/Science/sandejuly99/article1_e.html

BIBLIOGRAPHY

- [30] Vrbancic F., "The ubiquitous radio frequency identification technology used for livestock breeding," *MIPRO*, 2010 Proceedings of the 33rd International Convention, pp.653,655, 24-28 May 2010.
- [31] Z. He, "Energy-efficient integrated camera and sensor system design for wildlife activity monitoring," *IEEE International Conference on Multimedia and Expo, ICME 2009*, pp.1580-1581, June 28 2009-July 3 2009.
- [32] L.D. Mech and S.M. Barber, "A critique of wildlife radio-tracking and its use in national parks: a report to the U.S. National Park Service," *U.S. Geological Survey, Northern Prarie Wildlife Reserch Center*, Jamestown, N.D. 78, 2002.
- [33] J.J. Millspaugh and J.M. Marzluff, "Radio Tracking and Animal Populations," *Academic Press*, San Diego, California, USA, 2001.
- [34] L.D. Mech, "A Handbook Of Animal Radio-tracking," *Univ. of Minn. Press*, 1983.
- [35] NASA satellite Tracking of Threatened Species. http://sdc.d.gsf.nasa.gov/ISTO/satellite_tracking/, 2002.
- [36] P. Juang, H. Oki, Y. Wang, M. Martonosi, L.-S. Peh, and D. RUBenstein, "Energy-efficient computing for wildlife tracking: Design tradeoffs and early experiences with Zebranet," *Tenth International Conference on Architectural Support for Programming Languages and Operating Systems (ASPLOS-X)*, San Jose, CA, October 5-9, 2002.
- [37] S.I. Chakchai, P. Comdet, T. Smarn, W. Nutnicha, W. Kasidit, K. Urachart, W. Boonsup, and S. Saiyan, "Mobile Animal Tracking Systems using Light Sensor for Efficient Power and Cost Saving Motion Detection," *8th International Symposium on Communication Systems, Networks and Digital Signal Processing (CSNDSP)*, pp. 1-6, 2012.
- [38] M. Dominguez-Morales, A. Jimenez-Fernandez, D. Cascado-Caballero, A. Linares-Barranco, R. Paz, G. Jimenez-Moreno, and R. Soriguer, "Technical viability study for behavioral monitoring of wildlife animals in Donana: An 802.15.4 coverage study in a Natural Park," *Proceedings of the International Conference on Data Communication Networking (DCNET)*, pp.1-4, 18-21 July 2011.
- [39] S. Ehsan, M. Brugger, K. Bradford, B. Hamdaoui, and Y. Kovchegov, "Sufficient Node Density Conditions on Delay-Tolerant Sensor Networks for Wildlife Tracking and Monitoring," *IEEE Global Telecommunications Conference (GLOBECOM 2011)*, pp.1-6, 5-9 Dec. 2011.

- [40] D.M. Jun, D.L. Jones, T.P. Coleman, W.J. Leonard, and R. Ratnam, "Practical sensor management for an energy-limited detection system," *IEEE International Conference on Acoustics, Speech and Signal Processing (ICASSP)*, pp.1641-1644, 25-30 March 2012.
- [41] L. Long, D.M. Jun, and D.L. Jones, "Energy-efficient detection system in time-varying signal and noise power," *IEEE International Conference on Acoustics, Speech and Signal Processing (ICASSP)*, pp.2736-2740, 26-31 May 2013.
- [42] L. Karim, and N. Nasser, "Energy Efficient and Fault Tolerant Routing Protocol for Mobile Sensor Network," *IEEE International Conference on Communications (ICC)*, pp.1-5, 5-9 June 2011.
- [43] J. Kiepert, and L. Sin Ming, "A unified wireless sensor network framework," *IEEE International Systems Conference (SysCon)*, pp.1-6, 19-22 March 2012.
- [44] S. Sivaramakrishnan, and A. Al-Anbuky, "Analysis of network connectivity: Wildlife and Sensor Network," *Telecommunication Networks and Applications Conference (ATNAC)*, pp.1-6, 10-12 Nov. 2009.
- [45] S. Sivaramakrishnan, A. Al-Anbuky, and B.B. Breen, "Adaptive sampling for node discovery: Wildlife monitoring & sensor network," *16th Asia-Pacific Conference on Communications (APCC)*, pp.447-452, Oct. 31 2010-Nov. 3 2010.
- [46] S.A.B. Awwad, C.K. Ng, N.K. Noordin, and M.F.A. Rasid, "Cluster based routing protocol for mobile modes in wireless sensor network," *International Symposium on Collaborative Technologies and Systems*, pp. 233-241, 2009.
- [47] F. Bajaber and I. Awan, "Dynamic/Static Clustering Protocol for Wireless Sensor Network," *Second UKSIM European Symposium on Computer Modeling and Simulation*, pp. 524-529, 2008.
- [48] D.-S. Kim, and Y.-J. Chung, "Self-Organization Routing Protocol Supporting Mobile Nodes for Wireless Sensor Network," *Proceedings of the First International Multi-Symposiums on Computer and Computational Sciences (IMSCCS'06)*, 2006.
- [49] A. Duresia, V. Paruchuri, and L. Barolli, "Clustering Protocol for sensor networks," *20th International Conference on Advanced Information Networking and Applications*, vol. 2, 2006.
- [50] Y.P. Chen, A.L. Liestman, and J. Liu, "A hierarchical energy-efficient framework for data aggregation in wireless sensor networks," *Vehicular Technology, IEEE Transactions on*, vol.55, no.3, pp.789,796, May 2006.

BIBLIOGRAPHY

- [51] A. Lindgren, C. Mascolo, M. Loneragan, and B. McConnell, "Seal-2-Seal: A delay-tolerant protocol for contact logging in wildlife monitoring sensor networks," *5th IEEE International Conference on Mobile Ad Hoc and Sensor Systems, MASS 2008*, pp.321,327, Sept. 29 2008-Oct. 2 2008.
- [52] P. Mathur, R.H. Nielsen, N.R. Prasad, R. Prasad, "Wildlife conservation and rail track monitoring using wireless sensor networks," *4th International Conference on Wireless Communications, Vehicular Technology, Information Theory and Aerospace & Electronic Systems (VITAE)*, pp.1-4, 11-14 May 2014.
- [53] I. F. Akyildiz, Su W., Sankarasubramaniam Y., and Cayirci E., "A survey on sensor networks," *IEEE Communications Magazine*, vol.40, no.8, pp.102-114, Aug. 2002.
- [54] A.R. de Carvalho, A.D. Ribas, V.F. da Camara Neto, E.F. Nakamura, and C.M. Figueiredo, "An RSSI-based navigation algorithm for a mobile robot in Wireless Sensor Networks," *IEEE 37th Conference on Local Computer Networks (LCN)*, pp.308-311, 22-25 Oct. 2012.
- [55] A. Barati, M. Dehghan, H. Barati, and A.A. Mazreah, "Key Management Mechanisms in Wireless Sensor Networks," *Second International Conference on Second International Conference on Sensor Technologies and Applications*, pp.81-86, 25-31 Aug. 2008.
- [56] H. Leung, S. Chandana, and W. Shuang, "Distributed sensing based on intelligent sensor networks," *IEEE Circuits and Systems Magazine*, vol.8, no.2, pp.38-52, Second Quarter 2008.
- [57] J.M. Kahn, R.H. Katz, and K.S.J. Pister, "Mobile Networking for Smart Dust," *ACM/IEEE Intl. Conf. on Mobile Computing and Networking (MobiCom 99)*, Seattle, WA, August 17-19, 1999.
- [58] G. Pottie and W. Kaiser, "Wireless integrated network sensors," *Communications of the ACM*, vol. 43, no. 5, pp. 51-58, May 2000.
- [59] Bulusu et al., "Scalable Coordination for Wireless Sensor Networks: Self-Configuring Localization Systems," *ISCTA 2001*, Ambleside, U.K., July 2001.
- [60] C. Shen, C. Srisathapornphat, and C. Jaikaeo, "Sensor Information Networking Architecture and Applications," *IEEE Pers. Commun.*, pp. 52-59, Aug. 2001.
- [61] K. Sohrabi et al., "Protocols for Self-Organization of a Wireless Sensor Network," *IEEE Pers. Commun.*, pp. 16-27, Oct. 2000.

-
- [62] W. R. Heinzelman, A. Chandrakasan, and H. Balakrishnan, "Energy-Efficient Communication Protocol for Wireless Microsensor Networks," *IEEE Proc. Hawaii Int'l. Conf. Sys. Sci.*, pp. 1-10, Jan. 2000.
- [63] V. Rodoplu and T. H. Meng, "Minimum Energy Mobile Wireless Networks," *IEEE JSAC*, vol. 17, no. 8, pp. 1333-1344, Aug. 1999.
- [64] Skolnik M., "Radar Handbook," *3rd Edition, McGraw-Hill*, 2008.
- [65] Krohne Messtechnik GmbH & Co. KG, "Fundamental of Radar Technology for Level Gauging," *4th Edition*, 2007.
- [66] T. Augustynek, and A. Battaglia, "Retrieving hydrometeor motions using space-borne EarthCARE Doppler radar," *13th International Radar Symposium (IRS)*, pp.509-512, 23-25 May 2012.
- [67] J.H. Dunn, and D.D. Howard, "RADAR Target Amplitude, Angle, and Doppler Scintillation from Analysis of the Echo Signal Propagating in Space," *IEEE Transactions on Microwave Theory and Techniques*, vol.16, no.9, pp.715-728, Sep 1968.
- [68] P. H. Hildebrand, C. A. Walther, C. L. Frush, J. Testud, and F. Baudin, "The ELDORA/ASTRAIA Airbone Doppler Weather Radar: Goals, Design, and First Field Tests," *Proceedings of the IEEE*, vol. 82, No. 12, December 1994.
- [69] J. P. Webster, and R. Lukas, "TOGA-COARE: The TOGA coupled ocean-atmosphere response experiment," *Bull. Amer. Meteor. Soc.*, vol. 73, pp. 1377-1416, 1992.
- [70] T. Nakazawa, "Tropical super-clusters under intraseasonal variation," in *Japan-US Workshop on the ENSO Phenomena*, Univeristy of Tokyo, Meteorology Rep. 88-1, Dept. of Meterorology, Geophysical Institute, pp.76-78, 1988.
- [71] P. Komatineni, N. Nagarajan, M. M. Wadood, G. Mirzaei, J. Ross, M. M. Jamali, P. V. Gorsevski, J. Frizado, and V. P. Bingman, "Quantification of bird migration using Doppler Weather Surveillance Radars (NEXRAD)," *IEEE Radar Conference (RADAR)*, pp. 1-4, April 29 2013-May 3 2013.
- [72] Global Wind Energy Council, from <http://www.gwec.net/index.php?id=121>
- [73] U.S. Fish and Wildlife Services, from <http://www.fws.gov/birds/mortality-fact-sheet.pdf>
- [74] H. Zhou, "Dual-Doppler radar three-dimensional wind field retrieval software system and applications," *International Conference on Computer Science and Service System (CSSS)*, pp. 360-365, 27-29 June 2011.

BIBLIOGRAPHY

- [75] W. Li, and Y. Xie, "Multi-grid Analysis of the Three-Dimensional Doppler Radial Velocity: Idealized Cases Study," *Fifth International Joint Conference on Computational Sciences and Optimization (CSO)*, pp. 813-816, 23-26 June 2012.
- [76] M. W. Lang, G. W. McCarty, J. C. Ritchie, A. M. Sadeghi, W. D. Hively, and S. D. Eckles, "Radar Monitoring of Wetland Hydrology: Dynamic Information for the Assessment of Ecosystem Services," *IEEE International Geoscience and Remote Sensing Symposium, IGARSS 2008*, vol. 1, pp. I-261,I-264, 7-11 July 2008.
- [77] Y. K. Kwag, "An Airborne Radar System with Adaptive MTD Doppler Compensation Scheme usgin DSP Based Real-Time Spectral Estimation," *IEEE Radar Conference*, pp. 1-5, 26-30 May 2008.
- [78] D. C. Schleher, "MTI and pulsed Doppler radar," *Artech House*, pp. 344-355, 1991.
- [79] M. I. Skolnik, "Introduction to radar," *McGraw Hill*, ch. 3, 2000.
- [80] Galati, "Adavanced radar techniques and systems," *IEE Press, London, UK*, ch. 6, 1993.
- [81] Y. Huang et al, "Adaptive clutter suppression scheme with high performance," *IEEE Proceiding of ICSP*, pp. 1818-1821, 2000.
- [82] Y. S. Lee, P. N. Pathirana, C. L. Steinfort, and T. Caelli, "Monitoring and Analysis of Respiratory Patterns Using Microwave Doppler Radar," *IEEE Journal of Translational Engineering in Health ans Medicine*, vol. 2, pp. 1-12, 2014.
- [83] J. H. Oum, D. W. Kim, and S. Hong, "Two frequency radar sensor for non-contact vital signal monitor," *IEEE MTT-S International Microwave Symposium Digest*, pp. 919-922, June 2008.
- [84] Y. Yan, C. Li, X. Yu, M. D. Weiss, and J. Lin, "Verification of a non-contact vital sign monitoring system using an infant simulator," *Anual International Conference of the IEEE on Engineering in Medicine and Biology Society, EMBC 2009*, pp. 4836-4839, 3-6 Sept. 2009.
- [85] W. Xu, C. Gu, C. Li, and M. Sarrafzadeh, "Robust Doppler radar demodulation via compressed sensing," *Electronic Letters*, vol. 48, No. 2, pp. 1428-1430, October 25 2012.
- [86] C. Gu et al., "An instruments-built Doppler radar for sensing vital signs," *8th International Symposium on Antennas, Propagation and EM Theory, ISAPE 2008*, pp.1398-1401, 2-5 Nov. 2008.

- [87] A. Tariq, and H. Ghafouri-Shiraz, "Vital signs detection using Doppler radar and continuous wavelet Transform," *Proceedings of the 5th European Conference on Antennas and Propagation (EUCAP)*, pp.285,288, 11-15 April 2011.
- [88] O. Boric-Lubecke, V. M. Lubecke, I. Mostafanezhad, B.-K. Park, W. Mas-sagram, and B. Jekanovic, "Doppler Radar Architectures and Signal Processing for Heart Rate Extraction," *Microwave Review*, December 2009.
- [89] X. Lai, H. Torp, and K. Kristoffersen, "An Etended Autocorrelation Method for Estimation of Blood Velocity," *IEEE Transactions on Ultrasonic, Ferro-electrics, and Frequency Control*, Vol. 44, No. 6, November 1997.
- [90] P. Misans, and M. Terauds, "CW Doppler Radar Based Land Vehicle Speed MEasurement Algorithm Using Zero Crossing and Least Squares Method," *13th Biennial Baltic Electronics Conference (BEC2012)* Tallinn, Estonia, October 3-5, 2012.
- [91] J. H. Lim, I.-J Wang, and A. Terzis, "Tracking A Non.cooperative Mo-bile Target Usign Low-Power Pulsed Doppler Radars," *5th IEEE Interna-tional Workshop on Practical Issues in Building Sensor Network Applica-tions (SenseApp 2010)*, Denver, Colorado.

BIBLIOGRAPHY

Appendix A

Complete Circuitual Scheme of the WSN Node-Sensors Interfacing Board

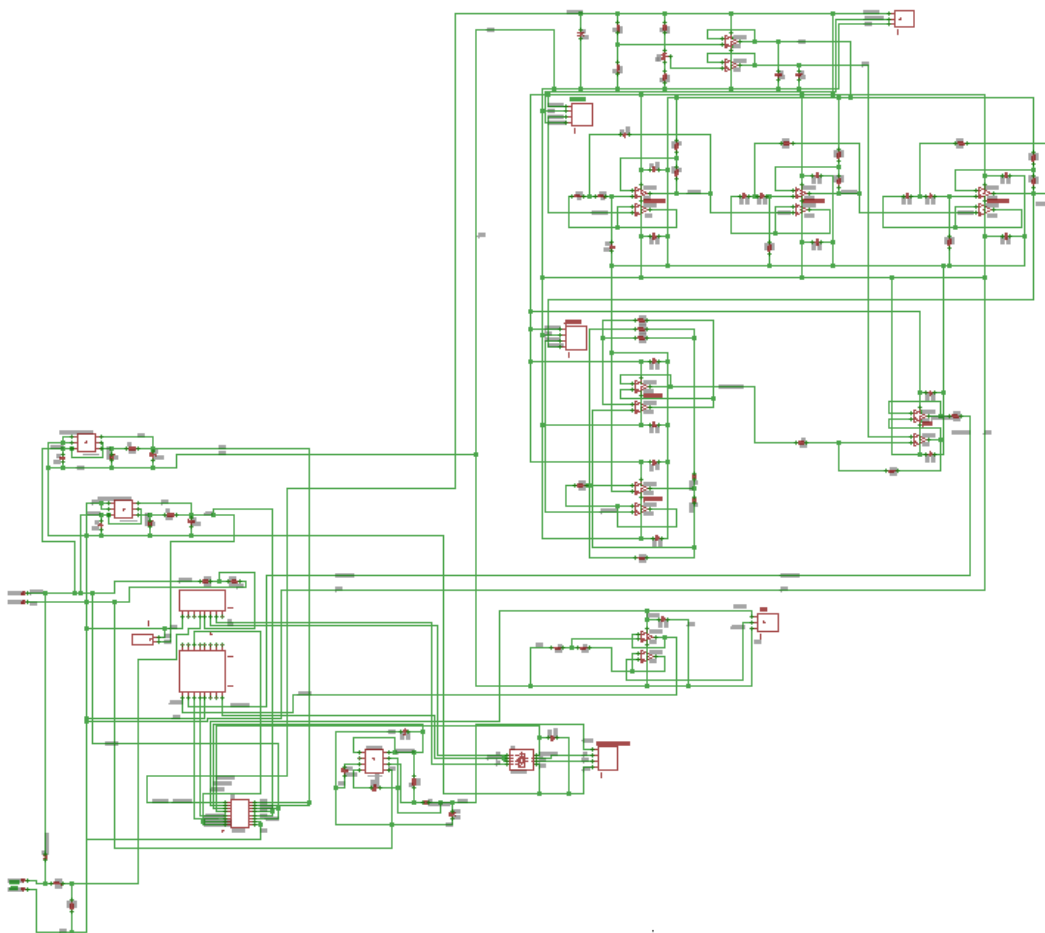


Figure A.1: Circuitual scheme of the WSN node-sensors interfacing board.
